

THE CRYSTAL STRUCTURE OF THE  
SILVER PERCHLORATE ADDUCT OF IRON(III) TRISACETYLACETONATE

by

M.M. THACKERAY B.Sc. (Hons.)

The University of Cape Town

A thesis submitted in fulfilment of the requirements for the degree of Master of Science of the University of Cape Town.

The copyright of this thesis is held by the University of Cape Town.

Reproduction of the whole or any part may be made for study purposes only, and not for publication.

Department of Chemistry  
University of Cape Town.

May 1973.

The copyright of this thesis vests in the author. No quotation from it or information derived from it is to be published without full acknowledgement of the source. The thesis is to be used for private study or non-commercial research purposes only.

Published by the University of Cape Town (UCT) in terms of the non-exclusive license granted to UCT by the author.

## ACKNOWLEDGEMENTS

The author wishes to thank his supervisor Dr. L.R. Nassimbeni for his invaluable assistance and enthusiasm throughout the course of this work.

The author is indebted to Dr. G. Gafner and Dr. G. Kruger of the C.S.I.R. for their assistance in the collection of intensity data from the C.S.I.R. diffractometer. The author also wishes to thank Dr. G.V. Fazakerley, Mr. M.R. Cairns and Mr. A.L. Rodgers for their interest and for useful discussion in producing this thesis.

The author finally wishes to thank his parents, the Council for Scientific and Industrial Research, and the University of Cape Town for financial aid.

# INDEX

	Page
1. INTRODUCTION	
1.1 Metal $\beta$ -Ketoenolates	1
1.2 Iron Acetylacetonate	2
1.3 Reactivity of the Metal Acetylacetonates	2
1.4 The Perchlorate Ion	4
1.5 Silver Perchlorate	4
1.6 The Silver Ion, $\text{Ag}^{+1}$	4
1.7 Complexes of Transition Metals	6
1.8 Complexes of the Silver Ion	7
1.9 Interaction of Metal Acetylacetonates with the Silver Ion	9
1.10 Infrared Spectral Data	10
a) The Infrared Spectra of Metal Acetylacetonates	11
b) The Interpretation of the Infrared Spectrum of $\text{Fe}(\text{acac})_3 \cdot \text{AgClO}_4 \cdot \text{H}_2\text{O}$	14
c) Band Assignments	14
d) The Structure of the Ferric Acetylacetonate Silver Perchlorate Adduct as Inferred from Spectral Data	19
e) The Hydrate Molecule	19
2. OBJECT OF RESEARCH	21
3. PREPARATION AND CHARACTERIZATION OF THE COMPLEX	
3.1 Preparation of the complex	23
3.2 Chemical Analysis of the crystals	23
4. SOLVING THE STRUCTURE	
4.1 Introduction	25
4.2 PART A.	
I. DATA COLLECTION BY VISUAL METHODS	
a) Apparatus	25
b) Finding the crystallographic axes	26
c) The Determination of the Unit Cell Parameters	26
d) The Density of the crystals	30
e) The Number of Molecules per Unit Cell	30
f) The Determination of the Space Group	31

	Page
g) Intensity Measurements	
(i) The Choice of a Suitable Crystal	31
(ii) The Alignment of the Crystal	33
(iii) Measurement of the Intensities	33
h) Correction of the Intensities	35
 II. SOLVING THE STRUCTURE	
a) The Patterson Synthesis	35
b) The Location of the Silver Ion	37
c) Model I	41
d) The Location of Atoms by Fourier Methods	42
(i) The Scattering Factor	42
(ii) The Structure Factor	42
(iii) The Fourier Synthesis	43
e) Model II	48
f) The Misinterpretation of the Patterson Map. Model I	53
g) The Difference Fourier	53
h) Refinement of the Structure	58
i) The Hydrate Molecule	60
j) The Program "ORTEP" : Illustrations of the Molecular Structure; Bond Lengths and Angles	62
 4.3 PART B.	
I. DATA COLLECTION FROM THE DIFFRACTOMETER	67
II. FINAL REFINEMENT OF THE STRUCTURE	69
a) Bond Lengths and Angles	72
b) Least Squares Planes	72
c) Illustrations of the Molecular Structure	76
 5. DISCUSSION	80
5.1 Gross Structural Features of $\text{Fe}(\text{acac})_3 \cdot \text{AgClO}_4 \cdot \text{H}_2\text{O}$	82
5.2 The Iron Acetylacetonate Molecule: Bond Lengths and Angles	83
5.3 The Coordination Sphere of the Silver Ion	87
a) Silver to Oxygen Bonding	87
b) Silver to Carbon Bonding	88
c) The Coordination Number of the Silver Ion as Inferred from Visual Data	90
d) The Coordination Number of the Silver Ion as Inferred from Diffractometer Data	91
e) Confirmation of the Trigonal Planar Arrangement of $\text{O}_8, \text{O}_{11}, \text{C}_{13}$ around the Silver Ion	93

	Page
5.4 The Planarity of the Chelate Rings	94
5.5 Thermal Motion of the Methyl Groups	98
5.6 The Perchlorate Ion	98
5.7 Hydrogen Bonding	100
5.8 The Structure as Interpreted from Infrared Spectral Data	101
5.9 Intermolecular Structure : Special Projections of the Structure	105
5.10 A Stereoscopic Illustration	105

Appendix A.

Appendix B.

## 1. INTRODUCTION

### 1.1 METAL $\beta$ - KETOENOLATES

$\beta$ -diketones exhibit keto-enol tautomerism (Fig. 1) and react with metal cations to form complexes in which the metal replaces the enolic hydrogen and a six membered ring is produced. (Fig. 2).

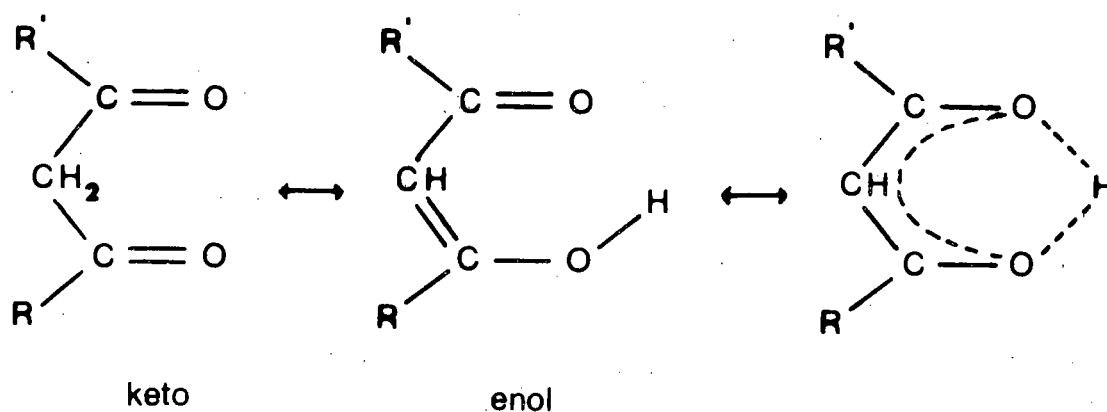


fig. 1

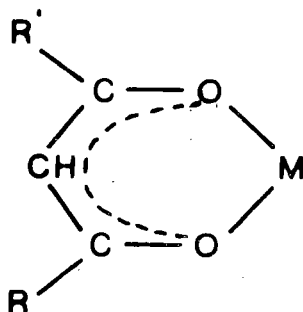


fig. 2

Since the enolate ion carries a single negative charge, trivalent metal atoms react with three enolate ions to give neutral molecules  $ML_3$  (where L is the  $\beta$ -diketone ligand). There are six donor oxygens to each metal atom. Such is the

case in ferric acetylacetonate ( $R = R' = \text{CH}_3$ ) in which the three rings are seen to be at right angles to one another producing an octahedral arrangement of the oxygen atoms about the central iron atom (Fig. 3).

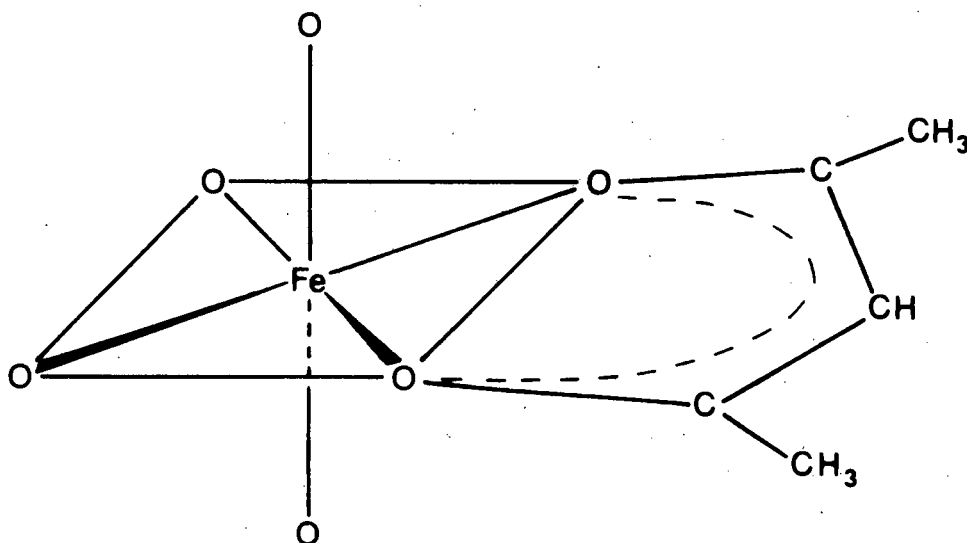


fig. 3

### 1.2 IRON ACETYLACETONATE

The crystal structure of ferric acetylacetonate was determined by Roof<sup>1</sup> in 1956 and refined by Iball and Morgan<sup>2</sup> in 1966. It was the first reported structure of a *tris*  $\beta$ -ketoenolate metal complex that was solved by X-ray diffraction methods. Fe - O bond lengths with a mean value of 1,99<sup>o</sup>A were observed and the mean O - Fe - O angle of 90,2<sup>o</sup> confirmed the regular octahedral arrangement of the oxygen atoms about the central iron atom.

### 1.3 REACTIVITY OF THE METAL ACETYLACETONATES

The exact nature of the acetylacetonate ring is not known although it has been postulated that the ring assumes

a "quasi aromatic" character as depicted by the broken line in figure 2. This arises through the delocalization of the four  $\pi$  electrons around part of the ring. In numerous metal acetylacetonates <sup>2-5</sup> metal to oxygen bond distances vary between 1,87 Å and 1,99 Å in contrast to the average carbon to carbon and carbon to oxygen distances of 1,38 Å and 1,28 Å respectively. This disproves any theory of complete resonance round the entire ring. The methyl substituents, being electron donors, contribute to the electronic character and reactivity of the acetylacetonate ring, but at the same time sterically retard chemical reaction.

Although they do not conform to the Hückel rule of aromaticity the chelate rings in metal acetylacetonates and related complexes undergo many reactions typical of aromatic systems<sup>6</sup>. The central hydrogen is known to be acidic and can be substituted by a variety of electrophilic reagents. Halogenation, nitration, thiocyanation and several Friedel Crafts reactions have been carried out in the metal acetylacetonates without rupture of the chelate rings. A concentration of electron density at the central carbon atom enables this atom to be a possible site for coordination with transition metals or ions<sup>7-10</sup>.

The oxygen atoms in  $\beta$ -ketoenolate complexes as well as the chelate rings themselves have been reported to function as sites for bond formation.

Fackler *et al*<sup>11</sup> have established hydrogen bond formation of  $\text{CH}_3\text{Cl}$ ,  $\text{CH}_3\text{OH}$  and other alcohols to  $\text{Mn}(\text{acac})_3$ . Numerous other authors<sup>12-14</sup> have reported the likelihood of hydrogen bond formation with metal  $\beta$ -ketoenolates.

In addition the ability of these sites to function as Lewis bases has been shown by the fact that many of the metal acetylacetonates polymerize through the  $\beta$ -diketone oxygens<sup>15</sup>.

#### 1.4 THE PERCHLORATE ION.

The perchlorate ion  $\text{ClO}_4^-$  is a very stable ion and is extremely reluctant to go over to the covalent state. Its structure has been well established. The four oxygen atoms are joined by single coordinate bonds to the central chlorine atom and are arranged tetrahedrally around it. The extreme stability of this ion has been attributed to its symmetry and to the fact that the chlorine atom has all of its valence electrons shared. Many of the perchlorates, especially those of the heavy metals are known to be deliquescent<sup>16</sup>.

An important property of the perchlorate ion is its low tendency to serve as a ligand in complexes<sup>17</sup>. The perchlorates have been used in the study of complex formation. When no other donor is present to compete there are indications that the perchlorate ion exercises a donor capacity. This is indicated in the complexes  $(\text{CH}_3)_3\text{SnClO}_4$  and  $[\text{Co}(\text{MeSC}_2\text{H}_4\text{SMe})_2(\text{ClO}_4)_2]$ . Shifts observed in the infrared spectrum which resulted from the tetrahedral symmetry of the  $\text{ClO}_4^-$  ion changing upon coordination, gave evidence for this coordination<sup>18</sup>.

#### 1.5 SILVER PERCHLORATE

Silver perchlorate is very soluble in water and forms the stable monohydrate  $\text{AgClO}_4 \cdot \text{H}_2\text{O}$ . It is also deliquescent. An odd feature of silver perchlorate is that it is also soluble in organic solvents notably toluene. Like most other metal perchlorates silver perchlorate is explosive and must be handled with care.

#### 1.6 THE SILVER ION, $\text{Ag}^{+1}$ .

The electronic configuration of this ion is  $1s^2 2s^2 2p^6 3s^2 3p^6 4s^2 3d^{10} 4p^6 4d^{10}$ .

The univalent state Ag(1) is the normal and dominant oxidation state for silver. The ion has a great tendency to form complex compounds as a result of its high polarizability and its low position on the electrochemical series<sup>19</sup>.

Ag(1) shows a pronounced tendency to exhibit linear two fold coordination as shown in the compounds AgCN (Fig. 4) and AgSCN (Fig. 5)<sup>20</sup>.

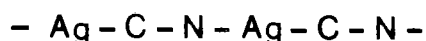


fig. 4

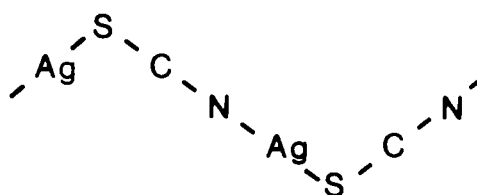


fig. 5

The small energy difference between the filled  $d_z^2$  orbital and the empty 5s orbital permits hybridization of these orbitals. This results in a linear configuration about the silver ion.

However the coordination number of the silver ion is dependent on the nature of the ligands and cases of trigonal<sup>21,22</sup> and tetrahedral<sup>23-25</sup> type bonding of the silver ion have been reported. In addition Ag(1) is also known to exhibit octahedral coordination<sup>26</sup> and even a number of cases of five fold coordination<sup>27</sup> have been reported.

1.7 COMPLEXES OF TRANSITION METALS : Interaction between Metals and  $\pi$  Electron Systems.

A feature of the d group transition metals is their ability to form  $\pi$  complexes with a variety of unsaturated organic ligands. In many of these complexes the metal atoms are in low positive, zero or negative oxidation states. It is a property of the ligands to be able to stabilize these low oxidation states. In addition to being able to donate electrons to  $\sigma$  type orbitals associated with a metal, the ligands possess vacant  $\pi$  orbitals. High electron density on the metal atom can then be delocalized onto the ligands. In  $\pi$  complexes therefore, both donation and back acceptance by the ligand are accomplished by use of ligand  $\pi$  orbitals.

In describing the interaction between transition metals and  $\pi$  bonding ligands, it is worthwhile to consider the Dewar-Chatt<sup>28</sup> Molecular Orbital description of the bonding between the metal and a mono-olefin. This is the generally accepted description of this type of bonding which is consistent with observed structural parameters.

The bonding consists of two separate components. These are illustrated in the figures below.

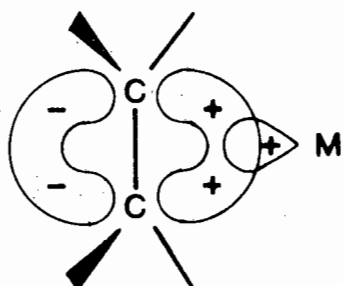


fig. 6a

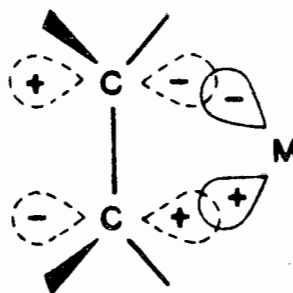


fig. 6b

Fig. (6a) depicts the donation of  $\pi$  electrons from the olefin into the  $\sigma$  type acceptor orbital of the metal atom. Fig. (6b) depicts the back donation of available  $\pi$  electrons from a filled metal d orbital into antibonding orbitals on the carbon atom. The donation of the electrons from the olefin to the metal and the introduction of electrons from the metal d orbital into the antibonding orbitals of the carbon atoms effectively increase the C-C bond length but to a lesser extent reduce its double bond character.

Similar bonding might be expected to occur between the silver ion and the unsaturated region of the acetylacetonate ring.

### 1.8 COMPLEXES OF THE SILVER ION

The existence of donor-acceptor complexes between aromatic moieties and Ag(I) has been known for some time.

A.E. Hill<sup>29-31</sup> reported the complexation of the silver ion with benzene and toluene as early as 1921 during the course of phase equilibrium studies.

In a review on the  $\pi$  Complex Theory<sup>32</sup> M.J.S. Dewar discussed the interaction between the silver ion and an olefin. Andrews and Keefer<sup>33-35</sup> in a series of articles reported the solubilities of certain aromatic hydrocarbons and substituted benzene compounds in aqueous silver nitrate. Data obtained was used to calculate equilibrium constants for the formation of the water soluble complexes  $\text{AgAr}^+$  and  $\text{Ag}_2\text{Ar}^{++}$ .

Winstein and Lucas<sup>36</sup> proposed the following structure for the benzene -  $\text{AgClO}_4$  complex. In the 1:1 complex  $\text{AgAr}^+$ , (Fig. 7a), the silver ion is pictured as being bonded to the aromatic nucleus from a position above the ring and

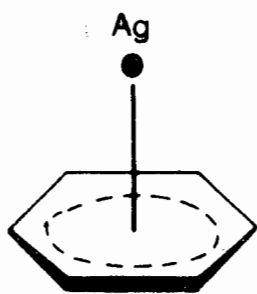


fig. 7a

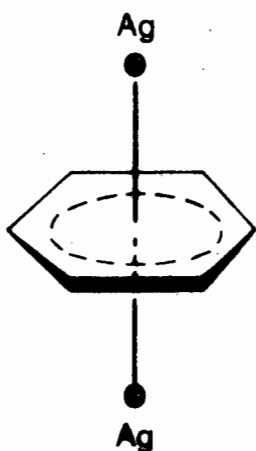


fig. 7b

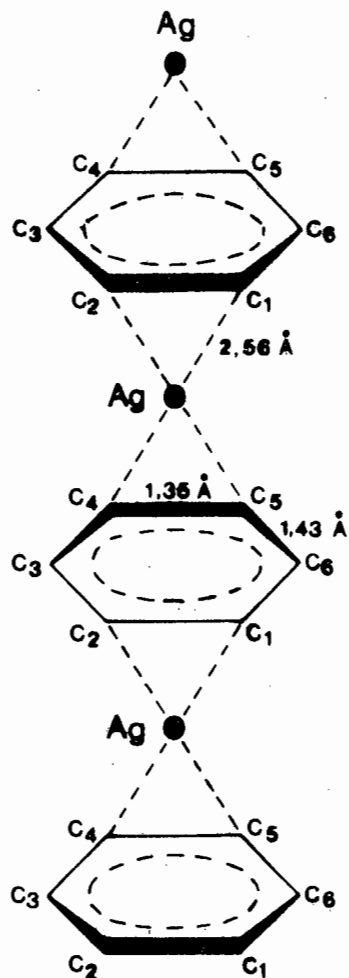
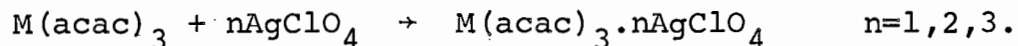
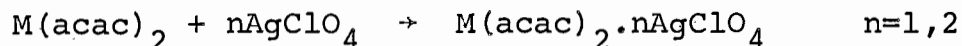


fig. 7c

bis-(o-xylene)<sup>39</sup>, bis-(m-xylene)<sup>23</sup>, Indene<sup>21</sup>, Anthracene<sup>40</sup>, Naphthalene<sup>40</sup>, Dioxane<sup>26</sup> and Adiponitrile<sup>24</sup>. Apart from the Dioxane and Adiponitrile complexes these structures may be described as layer structures. These layers are composed of  $\text{AgClO}_4$  (ionic) material and aromatic material which are alternately stacked to make the crystal structure.

#### 1.9 INTERACTION OF METAL ACETYLACETONATES WITH THE SILVER ION

Ginsberg<sup>41</sup> and Oestreich<sup>42</sup> have reported adduct formation which occurs between silver (I) salts and metal  $\beta$ -ketoenolates. When silver perchlorate dissolved in organic solvents is mixed with a solution of the metal  $\beta$ -ketoenolate, compounds precipitate which contain up to one  $\text{AgClO}_4$  molecule per chelate ring.



Ginsberg reports from infrared spectral data that in the structure of  $\text{Cu}(\text{acac})_2 \cdot 2\text{AgClO}_4$  the silver ions are located above the ring and in the immediate vicinity of the methylene carbon atom. This postulate is in agreement with the theory of the nature of the acetylacetonate ring as the central carbon atom has high electron density and is a probable site for coordination with a metal ion such as silver.

W.H. Watson Jr. and Chi-Tsun Ling<sup>7</sup> reported the crystal structure of Trisilver dinitrate tris(acetylacetonato)nickelate II monohydrate. In this compound all three silver ions are apparently bonded to a central "methylene" carbon atom of one ring ( $\text{Ag} - \text{C}:2,34 \overset{\text{O}}{\text{Å}}$ ) and to an oxygen of an adjacent ring ( $\text{Ag} - \text{O}:2,46 \overset{\text{O}}{\text{Å}}$ ). One of the silver ions is bonded to an oxygen of a nitrate ion and also to an oxygen of a water molecule giving the  $\text{Ag}(1)$  ion a coordination number of four. The other two  $\text{Ag}(1)$  ions obtain their coordination number of four by bonding to two oxygens of two different nitrate groups. The silver and nitrate ions form spiral chains together with the tris(acetylacetonate) nickelate II ion.

This is the only reported crystal structure of the silver ion with a metal  $\beta$ -ketoenolate that has been solved by X-ray diffraction techniques.

#### 1.10 INFRARED SPECTRAL DATA

By studying the differences between the infrared spectra of the parent compound and the silver perchlorate adduct, information regarding the structural features of the complex

can be obtained in terms of band shifts that occur when the adduct is formed.

A theoretical analysis of the infrared spectra of acetylacetonate chelates has been given by Nakamoto *et al.*<sup>43-45</sup>

Kline, Ginsberg and Ostreich<sup>46</sup> have reported the infrared spectra of various metal acetylacetonates together with their mono, di and triargentated adducts.

A Beckman I.R. 12 Spectrophotometer was used to obtain the infrared spectra of ferric acetylacetonate and that of the monoargentated adduct. These spectra are reproduced on pages 12 & 13.

The silver ion adduct retains the gross spectral characteristics of the parent chelate and only small changes in band frequencies are observed.

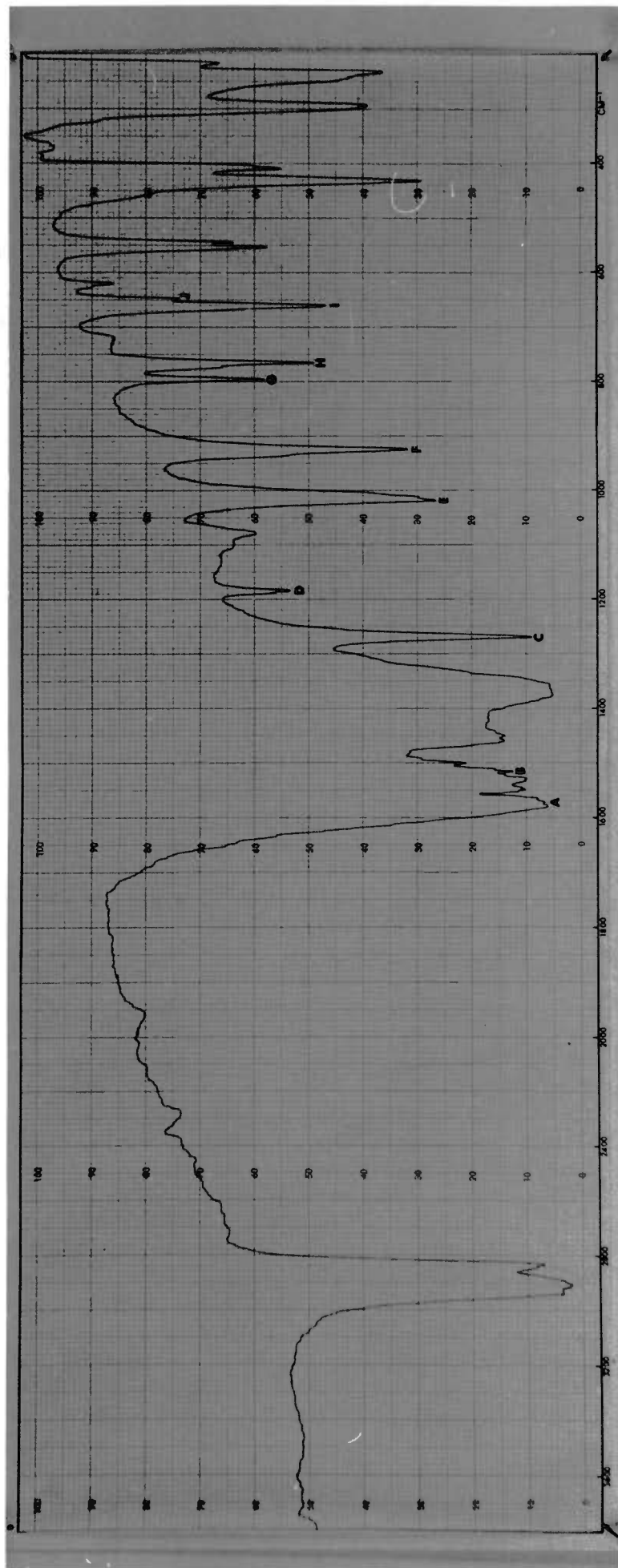
#### 1.10a The Infrared Spectra of Metal Acetylacetonates

Much work has been done on assigning bands to the vibrational modes of metal acetylacetonates. It must be pointed out that some confusion has arisen as to the correct assignment of the C=C and C=O bands which both appear on the spectrum between  $1500\text{ cm}^{-1}$  and  $1600\text{ cm}^{-1}$ . [See Table II].

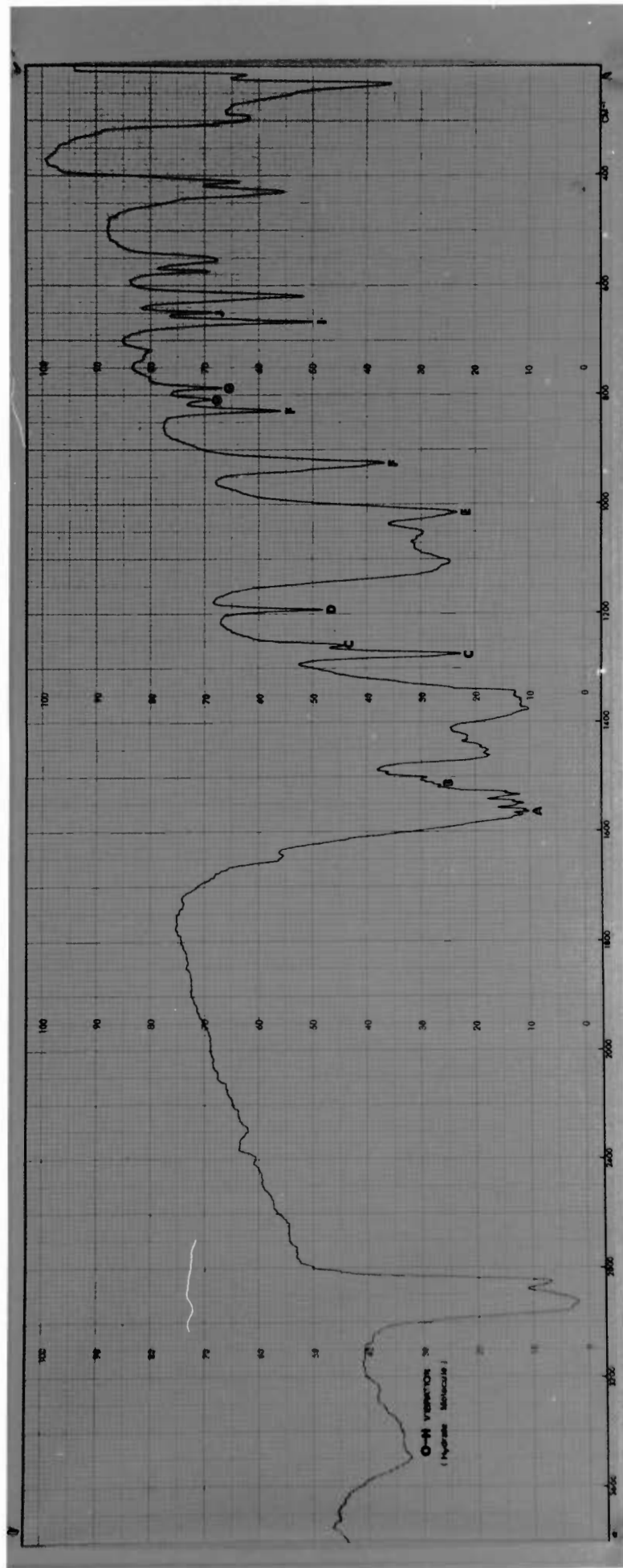
Two independent treatments of metal acetylacetonates<sup>43, 47</sup> have both led to the assignment of the band at higher frequency to a C=C stretch and the band at lower frequency to a C=O stretch. More recent analyses however have led to a reversal of these assignments<sup>48, 49</sup> which have been verified by <sup>18</sup>O labelling studies<sup>50</sup>.

As the question as to which of these two interpretations is still open to some debate it was decided to tackle the infrared spectrum of the adduct using one of these interpretations.

The Infrared Spectrum of  $\text{Fe}(\text{acac})_3 \cdot (\text{Nujol mull})$



The Infrared Spectrum of  $\text{Fe}(\text{acac})_3 \cdot \text{AgClO}_4 \cdot \text{H}_2\text{O}$  (Nujol mull)



The report by Kline *et al.*<sup>46</sup> allows for the former of these two assignments i.e. the band at higher frequency to a C=C stretch. The next section has been based on this interpretation of the band frequencies. It must be noted however that this treatment is not necessarily the correct one, in which case a different interpretation of the structure of the complex from infrared studies will have to be given.

Whatever the structure of the monoargentated complex is, it is theoretically expected that if the silver ion is located above the ring it will remove some of the  $\pi$ -electron density from the ring to form weak bonds with the ring. This should effectively reduce both the C=C and C=O stretching frequencies. Simple distortion of the rings caused by the close proximity of the silver ion may also be considered to account for small shifts in the C=C and C=O band frequencies.

#### 1.10b The Interpretation of the Infrared Spectrum of $\text{Fe}(\text{acac})_3 \cdot \text{AgClO}_4 \cdot \text{H}_2\text{O}$

The important band frequencies obtained in the above spectra have been compared with those reported by Kline, Ginsberg and Oestreich<sup>46</sup>. These are listed in Table I. The interpretation of the band frequencies of the various vibrational modes A to J, is that given by Kline, Ginsberg and Oestreich<sup>46</sup>.

#### 1.10c Band Assignments

Adduct formation causes a reduction in the infrared C=C frequencies near  $1580 \text{ cm}^{-1}$ . This is expected as the C=C stretching frequency of an olefin is shifted to lower wave numbers upon complexing the olefin with silver.

TABLE I.

SPECTRAL DATA OF FERRIC ACETYLACETONATE AND ITS MONOARGENTATED  
ADDUCT.

Band	Assignment	Kline, Ginsberg and Oestreich		This work	
		Fe(acac) <sub>3</sub> cm <sup>-1</sup>	Fe(acac) <sub>3</sub> .AgClO <sub>4</sub> cm <sup>-1</sup>	Fe(acac) <sub>3</sub> cm <sup>-1</sup>	Fe(acac) <sub>3</sub> .AgClO <sub>4</sub> cm <sup>-1</sup>
A	C=C	1578	1572	1582	1572
B	C=O	1528	1532	1524	1524 v.w.
C	C=C+C-CH <sub>3</sub>	1274	1274	1278	1281
			1261		1265
D	C-H i.p.	1190	1194	1193	1199
E	CH <sub>3</sub>	1023	1016	1026	1023
F	C=O+C-CH <sub>3</sub>	928	927	933	933
			834		836
G	C-H o.o.p.	802	810	804	815
			791		793
H		773	-	774	-
I	Ring def. + M-O.	667	668	669	672
J		654	654	656	656

The donation of  $\pi$  electron density to the attached silver ion causes a decrease in the C-C bond order and consequently a shift in the frequency of the absorption band. It is therefore expected that a similar frequency shift will be observed when Ag(I) ions are complexed by the unsaturated ligands in acetylacetonate chelates. Such a frequency was observed, and is indicated by Band A in Table I.

Band B is mainly due to the C=O stretching vibration.

The next band, C, contains the C=C stretching component coupled with the C-CH<sub>3</sub> stretching mode. This band is seen to be split in the spectrum of the mono adduct.

Band D is attributed to the C-H in plane bend.

Band E is the methyl rocking frequency and is shifted only slightly by complex formation.

Band F, which is the C-CH<sub>3</sub> stretching frequency coupled with the C=O stretching mode is unshifted although it is split in the argentated complex.

Band G is assigned the C-H out-of-plane bend. It is believed that the band is split by the silver ions giving rise to absorption at higher frequencies.

Band H is not present in the adduct spectrum. It is considered that this may be a molecular mode which the attachment of the silver ion disrupts.

Little explanation of bands I and J has been given. It is thought that these bands may be due to a metal to oxygen stretch or due to ring deformation.

Metal to oxygen stretching vibrations were observed in the region of 300 cm<sup>-1</sup>.

The spectral data of numerous metal acetylacetonates together with the spectral data of their mono, di and tri-argentated adducts has been grouped in Table II. From a study of the spectra of these argentated complexes Kline *et al.*<sup>46</sup> formulated two types of structures for these adducts.

TABLE II  
BAND FREQUENCIES (in  $\text{cm}^{-1}$ ) OF SILVER ION ADDUCTS OF  
OCTAHEDRAL METAL ACETYLACETONATES.

Band	Assignment	Co(acac) <sub>3</sub>	1AgClO <sub>4</sub>	3AgClO <sub>4</sub>	Fe(acac) <sub>3</sub>	1AgClO <sub>4</sub>	3AgClO <sub>4</sub>
A	C=C	1582	1571	1550	1578	1572	1576
B	C=O	1533	1533	1500	1528	1532	1505
C	C=C+C-CH <sub>3</sub>	1280	1283	1272	1274	1274	1268
			1272			1261	
D	C-H i.p.	1191	1201	1198	1190	1194	1185
E	CH <sub>3</sub>	1015	1023	-	1023	1016	-
F	C=O+C-CH <sub>3</sub>	935	937	935	928	927	920
			825	828		834	826
			808	-	-		
G	C-H o.o.p.	782	782	-	802	810	-
						791	-
H		775	-	-			
I	Ring def.	768			773	-	-
	+ M-O	674	678	674	667	668	672
J					654	654	654

Band	Assignment	Co(acac) <sub>3</sub> ·2H <sub>2</sub> O	1AgClO <sub>4</sub>	2AgClO <sub>4</sub>	Ag(Ni (acac) <sub>3</sub> )	1AgNO <sub>3</sub>	2AgNO <sub>3</sub> ·H <sub>2</sub> O
A	C=C	1602	1582	1572	1600	1600	1577
B	C=O	1515	1529	1502	1515	-	1497
C	C=C+C-CH <sub>3</sub>	1256	1276	1252	1264	1242	1277
			1248		1244		1244
D	C-H i.p.	1198	1198	1203	1185	1185	1188
					1020	-	-
E	CH <sub>3</sub>	1020	-	-	1014	1008	1014
F	C=O+C-CH <sub>3</sub>	930	925	930	929	922	-
			825	844	918	-	916
G	C-H o.o.p.	788	-	-	-		-
		769	-	-			
H		763			772	-	-
I	Ring def. +	669	673	693	-	-	669
	M-O.						
J		-	-	649	648	651	645

Note: The dash indicates that the band concerned had either disappeared completely or shifted radically to a new region of the spectrum.

### Structure 1

In the first instance a structure for the mono adducts of octahedral metal acetylacetonates was predicted. In general these complexes displayed the following important spectral features. The C=C absorption band, A, was found at slightly lower frequency than in the parent chelate. The C=O stretching frequency, B, appeared at slightly higher frequency. The methyl rocking frequency E was generally unaltered. The out-of-plane bending mode G was shifted but the in plane bending mode was not greatly changed.

In this structure the silver ion was believed to be located directly above the C=C region of the chelate ring. This was the best position for  $\pi$  bonding to be accomplished. An increase in the double bond character of the C=O bonds was considered to be due to a slight change in the electron density in the ring. Kline *et al.* thought this to be a consequence of the localization of electron density at the silver ion site.

### Structure 2

In the second type of structure viz. the di and tri-argentated complexes, the silver ions were thought to be bonded to the oxygen atoms of adjacent rings as well as to the C=C regions. The C=C band, A was more radically shifted to lower frequency than was found for the mono adducts. The C=O band, B was lowered in this case to about  $1500 \text{ cm}^{-1}$ . The methyl group rocking frequency and the out-of-plane bending mode G were also shifted more radically than was found in the monoargentated complexes. Interaction of the silver ion with a carbonyl group placed the silver close to one of

be ruled out.

The infrared spectrum of the mono argentated complex yielded a broad band at ca.  $3500\text{ cm}^{-1}$  indicating an O-H stretching mode. This band was not observed in the spectrum of ferric acetylacetonate.

From the analysis figures of the adduct (Section 3.2) the presence of a water molecule was also inferred.

This information implied that a hydrate molecule was to be found in the structure.

## 2. OBJECT OF RESEARCH.

The interaction of the silver ion with ring type systems has been of interest for many years.

Apart from the well known benzene- $\text{AgClO}_4$  structure it is only recently that crystal structures of  $\text{AgClO}_4$  with  $\pi$  electron donor molecules have been investigated by X-ray techniques.

Most of these complexes may be described as having "layer type" structures. These layer structures are composed of  $\text{AgClO}_4$  (ionic material) and aromatic moieties, which are alternately stacked to make the crystal structure.

An obvious exception to this "layer type" packing would be expected in the interaction of the silver ion with the chelate rings of metal acetylacetonates. Adduct formation between the silver(I) ion and metal  $\beta$ -ketoenolates has been described by Ginsberg and Oestreich [See Section 1.9]

Structural investigation of these compounds has been limited only to the complex Trisilver dinitrate tris(acetylacetonato)nickelate(II) monohydrate. No crystallographic structure of a mono argentated complex of any metal acetylacetonate has yet been published.

The geometric details of the mono argentated complex of iron acetylacetonate would yield further information regarding the interaction between the silver ion and  $\pi$  electron systems, especially as the silver ion has been reported to exhibit coordination numbers varying widely from two to six.

Two types of structure for argentated complexes of metal acetylacetonates have been postulated from infrared data<sup>4,6</sup>. One of these types has been predicted for the mono argentated complex of iron acetylacetonate.

Investigation of the crystal structure of the iron acetylacetonate silver perchlorate adduct by X-ray diffraction methods would provide the ultimate answer as to the true structure of the molecule.

### 3. PREPARATION AND CHARACTERIZATION OF THE COMPLEX.

#### 3.1 PREPARATION OF THE COMPLEX

Silver perchlorate (0.10 gm) was dissolved in toluene (10 ml) with gentle warming. Ferric acetylacetonate (0.17 gm) was also dissolved in toluene (10 ml) and added to the silver perchlorate solution. A deep red solution was formed on mixing together the orange acetylacetonate and the colourless silver perchlorate solutions.

The adduct  $\text{Fe}(\text{acac})_3 \cdot \text{AgClO}_4 \cdot \text{H}_2\text{O}$  crystallized on slow evaporation of the toluene from watchglasses. The temperature was recorded as  $18^\circ\text{C}$ . The watchglasses were covered so as to allow a high vapour pressure of toluene to be in contact with the solution. No crystals of the complex were formed from solutions that were left in the open. In these cases only a dark red oil remained after evaporation of the toluene.

The crystals obtained were diamond shaped and plate-like (Fig. 8).

Unlike most silver perchlorate adducts which tend to be deliquescent, the crystals were found to be stable in air for several months. They did not decompose on exposure to X-radiation. As a precautionary measure the crystals were stored under vacuum in a dessicator.

#### 3.2 CHEMICAL ANALYSIS OF THE CRYSTALS

In a review on metal  $\beta$ -ketoenolates<sup>15</sup> Fackler has reported the formation of mono, di and triargentated complexes with ferric acetylacetonate.

The theoretical analysis figures for all these complexes are listed in Table III. Also given are the analysis figures

for  $\text{Fe}(\text{acac})_3 \cdot \text{AgClO}_4 \cdot \text{H}_2\text{O}$  and the experimentally found values.

TABLE III

Element	$\text{Fe}(\text{acac})_3 \cdot \text{AgClO}_4$ M.W.=560,2	$\text{Fe}(\text{acac})_3 \cdot 2\text{AgClO}_4$ M.W.=767,6	$\text{Fe}(\text{acac})_3 \cdot 3\text{AgClO}_4$ M.W.=975,0	$\text{Fe}(\text{acac})_3 \cdot \text{AgClO}_4 \cdot \text{H}_2\text{O}$ M.W.=578,2	Experimentally* Found
C	32,13%	23,45%	18,46%	31,13%	30,9%
H	3,75%	2,74%	2,15%	3,98%	3,9%
Ag	19,26%	28,11%	33,20%	18,66%	18,03%
Fe	9,96%	7,27%	5,72%	9,65%	9,51%

The experimental results indicate clearly that a 1:1 complex was formed. The difference in values between the unhydrated complex and the monohydrated adduct is small as expected, but the values favour a monohydrated complex. This information was not considered to be critical as the contribution of a water molecule to the total molecular weight of the compound is very small and it therefore did not alter the fact that a 1:1 compound had been formed. It was felt that if a water molecule did exist in the compound, its presence would certainly be revealed on a difference Fourier computed during the later stages of refinement of the structure.

\* The micro analyses for carbon and hydrogen were carried out by Mr. W.R.T. Hemsted of this department. The percentages of silver and iron in the complex were determined using atomic absorption techniques. The crystals were soluble in nitric acid.

## 4. SOLVING THE STRUCTURE

### 4.1 Introduction

This chapter has been divided into two parts.

Intensity data for the structure analysis of the complex was collected in two ways. In the first instance the structure was solved using intensity data obtained visually from photographic films. Data collection, the solution and refinement of the structure have been outlined in Part A.

In order to improve the atomic parameters it was decided to refine the structure further using more accurate data that is available from a diffractometer. Diffractometer data collection, refinement and the final solution of the structure have been reported in Part B.

### 4.2 PART A.

#### I. DATA COLLECTION BY VISUAL METHODS

##### Ia. APPARATUS

Rotation and Weissenberg photographs were taken using a Stoe (Heidelberg) and a Stoe (Darmstadt) goniometer. Precession photographs were taken using a Stoe (Heidelberg) precession goniometer. These goniometers were used in conjunction with a Philips PW 1120 and a Philips PW 1008 generator. The generators were operated at 20 mA and 40 kV. A copper target was used and Cu K $\alpha$  radiation obtained with the aid of a Nickel filter.

Kodak "Kodirex" photographic film was employed in the collection of intensity data. The film was developed in Kodak Rapid X-ray Developer for 5 minutes at 20°C during which time it was continually agitated. It was immersed in a stop bath containing 3 per cent acetic acid solution and fixed for 5

the layer line spacings on the rotation photographs.

The unit cell length,  $a$ , is given by the equation

$$a = \frac{n\lambda}{\cos \arctan \frac{r}{x_n}} \quad (1)$$

where

$n$  = order of the layer line

$\lambda$  = wavelength of X-rays used (1,5418 Å)

$x_n$  = layer line spacing

$r$  = radius of the camera (2,865 cm)

The values of  $a$ ,  $b$ , and  $c$  obtained by this method are given in Table IV.

TABLE IV

Parameter	Length Å
a	12,01
b	11,57
c	16,95

These values were used for the preliminary investigation of the structure. For the refinement process more accurate data was necessary. Values of the axial lengths for refinement purposes were obtained from Weissenberg photographs as outlined below.

To obtain accurate reciprocal lattice constants  $a^*$ ,  $b^*$ , and  $c^*$ , the distance  $\delta$  between corresponding reflections on axial lines was accurately measured with a travelling microscope. The perpendicular distance between these spots,  $p$ , is related to  $\delta$  by the equation

$$p = \delta \sin \kappa \quad (2)$$

where  $\kappa$  is a constant for the camera ( $\tan \kappa = 2$ )  
(see Fig. 9).

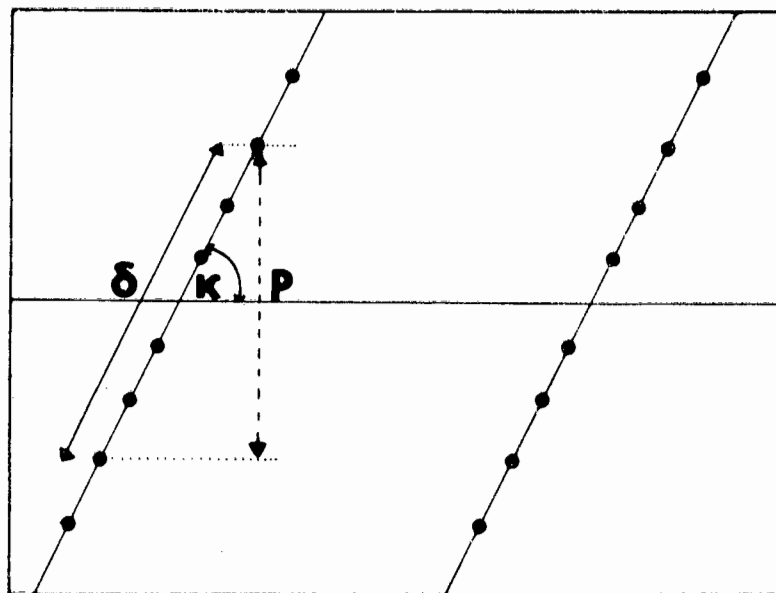


fig. 9

$\text{Now } p(\text{mm}) = \theta \text{ (degrees)}$

where  $\theta =$  Bragg angle for any one reflection.

The interplanar distance in reciprocal space  $d^*$ , is given by the Bragg Equation

$$\frac{1}{d^*} = \frac{2 \sin \theta}{n\lambda} \quad (3)$$

$d^*$  was calculated for numerous values of  $\theta$  corresponding to pairs of equivalent reflections on the axial lines.

As the values of  $d^*$  obtained from reflections on axial lines correspond directly to the reciprocal lattice constants,  $a^*$ ,  $b^*$ , and  $c^*$ , accurate values of these constants were obtained.

Zero and upper layer Weissenberg photographs confirmed that the space group was monoclinic with  $b$  the unique axis.

For a monoclinic crystal (2nd setting) the following conditions hold.

$$a = \frac{1}{a^*} \sin \beta$$

$$b = \frac{1}{b^*}$$

$$c = \frac{1}{c^*} \sin \beta$$

$$\beta = 180 - \beta^*$$

Volume of the unit cell =  $abc \sin \beta$ .

(ii) The Determination of  $\beta^*$ .

The angle  $\beta^*$  was measured in two ways.

- (a) directly from a precession photograph taken with the crystal precessing about the 'b' axis. This yielded a value of:-

$$\beta^* = 59,5^\circ \pm 0,50^\circ$$

$$\text{Hence } \beta = 120,5^\circ \pm 0,50^\circ$$

- (b) by the method of  $\omega$  separations<sup>51</sup> which yielded a value of:-

$$\beta^* = 58,75^\circ \pm 0,45^\circ$$

$$\text{Hence } \beta = 121,25^\circ \pm 0,45^\circ$$

As the values of  $\beta^*$  obtained by method (a) were taken from poor quality precession photographs, the final value of  $\beta^*$  used in the refinement process was that determined by method (b).

The final unit cell parameters and their standard deviations are given in Table V.

TABLE V

Parameter	Value	Standard Deviation
a	12,37 Å	0,02 Å
b	11,57 Å	0,02 Å
c	17,41 Å	0,01 Å
$\alpha$	90,00	-
$\beta$	121,25°	0,45°
$\gamma$	90,00	-

Id. THE DENSITY OF THE CRYSTALS

The approximate density of the crystals was determined by the flotation method. Solutions of thallium malonate, varying in concentration, were employed for this purpose. No accurate value was available as the crystals decomposed slowly in these solutions and other halocarbon liquids.

The approximate density was measured as 1,72 gm/cm<sup>3</sup>.

Ie. THE NUMBER OF MOLECULES PER UNIT CELL, n.

Using the equation

$$nM = a \times b \times c \times \sin \beta \times N \times \rho \quad (4)$$

where M = Molar mass of compound

abc Sin  $\beta$  = volume of the unit cell (cm<sup>3</sup>)

N = Avagadro's number (6,023 x 10<sup>23</sup>)

$\rho$  = observed density (1,72 gm/cm<sup>3</sup>)

the value of n = 3,94. This indicated that there were 4 molecules in the unit cell.

With n = 4 the calculated density was computed as 1,747 gm/cm<sup>3</sup>, assuming there was no hydrate molecule in the structure.

With a water molecule included in the structure  $\rho_c = 1,80$  gm/cm<sup>3</sup>.

If. THE DETERMINATION OF THE SPACE GROUP

From systematic absences observed on zero and upper layer Weissenberg photographs, the conditions for non extinction were found to be

h 0 0	no conditions
0 k 0	$k = 2n$
0 0 l	$l = 2n$
0 k l	no conditions
h 0 l	$l = 2n.$

These conditions yielded the unequivocal space group  $P2_1/c$ .

Ig. INTENSITY MEASUREMENTS

(i) Choice of a suitable crystal

An important factor which must be considered in determining a suitable crystal size is the absorption of the X-rays by the crystal<sup>52</sup>. The intensity  $I$  of a beam passing through a thickness  $\tau$  of crystal is given by the equation

$$I = I_0 e^{-\mu\tau} \quad (5)$$

where  $I_0$  = intensity of incident radiation

$\mu$  = linear absorption coefficient

The linear absorption coefficient is used to define the mass absorption coefficient  $\mu_m$

$$\text{where } \mu_m = \left(\frac{\mu}{\rho}\right)_\lambda \quad (6)$$

The linear absorption coefficient can be calculated if the chemical composition and density of the crystal and the mass absorption coefficients of every element in the crystal are known.

$$\text{i.e.} \quad \mu_{\lambda} = \rho \sum_n \left( \frac{P_n}{100} \right) (\mu_m)_{\lambda, E_n} \quad (7)$$

where  $\rho$  = density of the crystal (1,75 gm/cm<sup>3</sup>)

$P_n$  = percentage by weight of each element in the crystal

$(\mu_m)_{\lambda, E_n}$  = mass absorption coefficient for each element  $E_n$ , at a given wavelength (1,5418 Å).

The following values of  $\mu_m$  were used in the calculation

$$\mu_m (\text{Fe}) = 308 \text{ cm}^2/\text{gm}$$

$$\mu_m (\text{Ag}) = 218 \text{ cm}^2/\text{gm}$$

$$\mu_m (\text{Cl}) = 106 \text{ cm}^2/\text{gm}$$

$$\mu_m (\text{O}) = 11,5 \text{ cm}^2/\text{gm}$$

$$\mu_m (\text{C}) = 4,6 \text{ cm}^2/\text{gm}$$

$$\mu_m (\text{H}) = 0,435 \text{ cm}^2/\text{gm}$$

Insertion of these values into Equation 7 yielded

$$\mu_{\lambda} = 147,6 \text{ cm}^{-1}$$

The optimum thickness  $t$ , for a crystal to be used in data collection is given by the equation

$$t = \frac{2}{\mu_{\lambda}} \quad (8)$$

Hence  $t = 0,014 \text{ cm}$ .

All the crystals that were prepared were plate-like and had unequal dimensions. The crystals were fragile and could not be spherically ground. In order to minimize absorption effects a small crystal having dimensions 0,030 cm x 0,020 cm x 0,005 cm was chosen for data collection.

The average radius of this crystal for rotation about the 'b' axis was 0,085 cm. Hence  $\mu R = 1,3$ .

The absorption correction  $A^*$  for  $\mu R = 1,3$  varied from

7,96 at  $\theta = 0^\circ$  to 4,27 at  $\theta = 90^\circ$ . Although this change was significant the structure analysis was carried out without any absorption correction being made. Absorption effects were minimized by the choice of a small crystal.

(ii) The Alignment of the Crystal

Due to the shape of the crystal it was not possible to align the crystal optically.

The crystal was accurately aligned by the method described by Weisz and Cole<sup>53</sup>. In this method a composite photograph of a stationary crystal was taken using unfiltered radiation. The crystal was initially irradiated with the one goniometer arc parallel to the X-ray beam. The crystal was then rotated through  $180^\circ$  and exposed to X-radiation for a period that was twice as long as the initial irradiation.

From the composite cylindrical Laue photograph obtained, the errors in the two goniometer arcs were calculated. The arcs were adjusted accordingly.

(iii) Measurement of the Intensities

A crystal having the dimensions 0,030 x 0,020 x 0,005 cm was selected for data collection. The crystal was mounted at the end of a glass rod with the Y axis parallel to the oscillation axis. It was aligned by the method outlined above. By virtue of the space group, oscillation of the crystal about this axis yielded the greatest number of non-equivalent reflections.

A non-integrating Weissenberg goniometer was used and the data collected by the multiple film method<sup>54</sup>. In this method a pack of four photographic films was used for each X-ray photograph instead of a single film. Each film of the pack acted as an absorber of the radiation and reduced the

the X-ray reflection intensities on the underlying film by a factor  $f$ . The intensities of the strongest reflections were measured from spots on films of the pack farthest from the crystal and the weak reflections were estimated from the spots on the films nearest the crystal. The intensities of all the reflections were scaled up so as to get the final values of all the intensities on one film. The film factors  $f$  were found to vary between 2,20 to 2,33 and an average value was taken for scaling purposes.

The zero and upper layer intensities were collected by the equi-inclination technique<sup>55</sup>. Data was collected from the  $h0l$ ,  $h1l$ ,  $h2l$ ,  $h3l$ ,  $h4l$  and  $h5l$  layer lines.

All the spots were assigned Miller Indices and their intensities measured visually with the aid of an intensity strip<sup>56</sup>. The intensity strip contained a series of spots whose relative intensities were known. This strip was constructed in the following manner. A beam of X-rays was allowed to fall on a film for 'a' seconds. The film was then shifted and re-irradiated for 'ar' seconds, then after displacing the film again for 'ar<sup>2</sup>' seconds etc. A value of  $r = \sqrt{2}$  was chosen as this gave a sufficiently good graded series of spots in which the intensity of a spot for exposure 'ar' seconds was just distinguishably greater than the intensity of the spot made in 'a' seconds.

A total of 1102 reflections was measured by comparison with the spots on the intensity strip. 101 weak reflections were discarded (see Section IIh, page 59) leaving 1001 reflections for the final refinement.

The observed intensities were punched onto computer cards and corrected for geometric and physical factors.

## Ih. CORRECTION OF THE INTENSITIES

The program "COREC" was used to correct the intensities for the following factors.

- a) Spot-splitting and Spot Shape<sup>57</sup>
- b) Lorentz and polarisation factors<sup>58</sup>

No attempt was made at this stage to scale the intensities of the different layer lines. It was decided to allow the scaling to be automatically performed in the least squares refinement.

No correction was made for absorption [see Section 4.2 I(g)].

## II. SOLVING THE STRUCTURE

### IIa. THE PATTERSON SYNTHESIS

The Patterson synthesis provides a method whereby the positions of the heavy atoms in the unit cell may be located without a prior knowledge of the phases.

The Patterson function<sup>59</sup>,

$$P(u,v,w) = \sum_{h=-\infty}^{\infty} \sum_{k=-\infty}^{\infty} \sum_{l=-\infty}^{\infty} F_0^2 \cos 2\pi (hu + kv + lw) \quad (9)$$

is a Fourier summation which is carried out using the phaseless quantities  $F_0^2$  as coefficients

where  $F_0^2$  = observed intensity of an  $h, k, l$  reflection

$u, v, w$  = fractional coordinates of the Patterson cell.

Whereas a Fourier synthesis uses the phase dependent structure factors,  $F_0$ , as coefficients and shows the distribution of electron density in the unit cell, the Patterson function is calculated with  $F_0^2$  values as coefficients and has peaks corresponding to all the interatomic vectors.

Thus for a pair of points in real space having coordinates  $(x_1, y_1, z_1)$  and  $(x_2, y_2, z_2)$  there exists a peak at a point

(u,v,w) in vector space such that

$$u = x_2 - x_1$$

$$v = y_2 - y_1$$

$$w = z_2 - z_1$$

If there are N molecules in the unit cell there are  $N^2$  vector peaks in the Patterson map. N of these are found at the origin and correspond to the vectors from each atom to itself. The remaining  $N(N-1)$  vectors are distributed throughout the Patterson cell.

The volume V of each peak depends on the number of electrons and the scattering angle  $\theta$  associated with each of the two atoms between which the vector is defined.

For zero scattering angle the volume of the peak V is given by

$$V = k Z_i Z_j \quad (10)$$

where  $Z_{i,j}$  are the atomic numbers of atoms i and j, and k is a proportionality constant.

It must be pointed out that the peak height is not a completely true measure of the peak volume<sup>60</sup>. However peak heights are commonly used as an approximation of their volumes.

The importance of the peak height relationship is that the vector peaks created by the heavy atom interactions stand out strongly against the background of heavy-light and light-light atom interactions.

A Patterson peak has a broader base than an electron density peak<sup>60</sup> and as the cell of the Patterson synthesis has the same size as the true unit cell the peaks on a Patterson map are more densely packed. This tends to create a good deal of peak overlap. The result of this overlap is that the

light atom interactions are generally swamped by the background. On the other hand peaks which do stand out may be accentuated by the overlap of peaks from other interactions. For these reasons, when atom interactions are originally being located on Pattersons maps, not too much importance must be given to the heights of the peaks.

From the heavy atom interactions generated on Patterson maps it is possible to deduce the positional coordinates of the heavy atom in real space. Once the position of the heavy atom is known, lighter atoms may be discovered by successive Fourier syntheses. [See Section IIId. page 42].

#### I Ib. THE LOCATION OF THE SILVER ION

##### Computation of the Patterson Map

As the intensity for a given reflection is proportional to  $F_o^2$ , a three dimensional Patterson map for the whole unit cell was computed using the corrected observed intensities. The program "CENTROSY" was used for this purpose.

The space group  $P2_1/c$  demands that the four equivalent atoms of the four molecules in the unit cell are to be found in the equivalent positions<sup>61</sup>:

$$x, y, z; \bar{x}, \bar{y}, \bar{z}; \bar{x}, \frac{1}{2}+y, \frac{1}{2}-z; x, \frac{1}{2}-y, \frac{1}{2}+z;$$

The 4 x 4 positions of the vector peaks arising from Ag - Ag interactions were derived in terms of the coordinates of the equivalent positions. These are shown in Table VI.

TABLE VI

ATOMIC POSITION	1 $x, y, z$	2 $\bar{x} \bar{y} \bar{z}$	3 $x, \frac{1}{2}y, \frac{1}{2}z$	4 $x, \frac{1}{2}y, \frac{1}{2}z$
1' $x, y, z$	1-1' $0, 0, 0$	2-1' $-2x, -2y, -2z$	3-1' $-2x, \frac{1}{2}, \frac{1}{2}-2z$	4-1' $0, \frac{1}{2}-2y, \frac{1}{2}$
2' $\bar{x}, \bar{y}, \bar{z}$	1-2' $2x, 2y, 2z$	2-2' $0, 0, 0$	3-2' $0, \frac{1}{2}+2y, \frac{1}{2}$	4-2' $2x, \frac{1}{2}, \frac{1}{2}+2z$
3' $\bar{x}, \frac{1}{2}y, \frac{1}{2}z$	1-3' $2x, -\frac{1}{2}, -\frac{1}{2}+2z$	2-3' $0, -\frac{1}{2}-2y, -\frac{1}{2}$	3-3' $0, 0, 0$	4-3' $2x, -2y, 2z$
4' $x, \frac{1}{2}y, \frac{1}{2}z$	1-4' $0, -\frac{1}{2}+2y, -\frac{1}{2}$	2-4' $-2x, -\frac{1}{2}, -\frac{1}{2}-2z$	3-4' $-2x, 2y, -2z$	4-4' $0, 0, 0$

### The Height of the Origin Peak

The origin peak consists of all the peaks created by vectors from each atom to itself. The peak at the origin is thus given by the equation

$$V(0,0,0) = k \sum_{i=1}^N z_i^2$$

(11)

Disregarding the water molecule, the theoretical height of the origin peak was calculated in the following way.

For one molecule the height of the peak is given by

$$\begin{aligned}
 1 \times \text{Ag} - \text{Ag} &= 1 \times 46^2 = 2116 \\
 1 \times \text{Fe} - \text{Fe} &= 1 \times 26^2 = 676 \\
 1 \times \text{Cl} - \text{Cl} &= 1 \times 18^2 = 324 \\
 10 \times \text{O} - \text{O} &= 10 \times 8^2 = 640 \\
 15 \times \text{C} - \text{C} &= 15 \times 6^2 = 540 \\
 21 \times \text{H} - \text{H} &= 21 \times 1^2 = \underline{21} \\
 &4317
 \end{aligned}$$

As there are four molecules in the unit cell the height of the origin peak has the theoretical height of  $4317 \times 4 = 17268$ .

From the Patterson map obtained, the origin peak was observed to have a height of 1733. This gave a conversion factor from theoretical peak height to expected peak height on the map as  $\frac{1733}{17268} = 0,1027$ .

From Table VI equivalent Patterson peaks were singled out and their general positions listed in Table VII. The multiplicity, theoretical and experimentally found peak heights have also been tabulated.

Two models based on two interpretations of the Patterson map have been given in terms of possible Ag-Ag interactions.

The molecule  $\text{Fe}(\text{acac})_3 \cdot \text{AgClO}_4 \cdot \text{H}_2\text{O}$  contains two heavy atoms, viz. Ag and Fe. The three major peaks in the Patterson map are therefore expected to be due to silver to silver, iron to iron, and silver to iron interactions.

The theoretical magnitude of the peak due to a single Ag-Ag interaction will be  $46 \times 46 = 2116$ , due to two Ag-Ag

interactions  $2 \times 2116 = 4232$  etc. The magnitudes of a single Fe-Fe peak and a Ag-Fe peak are 676 and 1196 respectively. These values must be reduced by the map factor of 0,1027 to put them onto the Patterson map scale.

The Ag-Ag peak being the largest theoretical peak is therefore expected to be the most pronounced peak on the Patterson map.

TABLE VII

POSSIBLE Ag - Ag INTERACTIONS

Patterson Peak Co-ordinates	Multiplicity	Theoretical Peak Height (scaled to origin height = 1733)	Experimentally Found MODEL I	Experimentally Found MODEL II
0,0,0	4	1733	1733	1733
$0, \frac{1}{2}, -2y, \frac{1}{2}$	2	434	772	772
$0, \frac{1}{2}, +2y, \frac{1}{2}$	2	434	772	772
$2x, \frac{1}{2}, \frac{1}{2} + 2z$	2	434	529	473
$-2x, \frac{1}{2}, \frac{1}{2} - 2z$	2	434	529	473
$2x, 2y, 2z$	1	217	302	222
$-2x, -2y, -2z$	1	217	302	222
$2x, -2y, 2z$	1	217	302	222
$-2x, 2y, -2z$	1	217	302	222

IIc. MODEL I

A Ag-Ag peak of multiplicity two was sought, having coordinates of the type  $0, \frac{1}{2}-2y, \frac{1}{2}$ . A large peak of magnitude 772 was located at the position 0,30,50, where the figures denote hundredths of the unit cell lengths. This was the largest peak on the Patterson map.

$$\text{Hence } \frac{1}{2} - 2y = \frac{30}{100}$$

$$\text{and } y = \frac{10}{100}$$

A peak having the general coordinates  $2x, \frac{1}{2}, \frac{1}{2}+2z$  was then sought. Two large peaks satisfied these coordinates. A peak of magnitude 529 was located at 18,50, 42 and another of magnitude 473 at 68, 50, 10. Both of these peaks were confirmed by rotation peaks having coordinates of the type  $2x, 2y, 2z$ .

At this stage there was no indication as to which of these two peaks represented the true Ag-Ag interaction. Both peaks were seen to have magnitudes close to the theoretical peak height of 434. For Model I it was decided to use the larger of the two peaks, as Ag-Ag interactions were expected to yield the largest peaks. The next section concerns the interpretation of the Patterson map using Model I. Model II is discussed in Section IIe on page 48.

The peak found at 18, 50, 42 corresponding to the coordinates  $2x, \frac{1}{2}, \frac{1}{2}+2z$  yielded the values

$$x = \frac{9}{100} \quad \text{and} \quad z = \frac{46}{100}$$

The position of the silver atom therefore had the coordinates 0,09, 0,10, 0,46.

Using the position of the silver atom a Fourier Map was calculated and an attempt made to locate the lighter atoms in the unit cell.

### IIId. LOCATION OF ATOMS BY FOURIER METHODS

#### (i) The scattering factor, $f_j$ .

The scattering power of an atom varies with the glancing angle  $\theta$  and decreases with values of  $\sin \theta / \lambda$ . For  $\theta = 0^\circ$  the scattering power is equal to the number of electrons possessed by the atom and is denoted by  $f_0$ .

Atoms in crystals are continually oscillating with appreciable amplitude from their rest positions. The effect of this motion is to alter the scattering power of the atom by multiplying  $f_0$  by a factor  $\exp - B(\sin^2 \theta) / \lambda^2$ .

$$\text{i.e. } f_j = f_0 e^{-B(\sin^2 \theta) / \lambda^2} \quad (12)$$

$B$ , the isotropic temperature factor is a parameter dependent on the magnitude of the vibration and is given by

$$B = 8\pi \bar{u}^2 \quad (13)$$

Where  $\bar{u}^2$  is the mean square displacement of the atoms from their rest positions.

In the initial stages of the structural investigation, all atoms that were placed in Fourier maps were assigned an arbitrary value of 3 for the isotropic temperature factor. These values were only changed on refining the structure.

In this investigation scattering factor tables<sup>63</sup> of Pd ( $Z = 46$ ) were used for silver. This was due to the fact that Ag ( $Z = 47$ ) in  $\text{AgClO}_4$  is found in the ionic state  $\text{Ag}^+$  ( $Z = 46$ ). For similar reasons scattering factor tables of Argon ( $Z = 18$ ) were used for chlorine. Normal scattering factor tables were employed for Fe ( $Z = 26$ ), O ( $Z = 8$ ) and C ( $Z = 6$ ). Scattering by the hydrogen atoms was not considered.

#### (ii) The Structure Factor, $F_{hkl}$ .

The structure factor  $F_{hkl}$ <sup>64</sup> is given by the expression

$$F_{hkl} = \sum f_j e^{2\pi i(hx+ky+lz)} \quad (14)$$

and is defined as the resultant of the  $j$  waves scattered in the direction  $hkl$  by the  $j$  atoms in the unit cell.

The magnitude of  $F_{hkl}$  is dependent on the scattering power and position of each atom, and its sign depends on the phase of the resultant wave.

(iii) The Fourier Synthesis<sup>65</sup>

The general expression used for calculating the electron density  $\rho$  at a point  $(x,y,z)$  in the unit cell is given by the exponential function,

$$\rho(x,y,z) = \frac{1}{V} \sum_{hkl} F_{hkl} e^{-2\pi i(hx+ky+lz)} \quad (15)$$

where  $V$  is the volume of the unit cell, and  $F_{hkl}$  is the structure factor.

Before the structure can be determined, it is necessary to have some knowledge of the phases of the resultant waves.

Initially the phases used are those given by the structure factors calculated from the position of the heavy atom alone, since the heavy atom controls to a large extent the phases of the structure factors for the complete model.

When the calculated phases are combined with the observed  $F_o$  values an electron density map is computed which has a resemblance to the electron density map of the true structure.

From this map new atomic parameters are assigned, new structure factors calculated, and a further knowledge of the phases obtained. In this way more accurate electron density maps are constructed. This process is continued until a satisfactory solution to the structure is achieved.

The accuracy of the structure is reflected in the value of the residual index  $R^{66}$ , where

$$R = \frac{\sum |\Delta F|}{\sum |F_o|} = \frac{\sum ||F_o| - |F_c||}{\sum |F_o|} \quad (16)$$

The lower the value of  $R$ , the more accurate the model is considered to be in terms of the true structure. When  $R \ll 0,25$  it is generally accepted that the structure is correct although small shifts in atomic and thermal parameters are still required.

Using the position of the silver ion obtained from the Patterson map, and scattering factor tables<sup>63</sup> for Pd ( $Z = 46$ ), structure factors were calculated and an electron density map computed for the whole unit cell. The program "CENTROSY" was also used for this purpose.

The value of  $R$  was 0,45 which was not significant at this stage.

The expected silver peak at 0,09, 0,10, 0,46 had a peak height of 997. An attempt was now made to locate the iron atom. As this was also a heavy atom it was expected to stand out strongly in the Fourier map. As the iron atom contains about half as many electrons as the silver ion, the peak due to the iron atom was expected, as a rough approximation, to be about half the size of the silver peak.

The Fourier map was scanned and a large peak of magnitude 371 located at 42 60 36. No other large peaks were found.

Although the ratio  $\frac{997}{371} = 2,69$  did not correspond well with ratio of the number of electrons associated with the silver ion and iron atom, viz.  $\frac{46}{26} = 1,77$ , it was decided that the peak of 371 was most likely an iron peak.

In order to check the validity of this assignment, iron

to iron, and all silver to iron interactions were calculated and the resulting vector peaks sought for on the Patterson map. The vector peaks due to these interactions are tabulated in Tables VIII, IX and X.

Table VIII lists all the Fe-Fe interactions and is drawn up in the same way as the Ag-Ag interactions were in Table VII.

Table IX shows the computation of all possible Ag-Fe and Fe-Ag interactions between the four silver atoms and the four iron atoms in a single unit cell. A Ag-Fe interaction at a point  $(x, y, z)$  has an equivalent Fe-Ag interaction at  $(-x, -y, -z)$ . Both sets of interactions have been tabulated so as to show how the total multiplicity of a silver to iron interaction at any one point in the unit cell is obtained.

The positions and multiplicities of identical peaks in Table IX have been reported in Table X. The theoretical and experimentally found peak heights of silver to iron interactions have also been tabulated.

From Table VIII there appears to be no direct correlation between the electron density peaks on the Fourier map and the vector peaks on the Patterson map created by the Fe-Fe interactions. Correlations between the Fourier peaks and vector peaks of silver to iron interactions were good although peak heights varied from 185 to 312 for peaks of multiplicity 2 (Table X).

The peak at  $0, \frac{1}{2} - 2y, \frac{1}{2}$  on the Patterson map due to the Fe-Fe interaction was seen to overlap the Ag-Ag peak (see Tables VII and VIII). Although large peaks were found at the appropriate Patterson positions for silver to iron interactions no confirmation of the Fe-Fe interactions was evident at the Patterson positions  $2x, \frac{1}{2}, \frac{1}{2} + 2z$  and  $2x, 2y, 2z$ .

TABLE VIII

## Fe - Fe INTERACTIONS

(based on the position of Fe at (0,42 0,60 0,36)).

PATTERSON PEAK POSITIONS		Multiplicity	Theoretical Peak Height (scaled to origin height=1733)	Experimentally Found
General Coordinates	Map co-ordinates (hundredths of the unit cell lengths)			
0,0,0	0, 0, 0	4	1733	1733
$0, \frac{1}{2}-y, \frac{1}{2}$	0 30 50	2	138	772
$0, \frac{1}{2}+y, \frac{1}{2}$	0 70 50	2	138	772
$2x, \frac{1}{2}, \frac{1}{2}+2z$	84 50 22	2	138	-40
$-2x, \frac{1}{2}, \frac{1}{2}-2z$	16 50 78	2	138	-40
$2x, 2y, 2z$	84 20 72	1	69	10
$-2x, -2y, -2z$	16 80 28	1	69	10
$2x -2y 2z$	84 80 72	1	69	10
$-2x 2y -2z$	16 20 28	1	69	10

In spite of the fact that Patterson peaks were not present for some Fe-Fe interactions, the iron atom was placed at 0,42, 0,60, 0,36 and a second Fourier computed. The residual factor dropped rather insignificantly to 0,43.

At this stage a difference Fourier\* with the iron and silver atoms subtracted was computed. From the Fourier map obtained a three dimensional model incorporating all the major peaks was constructed.

\*

For a brief discussion on the Difference Fourier see page 53.

No peaks were found that resembled any acetylacetonate ring in the vicinity of the iron atom, nor was it possible to locate a perchlorate ion.

It was decided at this stage to abandon work on this model and to attempt a different interpretation of the Patterson map.

TABLE IX  
SILVER TO IRON INTERACTIONS  
(based on Ag at 9,10,46 and Fe at 42,  
60,36 and their equivalent positions).

Ag - Fe INTERACTIONS														
			Ag (1)			Ag (2)			Ag (3)			Ag (4)		
			9	10	46	9	40	96	91	90	54	91	60	4
Fe (1)			406			185			312			499		
42	60	36	67	50	10	67	80	60	49	30	18	49	0	68
Fe (2)			312			499			473			222		
58	40	64	51	70	82	51	0	32	33	50	90	33	20	40
Fe (3)			185			406			499			312		
42	90	86	67	20	60	67	50	10	49	0	68	49	70	18
Fe (4)			499			312			222			473		
58	10	14	51	0	32	51	30	82	33	80	40	33	50	90
Fe - Ag INTERACTIONS														
			Fe (1)			Fe (2)			Fe (3)			Fe (4)		
			42	60	36	58	40	64	42	90	86	58	10	14
Ag (1)			473			312			222			499		
9	10	46	33	50	90	49	30	18	33	80	40	49	0	68
Ag (2)			222			499			473			312		
9	40	96	33	20	40	49	0	68	33	50	90	49	70	18
Ag (3)			312			406			499			185		
91	90	54	51	70	82	67	50	10	51	0	32	67	20	60
Ag (4)			499			185			312			406		
91	60	4	51	0	32	67	80	60	51	30	82	67	50	10

For each interaction the top figure represents the peak height. The bottom figures are the positional coordinates of the peak in hundredths of the unit cell lengths.

TABLE X

SILVER TO IRON INTERACTIONS

(derived from Table IX)

Peak Coordinates (hundredths of the unit cell lengths)	Multiplicity	Theoretical Peak Height (scaled to Origin Height = 1733)	Experimentally Found
49 0 68	4	492	499
51 0 32	4	492	499
33 50 90	4	492	473
67 50 10	4	492	406
49 30 18	2	246	312
51 70 82	2	246	312
49 70 18	2	246	312
51 30 82	2	246	312
33 20 40	2	246	222
33 80 40	2	246	222
67 80 60	2	246	185
67 20 60	2	246	185

IIe. MODEL IIThe Patterson Map: Location of the Silver Ion.

For Model II the Patterson Map was interpreted in the following way (refer to Table VII).

The large peak of magnitude 772 at 0,30,50 having the general coordinates  $0, \frac{1}{2}-2y, \frac{1}{2}$  was interpreted as an Ag-Ag.

interaction in the same way as it was for Model I. This gave the y coordinate of the silver ion as 0,10.

As mentioned in Section IIc, two peaks having coordinates of the type  $2x, \frac{1}{2}, \frac{1}{2} + 2z$  were located. The larger of the two peaks was used for Model I.

For Model II, the peak of magnitude 473 was taken as a Ag-Ag interaction. The x and z coordinates of the silver atom were calculated. The position of the silver atom was found to be at (34 10 30). Rotation peaks of the type  $2x, 2y, 2z$  having magnitudes of 222 confirmed that the silver ion had been located in a possible atom site. In fact the correlation between theoretical and experimentally found peak heights was noted to be much better than that observed for Model I.

With the silver ion at (34 10 30) a Fourier map was computed. The value of R was 0,488 in contrast to 0,45 at this stage for Model I. This was not considered important.

The expected silver peak was found on the map to have a height of 1031. The rest of the map was scanned for a possible iron peak. The second largest peak to be found had a height of 441 and was located at (16 90 38). For this model the ratio of peak heights  $\frac{1031}{441} = 2,33$  compared slightly more favourably with the ratio  $\frac{46}{26} = 1,77$ .

Apart from the equivalent positions of this peak, no other peaks of this magnitude were found.

Assuming this peak to be the iron peak, iron to iron, and silver to iron vector peaks were calculated as they were for Model I. The theoretical and experimentally found vector peaks for Model II are listed in Tables XI, XII, and XIII.

TABLE XI

Fe - Fe INTERACTIONS

(based on the Fe atom at 16,90,38)

PATTERSON PEAK POSITIONS		Multiplicity	Theoretical Peak Height (scaled to origin height = 1733)	Experimentally Found
General Co-ordinates	Map Co-ordinates (in hundredths of the unit cell lengths)			
0, 0, 0	0, 0, 0	4	1733	1733
$0, \frac{1}{2}-2y, \frac{1}{2}$	0, 70, 50	2	138	772
$0, \frac{1}{2}+2y, \frac{1}{2}$	0, 30, 50	2	138	772
$2x, \frac{1}{2}, \frac{1}{2}+2z$	32, 50, 26	2	138	171
$-2x, \frac{1}{2}, \frac{1}{2}-2z$	68, 50, 74	2	138	171
$2x, 2y, 2z$	32, 80, 76	1	69	108
$-2x, -2y, -2z$	68, 20, 24	1	69	108
$2x, -2y, 2z$	32, 20, 76	1	69	108
$-2x, 2y, -2z$	68, 80, 24	1	69	108

All the Fe-Fe and Ag-Fe interactions resulted in peaks of considerable magnitude on the Patterson map, indicating a high probability that the positioning of the iron atom had been correct.

The Ag-Ag and Fe-Fe vector peaks at  $0, \frac{1}{2}-2y, \frac{1}{2}$  coincided with each other on the Patterson map. This overlap explained why the experimentally found peak heights for Ag-Ag and Fe-Fe interactions at this point were so much larger than their theoretical heights. Peak height correlations for the

other Ag-Ag and Fe-Fe interactions were very good (Tables VII and XI) as were the Ag-Fe interactions (Table XIII).

Using the positions of the silver ion and the iron atom a second Fourier was computed. The drop of the residual index from 0,488 to 0,399 was considered encouraging.

An attempt was made at this stage to locate the lighter atoms using a difference Fourier map.

TABLE XII

SILVER TO IRON INTERACTIONS

(based on Ag at 34 10 30 and Fe at  
16 90 38 and their equivalent positions)

Ag - Fe INTERACTIONS													
		Ag(1)			Ag(2)			Ag(3)			Ag(4)		
		34	10	30	66	90	70	34	40	80	66	60	20
84	Fe(1)	312			529			499			302		
40		50	70	18	82	50	58	50	0	68	82	20	8
12													
16	Fe(2)	529			312			302			499		
60		18	50	42	50	30	82	18	80	92	50	0	32
88													
84	Fe(3)	499			302			312			529		
10		50	0	68	82	80	8	50	30	18	85	50	58
62													
16	Fe(4)	302			499			529			312		
90		18	20	92	50	0	32	18	50	42	50	70	82
38													
Fe - Ag INTERACTIONS													
		Fe(1)			Fe(2)			Fe(3)			Fe(4)		
		84	40	12	16	60	88	84	10	62	16	90	38
34	Ag(1)	312			529			499			302		
10		50	30	82	82	50	58	50	0	32	82	80	8
30													
66	Ag(2)	529			312			302			499		
90		18	50	42	50	70	18	18	20	92	50	0	68
70													
34	Ag(3)	499			302			312			529		
40		50	0	32	82	20	8	50	70	82	82	50	58
80													
66	Ag(4)	302			499			529			312		
60		18	80	92	50	0	68	18	50	42	50	30	18
20													

For each interaction the top figure represents the peak height. The bottom figures are the positional coordinates of the peak in hundredths of the unit cell lengths.

TABLE XIIISILVER TO IRON INTERACTIONS

(derived from Table XII)

Peak Coordinates (in hundredths of the unit cell lengths)	Multiplicity	Theoretical Peak Height (scaled to origin height = 1733)	Experimentally Found
82 50 58	4	492	529
18 50 42	4	492	529
50 0 68	4	492	499
50 0 32	4	492	499
50 70 18	2	246	312
50 30 82	2	246	312
50 30 18	2	246	312
50 70 82	2	246	312
82 20 8	2	246	302
18 80 92	2	246	302
82 80 8	2	246	302
18 20 92	2	246	302

IIIf. THE MISINTERPRETATION OF THE PATTERSON MAP :

MODEL I.

From Table XIII an explanation of the Patterson peaks that were assigned to Model I can now be given.

It can be seen from Table VII that apart from the contribution to the origin peak, no Ag-Ag interaction was calculated to have a multiplicity greater than two. The theoretical height of a single Ag-Ag peak was 217, and therefore the largest Ag-Ag peak on the Patterson map had a theoretical height of 434.

On the other hand it can be seen from Table XIII that a number of Ag-Fe interactions had multiplicity factors of four. Since the theoretical height of a single Ag-Fe peak was 123, certain Ag-Fe peaks were expected to have theoretical heights of  $4 \times 123 = 492$ . This figure is in fact larger than a 2-fold Ag-Ag peak.

When the silver ion was being located in Model I, no consideration was given to the multiplicities of Ag-Fe interactions as the position of the iron atom was unknown at the time. It was therefore assumed that the largest of the two peaks having the general coordinates  $2x, \frac{1}{2}, \frac{1}{2}+2z$  would be a Ag-Ag peak.

It so happened that both a 2-fold Ag-Ag and a 4-fold Ag-Fe interaction had general coordinates of the type  $2x, \frac{1}{2}, \frac{1}{2}+2z$ . It was for these reasons that a Ag-Ag interaction had been easily misinterpreted for a Ag-Fe interaction.

IIIf. THE DIFFERENCE FOURIER

The Difference Fourier is a Fourier synthesis which is expressed in the following form<sup>6,7</sup>.

$$\Delta\rho = \frac{1}{V} \sum_{h} \sum_{k} \sum_{l} (|F_O| - |F_C|) e^{i\alpha_C} e^{-2\pi i(hx + ky + lz)} \quad (17)$$

where  $\alpha_C$  is the phase of the  $F_C$ .

This function provides a direct measure of the errors between the model and the true structure as implied by the  $F_O$ 's. In general atoms which have been correctly placed do not appear on a Difference Fourier. Those which have been misplaced appear as "holes" and those which are not placed at all appear as peaks. However holes and peaks are sometimes created even if the atoms have been correctly located. This occurs when errors in temperature parameters are assigned to the atoms.

Besides being used for the purpose of correcting the positions of those atoms already present, the difference synthesis may be employed for locating new atoms.

By subtracting out the electron density of correctly placed atoms in the structure, the peaks of other atoms are generally found to stand out more strongly, and a clearer picture of the electron density map is obtained. By subtracting out atoms, the difference synthesis also removes "ghost" peaks which sometimes occur through heavy atom interactions and are found midway between these atoms on Fourier maps<sup>68</sup>.

A Difference Fourier was computed with the silver and iron atoms omitted.

From this map the vicinity of the iron atom was scanned in an attempt to find the six oxygens of the three acetyl-acetate rings. These oxygen peaks, arranged almost octahedrally about the iron atom, were easily located. By

computing the positions of the remaining atoms of the rings all the peaks for these atoms with the exception of the methyl carbons were found.

A large peak of magnitude 118 was found which indicated the position of the chlorine atom. Ag-Cl and Fe-Cl interactions based on the positions of these atoms for this model were calculated. Peaks on the Patterson map confirmed the assignment of the positions for these atoms.

An attempt was made to locate the perchlorate oxygens. However the section of the map around the chlorine atom was crowded with diffuse peaks. Instead of assigning the most probable peaks to the oxygen atoms it was decided to compute another Fourier map, this time including all the ring atoms in the phasing model.

Table XIV shows the results of the Difference Fourier based on the known positions of the Ag and Fe atoms with both atoms subtracted.

TABLE XIV  
RESULTS OF THE DIFFERENCE FOURIER

ATOM	PEAK COORDINATES (in hundredths of the unit cell lengths)			PEAK HEIGHT
Ag	34	10	30	-146
Fe	16	90	38	-123
C1	38	0	14	118
O1	0	88	36	81
C2	96	88	42	45
C3	4	84	52	38
C4	18	86	56	49
O2	22	80	50	58
O3	16	72	34	51
C7	26	66	36	54
C8	38	70	40	28
C9	40	84	40	53
O4	34	90	40	85
O5	8	92	24	77
C12	10	6	22	27
C13	14	12	26	40
C14	16	14	34	34
O6	16	6	38	103

Insertion of the ring atoms into the next Fourier resulted in a drop of R to 0,331. From this map the methyl carbons were easily located. Only three perchlorate oxygen atoms were found. Using these three peaks the theoretical position of the fourth oxygen peak was calculated. This peak was seen to be hidden by the chlorine peak which appeared to be elongated in the direction of the 'y' axis.

A final Fourier was computed using the coordinates of all the atoms known and the calculated coordinates for the one perchlorate oxygen. The residual index fell to 0,286. The atomic parameters of the 28 atoms at this stage are listed in Table XV. The labelling system for the atoms is shown in Figs. 12 and 13.

TABLE XV

ATOM	POSITIONAL COORDINATES		
	X	Y	Z
Ag	0,34	0,10	0,30
Fe	0,16	0,90	0,38
C1	0,82	0,82	0,38
C2	0,96	0,88	0,42
C3	0,04	0,84	0,52
C4	0,18	0,86	0,56
C5	0,24	0,84	0,66
C6	0,24	0,52	0,33
C7	0,26	0,66	0,36
C8	0,38	0,70	0,40
C9	0,40	0,84	0,40
C10	0,54	0,88	0,42
C11	0,04	0,00	0,12
C12	0,10	0,06	0,22
C13	0,14	0,12	0,26
C14	0,16	0,14	0,34
C15	0,16	0,30	0,38
O1	0,00	0,88	0,36
O2	0,22	0,88	0,50
O3	0,16	0,72	0,34
O4	0,34	0,90	0,40
O5	0,08	0,92	0,24
O6	0,16	0,06	0,38
*O7	0,38	0,15	0,14
O8	0,34	0,94	0,20
O9	0,28	0,90	0,06
O10	0,50	0,94	0,16
Cl	0,38	0,00	0,14

\*The coordinates of this atom were calculated.

Using all the twenty eight known atomic parameters a three dimensional model of the unit cell was constructed (Fig. 10).

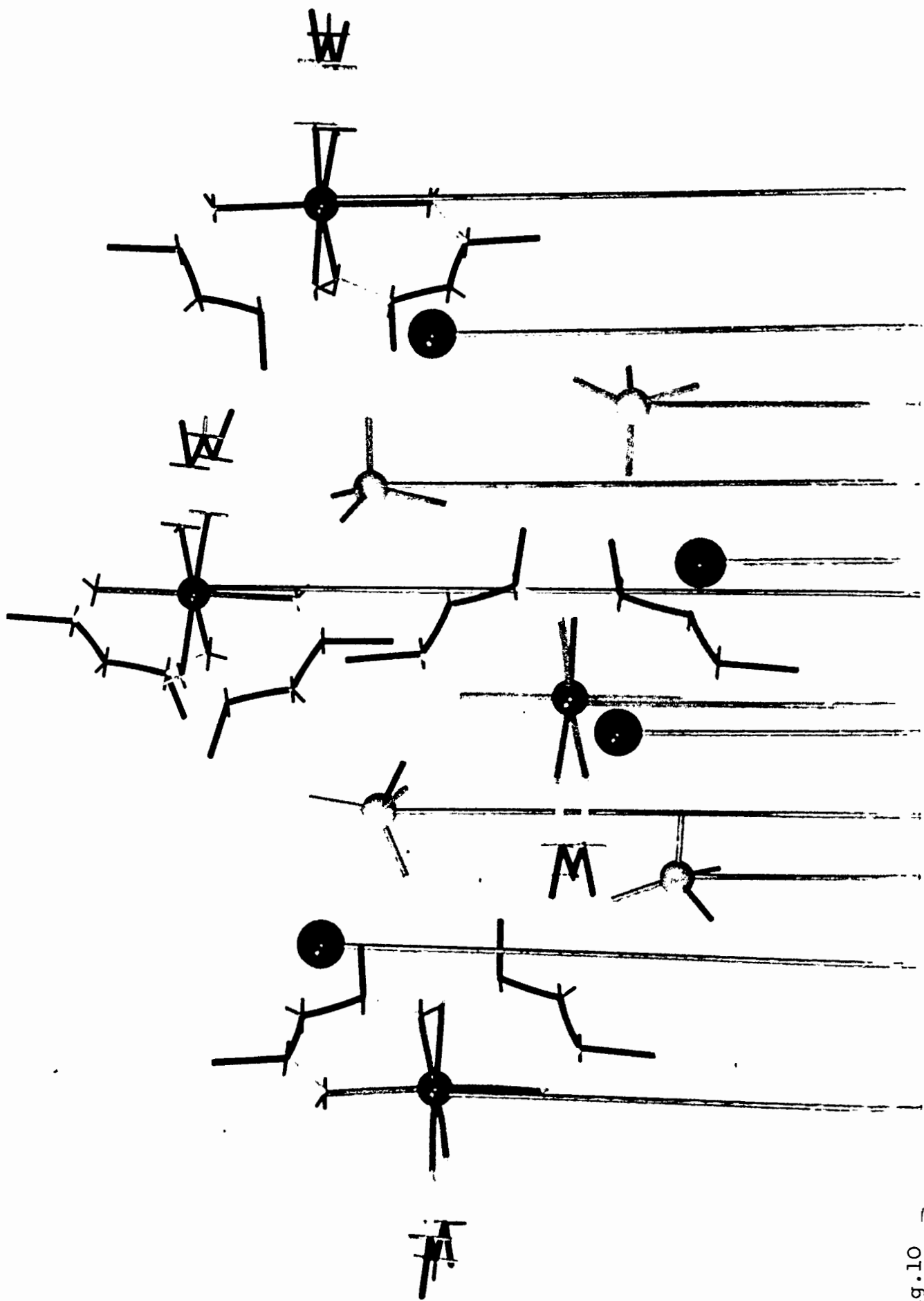


Fig.10

IIh. REFINEMENT OF THE STRUCTURE

The structure was refined by the method of least squares<sup>6,9</sup> using the program ORFLS.

All atoms were initially given an arbitrary value of  $3 \text{ \AA}^2$  for the isotropic temperature factor. The overall B was also assigned this value.

As six layer lines had been used for collecting the intensity data ( $h0l$  to  $h5l$ ) the first three cycles of refinement were used to refine the six scale factors and the overall B. At the end of the third cycle R was 0,274.

The isotropic temperature factors were varied with the positional parameters and after six cycles R had been reduced to 0,178. By the end of the sixth cycle shifts in both the positional parameters and the isotropic B values were very small. Continued refinement of these parameters would not have lowered the value of R any further.

The isotropic temperature factors of all the atoms except the perchlorate oxygens had values varying between  $1,6 \text{ \AA}^2$  and  $4,7 \text{ \AA}^2$  at the end of the sixth cycle. The B values of the perchlorate oxygen atoms had values ranging between  $9,5 \text{ \AA}^2$  and  $18,0 \text{ \AA}^2$ . These were considered alarmingly high. However similar magnitudes for the isotropic B's of perchlorate oxygens in other structures have been reported<sup>7,21</sup>. These high values have been attributed to the large thermal motion of these atoms.

The positional parameter shifts for these atoms was accordingly found to be somewhat larger than the shifts observed for the other atoms in the structure.

High B values are sometimes an indication that an atom has been misplaced. It seemed unlikely that this was so for the perchlorate oxygens as they were found to be arranged

more or less tetrahedrally around the chlorine atom as expected. Changes in their positional parameters were also seen to be very small.

However as a check on the coordinates of these four oxygen atoms, a difference Fourier was computed without using these oxygen atoms in the structure factor calculations. All of the twenty four atoms that were used in the structure factor calculations were subtracted. Four peaks corresponding to the perchlorate oxygens appeared in their expected positions.

Before carrying on with the refinement process, it was decided to discard some of the very weak reflections as their intensities could not be very accurately measured. This was justified as large errors in intensity measurements of reflections greatly affect the accuracy of the final structure.

Values of  $F_O$  and  $F_C$  were computed. For those reflections where there was found to be a great difference between  $F_O$  and  $F_C$  the ratio  $F_O/F_C$  was calculated.

If either of the conditions,

$$F_O/F_C < 0,50$$

or

$$F_O/F_C > 1,50,$$

indicating an error of fifty per cent or more between  $F_O$  and  $F_C$ , was seen to hold, then the intensities of these reflections were remeasured on the original photographs.

One hundred and forty reflections were remeasured and corrected for the factors described in Section 1h (page 35). One hundred and one reflections were still found to obey the above conditions and were therefore discarded.

One thousand and one reflections were used in the final stages of refinement. Three more cycles of isotropic least

squares refinement were carried out and the residual dropped to 0,151.

Thus nine cycles of isotropic least squares refinement were executed. Fig. 11 shows the variation of B with the number of cycles of refinement. The slight jump in B observed for all atoms after the sixth cycle arises as a result of removing the one hundred weak reflections from the data pack.

Anisotropic temperature factors were applied only to the heavy atoms Ag, Fe, and Cl. For anisotropic vibration the isotropic temperature factor B is replaced by six parameters  $\beta_{11}$ ,  $\beta_{22}$ ,  $\beta_{33}$ ,  $\beta_{12}$ ,  $\beta_{13}$ ,  $\beta_{23}$  which describe the size and orientation of the vibration ellipsoid.

For anisotropic vibration the temperature factor,  $T_{hkl}$ , is given by the expression<sup>7a</sup>

$$T_{hkl} = \exp [-(\beta_{11}h^2 + \beta_{22}k^2 + \beta_{33}l^2 + 2\beta_{12}hk + 2\beta_{13}hl + 2\beta_{23}kl)]$$

After three cycles of anisotropic least squares refinement had been applied to the heavy atoms, R reached its final value of 0,134. By this time all parameters had ceased to oscillate appreciably about their mean positions.

No attempt was made to locate the hydrogen atoms. (see Section 5.7).

### III. THE HYDRATE MOLECULE

It was not known at this stage whether one or more hydrate molecules were present in the structure or not. In an attempt to locate any such molecules, a difference Fourier was computed, subtracting out all the atoms except for a reference perchlorate oxygen peak.

The Fourier map was featureless except for the reference peak which had a height of 52, and another peak of magnitude 58 located at 50, 20, 38. As the peak heights compared

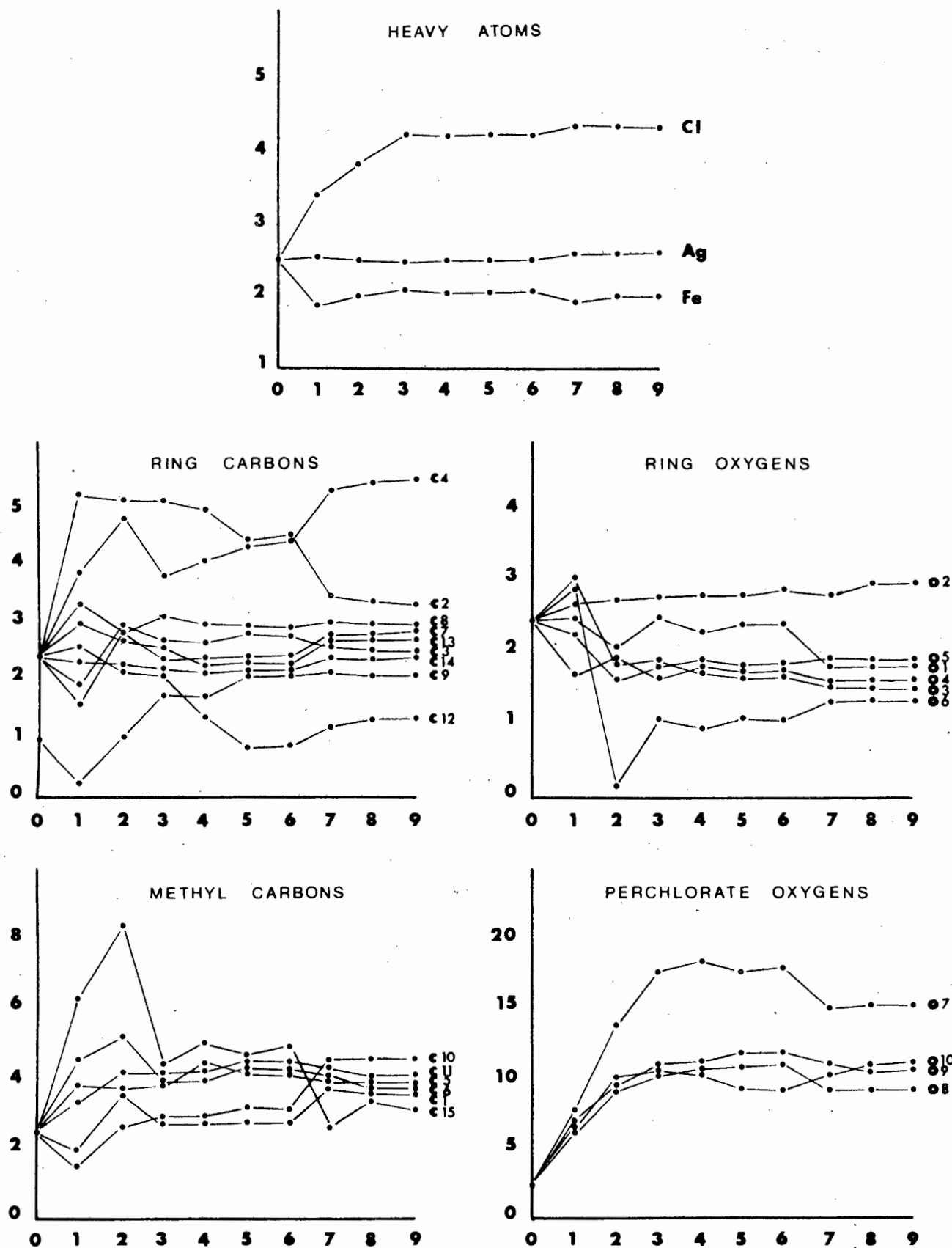


FIG. 11

The variation of the isotropic temperature factor,  $B$ , of each atom with the number of cycles of least squares refinement.

TABLE XVI

## FINAL ATOMIC FRACTIONAL COORDINATES AND THERMAL PARAMETERS (VISUAL DATA)

ATOM	x	y	z	B <sub>11</sub>	B <sub>22</sub>	B <sub>33</sub>	B <sub>12</sub>	B <sub>13</sub>	B <sub>23</sub>	ISOTROPIC B Å <sup>2</sup>
Ag	.34103 31	.09814 51	.30445 25	517 29	515 196	375 20	-60 48	217 20	-1 36	2,60
Fe	.15973 50	.89109 105	.37858 40	384 52	520 272	228 34	-74 78	123 35	30 61	1,99
C1	.37724 127	.99050 207	.13872 96	821 133	1456 391	499 82	156 165	348 90	67 124	4,39
C <sub>1</sub>	.82121 466	.84476 574	.38151 338	-	-	-	-	-	-	3,75
C <sub>2</sub>	.95544 444	.85479 580	.41754 327	-	-	-	-	-	-	3,39
C <sub>3</sub>	.04557 411	.85007 530	.51468 300	-	-	-	-	-	-	2,67
C <sub>4</sub>	.15872 585	.85293 693	.54720 426	-	-	-	-	-	-	5,66
C <sub>5</sub>	.25784 477	.84785 585	.65691 350	-	-	-	-	-	-	4,01
C <sub>6</sub>	.24784 460	.57499 764	.35139 336	-	-	-	-	-	-	3,81
C <sub>7</sub>	.26332 432	.69734 744	.36623 306	-	-	-	-	-	-	2,82
C <sub>8</sub>	.38376 423	.70889 682	.39195 307	-	-	-	-	-	-	2,97
C <sub>9</sub>	.41342 388	.83139 601	.40613 278	-	-	-	-	-	-	2,07
C <sub>10</sub>	.54023 477	.89995 723	.42254 353	-	-	-	-	-	-	4,74
C <sub>11</sub>	.02558 474	.00740 624	.10550 341	-	-	-	-	-	-	4,02
C <sub>12</sub>	.08128 343	.01439 580	.21672 271	-	-	-	-	-	-	1,33
C <sub>13</sub>	.12909 407	.13595 594	.24985 309	-	-	-	-	-	-	2,84
C <sub>14</sub>	.15403 407	.14678 625	.34688 340	-	-	-	-	-	-	2,60
C <sub>15</sub>	.16992 456	.24506 709	.38329 356	-	-	-	-	-	-	3,20
O <sub>1</sub>	.99242 222	.86379 330	.36431 171	-	-	-	-	-	-	1,81
O <sub>2</sub>	.23717 265	.86566 359	.51602 194	-	-	-	-	-	-	2,95
O <sub>3</sub>	.17102 228	.73029 384	.35501 170	-	-	-	-	-	-	1,48
O <sub>4</sub>	.32690 210	.91655 346	.39293 156	-	-	-	-	-	-	1,59
O <sub>5</sub>	.07443 221	.92614 379	.24475 173	-	-	-	-	-	-	1,85
O <sub>6</sub>	.15244 217	.05792 401	.39242 171	-	-	-	-	-	-	1,34
O <sub>7</sub>	.34325 733	.10181 919	.10659 547	-	-	-	-	-	-	15,19
O <sub>8</sub>	.35377 490	.94620 549	.20642 367	-	-	-	-	-	-	9,39
O <sub>9</sub>	.27910 556	.91387 674	.06973 401	-	-	-	-	-	-	10,91
O <sub>10</sub>	.49549 568	.95051 605	.14781 392	-	-	-	-	-	-	11,19
O <sub>11</sub>	.50000 -	.20000 -	.38000 -	This position was unrefined			-	-	-	-

The standard error is shown below each parameter

$B_{ij} = 10^5 \times \beta_{ij}$  where  $\beta_{ij}$  is the anisotropic thermal parameter

the hydrate oxygen). has been given in Fig. 13.

This program also yielded values of interatomic distances and bond angles. These have been listed in Tables XVII and XVIII. Standard errors were not computed with this program. The errors in the bond lengths and angles were only calculated for the more refined structure as obtained from the diffractometer data.

TABLE XVII  
INTERATOMIC BOND DISTANCES  
(derived from visual intensity data)

BONDING INTERACTIONS OF THE ACETYLACETONATE RINGS		BONDING INTERACTIONS OF THE PERCHLORATE ION	
BOND	LENGTH (Å)	BOND	LENGTH (Å)
Fe - O <sub>1</sub>	1,98 Å	Cl - O <sub>7</sub>	1,38 Å
Fe - O <sub>2</sub>	2,09	Cl - O <sub>8</sub>	1,45
Fe - O <sub>3</sub>	1,93	Cl - O <sub>9</sub>	1,48
Fe - O <sub>4</sub>	1,97	Cl - O <sub>10</sub>	1,46
Fe - O <sub>5</sub>	2,04		
Fe - O <sub>6</sub>	1,95	BONDING INTERACTIONS OF THE SILVER ION	
O <sub>1</sub> - C <sub>2</sub>	1,23	Ag - C <sub>13</sub>	2,32
O <sub>2</sub> - C <sub>4</sub>	1,34	Ag - O <sub>8</sub>	2,51
O <sub>3</sub> - C <sub>7</sub>	1,12	Ag - O <sub>4</sub>	2,66
O <sub>4</sub> - C <sub>9</sub>	1,38	Ag - O <sub>11</sub>	2,07 (un-refined)
O <sub>5</sub> - C <sub>12</sub>	1,15		
O <sub>6</sub> - C <sub>14</sub>	1,31	NON-BONDING INTERACTIONS OF THE SILVER ION	
C <sub>2</sub> - C <sub>3</sub>	1,47	Ag - C <sub>12</sub>	2,92
C <sub>3</sub> - C <sub>4</sub>	1,21	Ag - C <sub>14</sub>	2,83
C <sub>7</sub> - C <sub>8</sub>	1,32		
C <sub>8</sub> - C <sub>9</sub>	1,45		
C <sub>12</sub> - C <sub>13</sub>	1,52		
C <sub>13</sub> - C <sub>14</sub>	1,56		
C <sub>1</sub> - C <sub>2</sub>	1,44		
C <sub>4</sub> - C <sub>5</sub>	1,65		
C <sub>6</sub> - C <sub>7</sub>	1,43		
C <sub>9</sub> - C <sub>10</sub>	1,64		
C <sub>11</sub> - C <sub>12</sub>	1,69		
C <sub>14</sub> - C <sub>15</sub>	1,27		

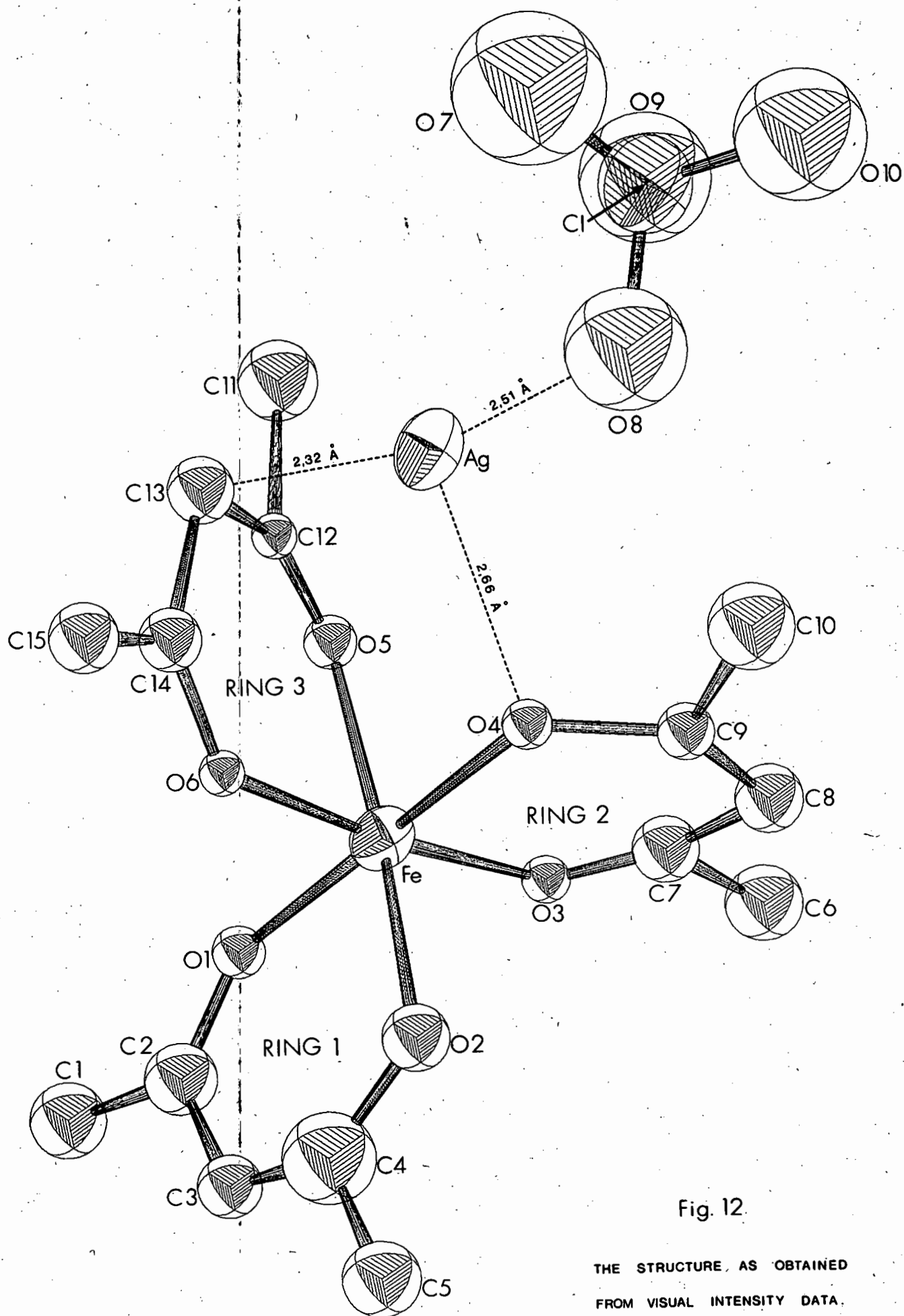


Fig. 12.

THE STRUCTURE, AS OBTAINED  
FROM VISUAL INTENSITY DATA.

TABLE XVIII

INTERATOMIC BOND ANGLES  $\theta$   
(derived from visual intensity data)

ANGLE	$\theta$ (degrees)	ANGLE	$\theta$ (degrees)	ANGLE	$\theta$ (degrees)
O <sub>1</sub> -Fe-O <sub>2</sub>	87,1	O <sub>1</sub> -C <sub>2</sub> -C <sub>1</sub>	118,1	C <sub>13</sub> -Ag-O <sub>8</sub>	108,0
O <sub>3</sub> -Fe-O <sub>4</sub>	89,1	O <sub>2</sub> -C <sub>4</sub> -C <sub>5</sub>	102,3	C <sub>13</sub> -Ag-O <sub>11</sub>	130,6
O <sub>5</sub> -Fe-O <sub>6</sub>	85,1	O <sub>3</sub> -C <sub>7</sub> -C <sub>6</sub>	106,0	O <sub>8</sub> -Ag-O <sub>11</sub>	117,1
		O <sub>4</sub> -C <sub>9</sub> -C <sub>10</sub>	105,7		
Fe-O <sub>1</sub> -C <sub>2</sub>	133,8	O <sub>5</sub> -C <sub>12</sub> -C <sub>11</sub>	111,5	C <sub>13</sub> -Ag-O <sub>4</sub>	89,2
Fe-O <sub>2</sub> -C <sub>4</sub>	118,7	O <sub>6</sub> -C <sub>14</sub> -C <sub>15</sub>	116,8	O <sub>8</sub> -Ag-O <sub>4</sub>	83,5
Fe-O <sub>3</sub> -C <sub>7</sub>	118,1			O <sub>11</sub> -Ag-O <sub>4</sub>	114,0
Fe-O <sub>4</sub> -C <sub>9</sub>	125,8	C <sub>1</sub> -C <sub>2</sub> -C <sub>3</sub>	121,0		
Fe-O <sub>5</sub> -C <sub>12</sub>	123,5	C <sub>3</sub> -C <sub>4</sub> -C <sub>5</sub>	121,7	O <sub>1</sub> -Fe-O <sub>3</sub>	90,3
Fe-O <sub>6</sub> -C <sub>14</sub>	133,4	C <sub>6</sub> -C <sub>7</sub> -C <sub>8</sub>	100,5	O <sub>1</sub> -Fe-O <sub>5</sub>	90,0
		C <sub>8</sub> -C <sub>9</sub> -C <sub>10</sub>	129,3	O <sub>1</sub> -Fe-O <sub>6</sub>	93,5
C <sub>2</sub> -C <sub>3</sub> -C <sub>4</sub>	122,9	C <sub>11</sub> -C <sub>12</sub> -C <sub>13</sub>	109,1	O <sub>2</sub> -Fe-O <sub>3</sub>	93,9
C <sub>7</sub> -C <sub>8</sub> -C <sub>9</sub>	107,3	C <sub>13</sub> -C <sub>14</sub> -C <sub>15</sub>	120,5	O <sub>2</sub> -Fe-O <sub>4</sub>	92,8
C <sub>12</sub> -C <sub>13</sub> -C <sub>14</sub>	107,8			O <sub>2</sub> -Fe-O <sub>6</sub>	91,2
		O <sub>7</sub> -Cl-O <sub>8</sub>	120,9	O <sub>3</sub> -Fe-O <sub>5</sub>	90,0
O <sub>1</sub> -C <sub>2</sub> -C <sub>3</sub>	120,9	O <sub>7</sub> -Cl-O <sub>9</sub>	106,3	O <sub>4</sub> -Fe-O <sub>5</sub>	90,1
O <sub>2</sub> -C <sub>4</sub> -C <sub>3</sub>	135,9	O <sub>7</sub> -Cl-O <sub>10</sub>	114,6	O <sub>4</sub> -Fe-O <sub>6</sub>	87,1
O <sub>3</sub> -C <sub>7</sub> -C <sub>8</sub>	153,2	O <sub>8</sub> -Cl-O <sub>9</sub>	91,2		
O <sub>4</sub> -C <sub>9</sub> -C <sub>8</sub>	124,1	O <sub>8</sub> -Cl-O <sub>10</sub>	114,3	O <sub>1</sub> -Fe-O <sub>4</sub>	179,4
O <sub>5</sub> -C <sub>12</sub> -C <sub>13</sub>	139,3	O <sub>9</sub> -Cl-O <sub>10</sub>	104,6	O <sub>2</sub> -Fe-O <sub>5</sub>	175,2
O <sub>6</sub> -C <sub>14</sub> -C <sub>13</sub>	122,6			O <sub>3</sub> -Fe-O <sub>6</sub>	173,8

PART B.I. DATA COLLECTION FROM THE DIFFRACTOMETER

Intensity data was collected using a Philips P.W.1100 computer controlled four-circle<sup>71</sup> X-ray diffractometer. A Philips P.W. 1130 3kW X-ray generator provided the radiation source for the diffractometer. The generator was operated at 50 kV and 20 mA. Molybdenum K<sub>α</sub> radiation ( $\lambda = 0,7107\text{\AA}$ ) was obtained with the aid of a Zr filter.

Preliminary Weissenberg and precession photographs had been used to determine relatively accurate unit cell parameters and to establish the space group as  $P2_1/c$ .

A crystal having dimensions 0,6 x 0,4 x 0,2 mm was mounted at the end of a thin glass rod and aligned on the diffractometer<sup>72</sup>. A least squares fit of the  $\chi$ ,  $\phi$ , and  $2\theta$  angles of 25 reflections accurately centred on the diffractometer was used to determine the lattice constants at room temperature.

The final parameters with their standard deviations obtained from the diffractometer are listed below.

$$a = 12,274 \text{\AA} \pm 0,005 \text{\AA}$$

$$b = 11,761 \text{\AA} \pm 0,005 \text{\AA}$$

$$c = 17,235 \text{\AA} \pm 0,005 \text{\AA}$$

$$\alpha = 90,00^\circ$$

$$\beta = 120,64^\circ \pm 0,12^\circ$$

$$\gamma = 90,00^\circ$$

The measured density (page 30) was  $1,72 \text{ gm/cm}^3$ . Using the diffractometer data and Equation (4), the density was calculated as  $\rho_c = 1,79 \text{ gm/cm}^3$ .

For the crystal used the average radius was 0,40 mm. The linear absorption coefficient for Mo radiation was

calculated using equation (7). The values of the mass absorption coefficients  $(\mu/\rho)_{0,7107}$  employed in this calculation were:

<u>Element</u>	<u><math>(\mu/\rho)_{0,7107}</math> (cm<sup>2</sup>/gm)</u>
Ag	25,80
Fe	38,50
Cl	11,50
O	1,31
C	0,625
H	0,380

Insertion of these values into equation (7) yielded

$$\mu = 17,62 \text{ cm}^{-1}$$

$$\text{Thus, } \mu R = 0,705$$

The diffractometer scanned the area in reciprocal space from  $\theta = 0^\circ$  to  $\theta = 20^\circ$ . The value of  $\mu R$  over this range varied only from 0,316 to 0,309. Hence no absorption corrections were made to the intensities.

A total number of 1977 independent reflections were measured of which 131 were systematically absent according to the space group conditions. Reflections were considered absent if their net intensity was less than two times the standard deviation of this value<sup>73</sup> i.e.  $I_{\text{rel}} < 2\sigma_I$ . 174 reflections fulfilled this criterion. These reflections were not used in the structure refinement. Finally 1672 reflections were retained as being non-zero.

The reflections were measured using the  $\omega$ - $2\theta$  scan technique<sup>74</sup>. In this scanning process the detector of the diffractometer rotates at an angular rate which is twice that of the crystal. In the  $\omega$  scan of a given reflection, the crystal, and hence the reciprocal lattice, rotates. The

result of this is that the lattice point in question is carried from outside the sphere of reflection to the inside. The  $\omega$  scan is similar to a photometric trace made parallel to the central line of the film on a zero layer Weissenberg photograph. In the  $2\theta$  scan the trace is made along the diagonal passing through reflections on a common central lattice row. In this way a given reflection is accurately centered so that a reasonable number of quanta are diffracted and detected during one pass through the reflecting position.

Three standard reflections were measured every thirty five reflections to ensure stability of operation and to monitor any crystal decomposition. The variation in intensity of a standard reflection was observed to be less than 5,3 per cent of the net intensity (\* 65,000 counts).

The take off angle, source to crystal distance and crystal to counter distance were  $6^\circ$ , 24 cm and 22 cm respectively. The receiving aperture at the counter was 2mm wide and 1mm high. The scan speed for  $\omega$  was  $0,02^\circ/\text{sec}$ . The background and scan times were both 50 sec.

Lorentz and polarization corrections were made to reduce the intensities to relative structure factors.

## II. FINAL REFINEMENT OF THE STRUCTURE

The positional coordinates of 28 atoms had already been determined and refined using visual intensity data (Part A). The residual index at the end of this refinement was 13,4%. A possible water molecule had also been located.

Using the more accurate diffractometer data and the coordinates of the atoms as obtained in Part A, the refinement process was continued using the program "ORFLS".

The scaling parameter for the intensity data was first

refined and after three cycles of refinement R was 17,5%. 3 Cycles of least squares refinement of the positional coordinates and the isotropic temperature factor reduced R to 13,9%. By this stage changes in the parameters were small and R would not have been lowered by any further refinement of these parameters.

At this stage it was decided to confirm the location of the water molecule. A difference Fourier was computed subtracting out all 28 atoms. The whole map was featureless except for a large peak found at 52 20 40. The position of this peak corresponded well with the peak found at 50 20 38 on the difference Fourier map computed using visual intensity data. It was finally concluded that the structure contained a single hydrate molecule.

In continuing the refinement process, 3 more cycles of isotropic refinement and refinement of the positional parameters reduced R to 10,3%. After 3 cycles of least squares anisotropic B refinement R had dropped to 7,0%.

Finally one last cycle of least squares anisotropic refinement and refinement of the positional parameters was executed.

R converged to its final value of 6,6%.

As no absorption corrections had been applied, and as high values of B had been recorded for the perchlorate oxygens this value of R was deemed very satisfactory.

The final atomic coordinates, isotropic and anisotropic temperature factors are listed together in Table XIX. Standard errors of these parameters are also tabulated.

Appendix A lists the values of the observed and calculated structure factors which were obtained after the last cycle of refinement.

TABLE XIX  
FINAL ATOMIC FRACTIONAL COORDINATES AND THERMAL PARAMETERS  
(DIFFRACTOMETER DATA)

ATOM	X	Y	Z	B <sub>11</sub>	B <sub>22</sub>	B <sub>33</sub>	B <sub>12</sub>	B <sub>13</sub>	B <sub>23</sub>	ISOTROPIC B. $\frac{\sigma^2}{A}$
Ag	.34101 13	.09827 13	.30448 10	813 406	699 348	456 211	-129 299	398 238	2 216	3,38
Fe	.15953 20	.89111 18	.37838 13	544 605	195 453	158 284	- 17 401	227 339	2 274	1,31
C <sub>1</sub>	.81589 173	.84933 164	.38354 139	784 5251	814 4562	765 3288	-130 3966	646 3572	-175 3199	3,74
C <sub>2</sub>	.95482 172	.85537 133	.42041 122	1211 5999	276 3382	584 2996	- 11 3507	738 3805	- 40 2580	2,87
C <sub>3</sub>	.04238 170	.84881 164	.51179 112	895 5500	837 4615	295 2534	27 4062	339 3331	- 44 2681	3,70
C <sub>4</sub>	.16746 189	.84994 136	.55164 109	1614 6817	313 3410	281 2417	65 3921	607 3616	74 2284	2,88
C <sub>5</sub>	.25433 222	.83669 182	.65526 122	1914 7905	972 5207	262 2501	508 5182	465 3708	216 2943	4,55
C <sub>6</sub>	.24344 180	.54476 133	.35243 134	1205 5911	169 3328	728 3165	18 3493	647 3771	- 75 2609	3,07
C <sub>7</sub>	.26447 155	.67508 128	.36618 97	832 4996	322 3521	206 2036	-62 3443	295 2680	- 23 2126	1,97
C <sub>8</sub>	.38312 161	.72058 130	.38913 106	915 5114	283 3650	303 2256	-54 3504	305 2760	- 25 2263	2,48
C <sub>9</sub>	.41081 148	.83503 138	.40072 93	690 4688	532 4021	107 1880	70 3531	168 2430	19 2139	2,02
C <sub>10</sub>	.53737 153	.87667 162	.42202 121	542 4609	795 4483	516 2655	-189 3653	344 2902	19 2806	3,54
C <sub>11</sub>	.02746 183	.01558 188	.10683 112	1078 5807	1205 5603	184 2267	-163 4628	177 3082	101 2850	4,27
C <sub>12</sub>	.08398 139	.01758 142	.21107 91	(514 -)	708 -	35 -	56 -	126 -	60)*	2,07
C <sub>13</sub>	.13041 147	.12122 134	.25617 95	731 4492	439 3564	144 1995	63 3237	141 2423	144 2166	2,32
C <sub>14</sub>	.15504 154	.14094 128	.34527 113	728 4636	207 3415	441 2634	104 3113	329 2869	47 2457	2,42
C <sub>15</sub>	.16771 202	.25932 142	.37970 131	1659 6993	162 3572	562 2903	112 3844	549 3801	3 2526	4,05
O <sub>1</sub>	-.01173 98	.87017 88	.36058 69	757 2998	484 2395	360 1488	-57 2150	373 1844	-34 1528	2,26
O <sub>2</sub>	.23429 104	.86647 89	.51228 66	972 3307	457 2411	199 1370	96 2218	209 1805	106 1454	2,59
O <sub>3</sub>	.17168 99	.72897 80	.35552 69	836 3125	208 2149	401 1519	-48 2094	431 1899	-65 1445	2,30
O <sub>4</sub>	.33130 93	.91270 80	.39597 64	730 2894	236 2012	312 1381	-69 2130	320 1691	-35 1400	1,86
O <sub>5</sub>	.07736 93	.92743 85	.24531 59	770 2855	415 2271	112 1177	-96 2065	186 1543	-20 1337	1,97
O <sub>6</sub>	.15700 97	.05933 78	.39752 65	885 3057	178 2067	280 1362	69 1920	351 1739	-21 1403	1,98
O <sub>7</sub>	.37308 534	.09789 236	.13581 499	12729 1591	1173 272	11406 1371	574 558	11630 1435	428 517	21,44
O <sub>8</sub>	.35235 275	.34892 171	.20545 156	5505 570	1367 216	1499 179	508 288	2461 296	291 167	10,03
O <sub>9</sub>	.27697 254	.93596 333	.06423 156	2754 398	4855 649	848 149	-752 422	248 202	-520 270	14,20
O <sub>10</sub>	.49073 196	.94905 153	.15009 199	2274 292	1073 185	3047 304	503 192	2216 273	254 194	10,34
Cl	.37814 49	-.00983 42	.13992 35	1233 1572	633 1102	605 780	- 3 1060	593 953	- 26 727	3,97
O <sub>11</sub>	.51321 124	.20359 113	.39319 84	1242 167	845 128	510 77	- 287 119	401 95	- 29 81	4,88

The standard deviation is shown below each parameter  
 $B_{ij} = 10^5 \beta_{ij}$  where  $\beta_{ij}$  is the anisotropic temperature factor

\*Signifies that these parameters were not refined.

### IIa. BOND LENGTHS AND ANGLES

Using the values of the final parameters, accurate bond lengths and angles were calculated with the aid of the program "ORFFE". These have been listed together with their standard errors in Tables XX, XXI, and XXII.

Table XX lists all bonded separations in the acetyl-acetate rings and in the perchlorate ion. Bonding interactions of the silver ion with certain atoms are also given.

Table XXI lists all the non-bonded separations which are of interest. All relevant bond angles are tabulated in Table XXII.

### IIb. LEAST SQUARES PLANES

The equation of a plane may be defined by the expression<sup>75</sup>

$$Lx + My + Nz - P = 0 \quad (19)$$

where,  $L^2 + M^2 + N^2 = 1$

$P$  = distance from the origin to the plane

$L, M, N$  = the cosines of the angles which the line makes with the  $x$ ,  $y$ , and  $z$  orthogonal axes respectively.

The perpendicular distance  $D$  from a point  $(x_1, y_1, z_1)$  to the plane defined in equation (19) is given by

$$D = Lx_1 + My_1 + Nz_1 - P \quad (20)$$

TABLE XX  
INTERATOMIC BONDED SEPARATIONS  
 (derived from diffractometer intensity data)

BONDING INTERACTIONS OF THE ACETYLACETONATE RINGS		BONDING INTERACTIONS OF THE PERCHLORATE ION	
BOND	LENGTH Å	BOND	LENGTH Å
Fe - O <sub>1</sub>	1,98 (1)	Cl - O <sub>7</sub>	1,27 (3)
Fe - O <sub>2</sub>	2,02 (1)	Cl - O <sub>8</sub>	1,41 (2)
Fe - O <sub>3</sub>	1,97 (1)	Cl - O <sub>9</sub>	1,41 (2)
Fe - O <sub>4</sub>	1,99 (1)	Cl - O <sub>10</sub>	1,39 (2)
Fe - O <sub>5</sub>	2,02 (1)		
Fe - O <sub>6</sub>	2,01 (1)	BONDING INTERACTIONS OF THE SILVER ION	
O <sub>1</sub> - C <sub>2</sub>	1,30 (2)	Ag - C <sub>13</sub>	2,29 (2)
O <sub>2</sub> - C <sub>4</sub>	1,32 (2)	Ag - O <sub>8</sub>	2,50 (2)
O <sub>3</sub> - C <sub>7</sub>	1,23 (2)	Ag - O <sub>11</sub>	2,25 (1)
O <sub>4</sub> - C <sub>9</sub>	1,31 (2)		
O <sub>5</sub> - C <sub>12</sub>	1,24 (2)		
O <sub>6</sub> - C <sub>14</sub>	1,31 (2)		
C <sub>2</sub> - C <sub>3</sub>	1,38 (2)		
C <sub>3</sub> - C <sub>4</sub>	1,32 (2)		
C <sub>7</sub> - C <sub>8</sub>	1,41 (2)		
C <sub>8</sub> - C <sub>9</sub>	1,38 (2)		
C <sub>12</sub> - C <sub>13</sub>	1,40 (2)		
C <sub>13</sub> - C <sub>14</sub>	1,42 (2)		
C <sub>1</sub> - C <sub>2</sub>	1,49 (2)		
C <sub>4</sub> - C <sub>5</sub>	1,55 (2)		
C <sub>6</sub> - C <sub>7</sub>	1,55 (2)		
C <sub>9</sub> - C <sub>10</sub>	1,49 (2)		
C <sub>11</sub> - C <sub>12</sub>	1,56 (2)		
C <sub>14</sub> - C <sub>15</sub>	1,49 (2)		

TABLE XXI

INTERATOMIC NON-BONDED SEPARATIONS  
(derived from diffractometer intensity data)

NON-BONDING INTERACTIONS		NON-BONDING INTERACTIONS	
INTERACTION	SEPARATION	INTERACTION	SEPARATION
Ag - O <sub>4</sub>	2,73 (1)	C <sub>2</sub> - C <sub>4</sub>	2,43 (3)
Ag - C <sub>12</sub>	2,87 (2)	C <sub>7</sub> - C <sub>9</sub>	2,45 (2)
Ag - C <sub>13</sub>	2,75 (2)	C <sub>12</sub> - C <sub>14</sub>	2,48 (2)
O <sub>1</sub> - O <sub>2</sub>	2,81 (2)	C <sub>13</sub> - O <sub>8</sub>	3,84 (3)
O <sub>3</sub> - O <sub>4</sub>	2,76 (2)	O <sub>8</sub> - O <sub>11</sub>	4,10 (3)
O <sub>5</sub> - O <sub>6</sub>	2,76 (1)	O <sub>11</sub> - C <sub>13</sub>	4,16 (3)
O <sub>7</sub> - O <sub>8</sub>	2,21 (4)	C <sub>13</sub> - O <sub>4</sub>	3,44 (2)
O <sub>7</sub> - O <sub>9</sub>	2,25 (6)	O <sub>8</sub> - O <sub>4</sub>	3,45 (2)
O <sub>7</sub> - O <sub>10</sub>	2,20 (3)	O <sub>11</sub> - O <sub>4</sub>	4,10 (3)
O <sub>8</sub> - O <sub>9</sub>	2,12 (3)		
O <sub>8</sub> - O <sub>10</sub>	2,33 (3)		
O <sub>9</sub> - O <sub>10</sub>	2,23 (3)		

TABLE XXII

INTERATOMIC BOND ANGLES,  $\theta$ 

(derived from diffractometer intensity data)

ANGLE	$\theta^\circ$	ANGLE	$\theta^\circ$	ANGLE	$\theta^\circ$
O <sub>1</sub> -Fe-O <sub>2</sub>	89,3(0,5)	O <sub>1</sub> -C <sub>2</sub> -C <sub>1</sub>	115,1(1,6)	C <sub>13</sub> -Ag-O <sub>8</sub>	106,2(0,8)
O <sub>3</sub> -Fe-O <sub>4</sub>	88,4(0,4)	O <sub>2</sub> -C <sub>4</sub> -C <sub>5</sub>	111,3(1,6)	C <sub>13</sub> -Ag-O <sub>11</sub>	132,7(0,5)
O <sub>5</sub> -Fe-O <sub>6</sub>	86,4(0,4)	O <sub>3</sub> -C <sub>7</sub> -C <sub>6</sub>	114,6(1,4)	O <sub>8</sub> -Ag-O <sub>11</sub>	119,4(0,7)
Fe-O <sub>1</sub> -C <sub>2</sub>	129,3(1,1)	O <sub>4</sub> -C <sub>9</sub> -C <sub>10</sub>	116,0(1,4)	C <sub>13</sub> -Ag-O <sub>4</sub>	86,0(0,4)
Fe-O <sub>2</sub> -C <sub>4</sub>	124,7(1,1)	O <sub>5</sub> -C <sub>12</sub> -C <sub>11</sub>	115,9(1,5)	O <sub>8</sub> -Ag-O <sub>4</sub>	82,3(0,5)
Fe-O <sub>3</sub> -C <sub>7</sub>	128,8(1,0)	O <sub>6</sub> -C <sub>14</sub> -C <sub>15</sub>	116,7(1,4)	O <sub>11</sub> -Ag-O <sub>4</sub>	110,5(0,4)
Fe-O <sub>4</sub> -C <sub>9</sub>	128,3(0,9)	C <sub>1</sub> -C <sub>2</sub> -C <sub>3</sub>	122,7(1,5)	O <sub>1</sub> -Fe-O <sub>3</sub>	91,8(0,4)
Fe-O <sub>5</sub> -C <sub>12</sub>	127,3(0,9)	C <sub>3</sub> -C <sub>4</sub> -C <sub>5</sub>	122,0(1,6)	O <sub>1</sub> -Fe-O <sub>5</sub>	88,5(0,4)
Fe-O <sub>6</sub> -C <sub>14</sub>	127,3(0,9)	C <sub>6</sub> -C <sub>7</sub> -C <sub>8</sub>	119,1(1,5)	O <sub>1</sub> -Fe-O <sub>6</sub>	92,5(0,4)
C <sub>2</sub> -C <sub>3</sub> -C <sub>4</sub>	127,7(1,6)	C <sub>8</sub> -C <sub>9</sub> -C <sub>10</sub>	120,5(1,5)	O <sub>2</sub> -Fe-O <sub>3</sub>	93,0(0,4)
C <sub>7</sub> -C <sub>8</sub> -C <sub>9</sub>	123,8(1,5)	C <sub>11</sub> -C <sub>12</sub> -C <sub>13</sub>	117,9(1,4)	O <sub>2</sub> -Fe-O <sub>4</sub>	90,9(0,4)
C <sub>12</sub> -C <sub>13</sub> -C <sub>14</sub>	122,8(1,4)	C <sub>13</sub> -C <sub>14</sub> -C <sub>15</sub>	120,2(1,4)	O <sub>2</sub> -Fe-O <sub>6</sub>	89,4(0,4)
O <sub>1</sub> -C <sub>2</sub> -C <sub>3</sub>	122,2(1,6)	O <sub>7</sub> -Cl-O <sub>8</sub>	111,4(2,2)	O <sub>3</sub> -Fe-O <sub>5</sub>	91,3(0,4)
O <sub>2</sub> -C <sub>4</sub> -C <sub>3</sub>	126,5(1,5)	O <sub>7</sub> -Cl-O <sub>9</sub>	113,8(3,7)	O <sub>4</sub> -Fe-O <sub>5</sub>	91,3(0,4)
O <sub>3</sub> -C <sub>7</sub> -C <sub>8</sub>	126,3(1,4)	O <sub>7</sub> -Cl-O <sub>10</sub>	111,8(1,7)	O <sub>4</sub> -Fe-O <sub>6</sub>	87,3(0,4)
O <sub>4</sub> -C <sub>9</sub> -C <sub>8</sub>	123,5(1,5)	O <sub>8</sub> -Cl-O <sub>9</sub>	97,7(1,7)	O <sub>1</sub> -Fe-O <sub>4</sub>	179,8(0,4)
O <sub>5</sub> -C <sub>12</sub> -C <sub>13</sub>	126,0(1,2)	O <sub>8</sub> -Cl-O <sub>10</sub>	113,3(1,5)	O <sub>2</sub> -Fe-O <sub>5</sub>	175,2(0,4)
O <sub>6</sub> -C <sub>14</sub> -C <sub>13</sub>	122,8(1,4)	O <sub>9</sub> -Cl-O <sub>10</sub>	108,0(1,7)	O <sub>3</sub> -Fe-O <sub>6</sub>	175,0(0,4)

If two planes,

$$L_1x + M_1y + N_1z - P_1 = 0$$

and  $L_2x + M_2y + N_2z - P_2 = 0$

intersect at an angle  $\theta$ , then

$$\cos \theta = L_1L_2 + M_1M_2 + N_1N_2 \quad (21)$$

In order to visualize the planarity of certain sections of the structure, a number of least squares planes<sup>76</sup> were calculated using the program "LSP" (Least Squares Plane). In this program the best least squares fit of a plane through a specified number of points was calculated. Perpendicular distances of a number of atoms to these planes were also calculated (Eqn 20). These have been recorded in Table XXIIIa and Table XXIIIb. In addition angles between various pairs of planes were determined. (Eqn 21). These have been tabulated in Table XXIV.

A listing of the plane parameters and the orthogonalized coordinates of the atoms used in the calculation of the least squares planes appears in Appendix B.

The planarity of the structure will be discussed more fully in the next section.

#### IIC. ILLUSTRATIONS OF THE MOLECULAR STRUCTURE

A good viewing projection of the molecule was obtained using the plotter program "ORTEP". This has been illustrated in Fig. 13. In addition [100], [010] and [001] projections were also computed. These are given at the end of Chapter 5. (Figs. 22, 23, 24).

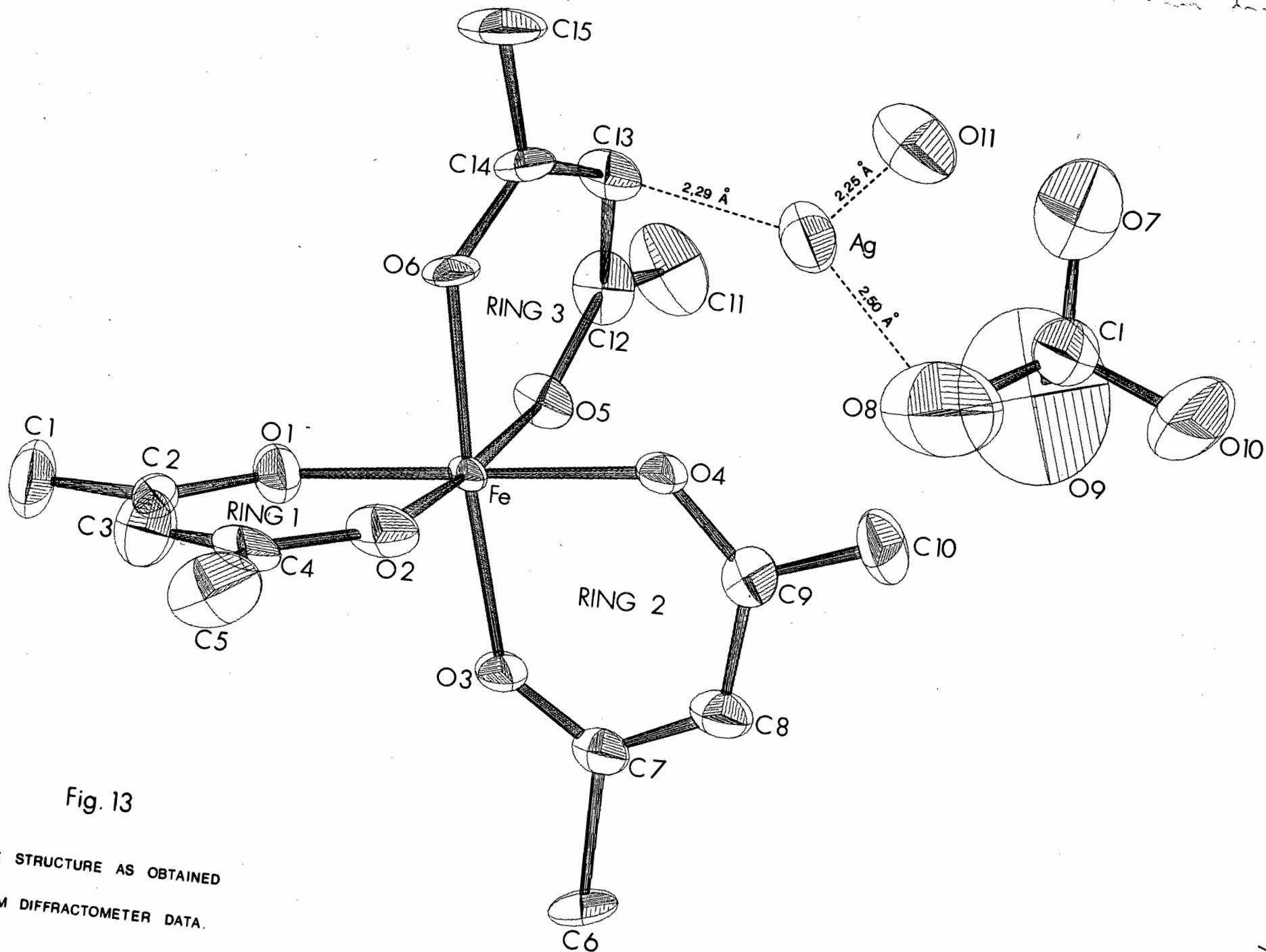


Fig. 13

THE STRUCTURE AS OBTAINED  
FROM DIFFRACTOMETER DATA.

TABLE XXIIIa

## LEAST SQUARES PLANES IN THE FERRIC ACETYLACETONATE MOLECULE

Plane Number	Atoms included in Least Squares Plane	Perpendicular Distance D of Atoms from Plane		Plane Number	Atoms included in Least Squares Plane	Perpendicular Distance D of Atoms from Plane	
		Atom	D (Å)			Atom	D (Å)
1	O <sub>1</sub>	O <sub>1</sub>	0,00	7	O <sub>1</sub>	O <sub>1</sub>	-0,01
	Fe	Fe	0,00		C <sub>1</sub>	C <sub>1</sub>	0,00
	O <sub>2</sub>	O <sub>2</sub>	0,00		C <sub>2</sub>	C <sub>2</sub>	-0,01
2	O <sub>3</sub>	O <sub>3</sub>	0,00		C <sub>3</sub>	C <sub>3</sub>	0,03
	Fe	Fe	0,00		C <sub>4</sub>	C <sub>4</sub>	-0,01
	O <sub>4</sub>	O <sub>4</sub>	0,00		C <sub>5</sub>	C <sub>5</sub>	-0,02
3	O <sub>5</sub>	O <sub>5</sub>	0,00		O <sub>2</sub>	O <sub>2</sub>	0,01
	Fe	Fe	0,00	8	O <sub>3</sub>	O <sub>3</sub>	-0,02
	O <sub>6</sub>	O <sub>6</sub>	0,00		C <sub>6</sub>	C <sub>6</sub>	0,00
4	O <sub>1</sub>	O <sub>1</sub>	-0,03		C <sub>7</sub>	C <sub>7</sub>	0,00
	O <sub>2</sub>	O <sub>2</sub>	0,04		C <sub>8</sub>	C <sub>8</sub>	0,02
	Fe	Fe	-0,03		C <sub>9</sub>	C <sub>9</sub>	0,00
	O <sub>4</sub>	O <sub>4</sub>	-0,03		C <sub>10</sub>	C <sub>10</sub>	-0,02
	O <sub>5</sub>	O <sub>5</sub>	0,04		O <sub>4</sub>	O <sub>4</sub>	0,01
5	O <sub>3</sub>	O <sub>3</sub>	-0,02	9	O <sub>5</sub>	O <sub>5</sub>	-0,04
	O <sub>4</sub>	O <sub>4</sub>	0,02		C <sub>11</sub>	C <sub>11</sub>	-0,13
	Fe	Fe	0,02		C <sub>12</sub>	C <sub>12</sub>	0,05
	O <sub>1</sub>	O <sub>1</sub>	0,01		C <sub>13</sub>	C <sub>13</sub>	0,22
	O <sub>6</sub>	O <sub>6</sub>	-0,02		C <sub>14</sub>	C <sub>14</sub>	0,06
6	O <sub>5</sub>	O <sub>5</sub>	-0,05		C <sub>15</sub>	C <sub>15</sub>	-0,14
	O <sub>6</sub>	O <sub>6</sub>	0,06		O <sub>6</sub>	O <sub>6</sub>	-0,02
	Fe	Fe	-0,01	The positive and negative signs indicate positions on opposite sides of the least squares plane			
	O <sub>2</sub>	O <sub>2</sub>	-0,05				
	O <sub>3</sub>	O <sub>3</sub>	0,06				

TABLE XXIIIb  
LEAST SQUARES PLANES (continued)

Plane Number	Atoms Included in Least Squares Plane	Perpendicular Distance D of Atoms from Plane.	
		Atom	D (Å)
10	C <sub>13</sub> O <sub>4</sub> O <sub>8</sub>	C <sub>13</sub>	0,00
		O <sub>4</sub>	0,00
		O <sub>8</sub>	0,00
		Ag	1,35
11	C <sub>13</sub> O <sub>4</sub> O <sub>11</sub>	C <sub>13</sub>	0,00
		O <sub>4</sub>	0,00
		O <sub>11</sub>	0,00
		Ag	-0,73
12	O <sub>4</sub> O <sub>8</sub> O <sub>11</sub>	O <sub>4</sub>	0,00
		O <sub>8</sub>	0,00
		O <sub>11</sub>	0,00
		Ag	-0,97
13	O <sub>8</sub> O <sub>11</sub> C <sub>13</sub>	O <sub>8</sub>	0,00
		O <sub>11</sub>	0,00
		C <sub>13</sub>	0,00
		Ag	0,17
14	O <sub>8</sub> O <sub>11</sub> C <sub>13</sub> Ag	O <sub>8</sub>	-0,03
		O <sub>11</sub>	-0,05
		C <sub>13</sub>	-0,04
		Ag	0,12

TABLE XXIV  
ANGLES BETWEEN LEAST SQUARES PLANES

INTERSECTING PLANES	ANGLE OF INTERSECTION
1 and 7	177° 6'
2 and 8	172° 51'
3 and 9	164° 13'

## 5. DISCUSSION

Complexes formed between aromatic moieties and the silver (I) ion were first described by A.E. Hill<sup>29,30</sup> in the early 1920's during the course of phase equilibrium studies.

Mulliken<sup>37</sup> and Dewar<sup>32</sup> both formulated theoretical models for the bonding of Ag (I) with aromatic compounds. The gross features of their models have since been verified by the crystal structures of the benzene-AgClO<sub>4</sub> complex<sup>38</sup> and the benzene-AgAlCl<sub>4</sub> complex<sup>27</sup>. Although a 1:1 interaction occurs between the silver ion and the aromatic compound in both these complexes, a fundamental difference between them exists. In the former case the silver ion is  $\pi$  bonded to two benzene rings with the result that a polymer of the type - Ar - Ag - Ar - Ag - is formed (Fig. 7c). In the latter complex no such polymer is formed and the silver ion is  $\pi$  bonded to only one benzene ring. However in this complex the silver ion also interacts with four chlorine atoms to yield the unusual coordination number of five.

Solution studies have indicated silver to aromatic ratios other than 1:1. Andrews and Keefer<sup>33-35</sup> have reported the existence of complexes of the type AgAr<sup>+</sup> and Ag<sub>2</sub>Ar<sup>2+</sup>. In addition several complexes of the type AgAr<sub>2</sub><sup>+</sup> have been described by E.A. Hall Griffith and E.L. Amma. These include the silver perchlorate complexes of biscyclohexylbenzene<sup>22</sup>, m-xylene<sup>23</sup> and o-xylene<sup>39</sup>:

E.A. Hall Griffith and E.L. Amma<sup>21</sup> have postulated that a basic distinction exists between the nature of the metal to carbon bond in Ag to aromatic and Ag to olefin complexes.

A "short" Ag-C bond of  $\overset{\text{O}}{\sim} 2,48 \text{ \AA}$  has been observed in most

Ag-aromatic complexes regardless of stoichiometry, anion and packing considerations (see Table XXVII). The adjacent carbon distance in these complexes is seen to vary widely from  $2,56 \overset{\circ}{\text{A}}$  to  $2,92 \overset{\circ}{\text{A}}$  indicating the asymmetry of the silver ion above the C=C bond (Fig. 14a).

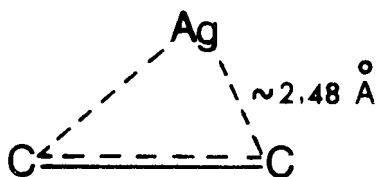


fig. 14a

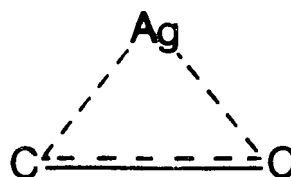


fig. 14b

In Ag to olefin complexes on the other hand the silver ion is seen to be symmetrically located above the carbon to carbon double bond (Fig. 14b). However no regularity in the Ag-C distance has been observed in these complexes, and Ag-C bond lengths vary from  $2,31 \overset{\circ}{\text{A}}$  to  $2,45 \overset{\circ}{\text{A}}$ . (Table XXVII).

In the latter type structure the Ag-C bond distances are seen to be significantly shorter than those in the Ag-aromatic type structure. This result is in agreement with the fact that olefins are stronger  $\pi$  bases than aromatics.

A fundamental difference exists between complexes of metal acetylacetonates and those involving metal to carbon bonds in aromatic and olefin type structures. From a consideration of molecular orbital theory<sup>77</sup> the position of greatest  $\pi$  electron density in aromatic and olefin compounds is found to be located between the two carbon atoms forming the double bond. In metal acetylacetonates

the location of greatest  $\pi$  electron density is directly above the "active methylene" carbon atom of the chelate ring. Hence packing in the silver to metal acetylacetonate complexes is expected to be different from the packing observed in Ag- aromatic and Ag- olefin type complexes. However the degree of basicity of the chelate rings in metal acetylacetonates may be assessed in terms of the Ag-C bond distance observed in these structures.

### 5.1 Gross Structural Features of $\text{Fe}(\text{acac})_3 \cdot \text{AgClO}_4 \cdot \text{H}_2\text{O}$

The structure of the ferric acetylacetonate silver perchlorate monohydrate molecule is shown in Fig. 13. The oxygen atoms of the chelate rings are seen to be arranged octahedrally around the central iron atom.

Although the silver ion is located in the vicinity of two chelate rings (Rings 2 and 3), it is apparently bonded to the central carbon atom of only one chelate ring. (Ring 3). In addition the silver ion is bonded to one perchlorate oxygen ( $\text{O}_8$ ) and to the hydrate oxygen ( $\text{O}_{11}$ ) to procure a coordination number of three. The four atoms  $\text{O}_8$ ,  $\text{O}_{11}$ ,  $\text{C}_{13}$  and Ag lie almost in the same plane. The coordination of the silver ion is discussed in greater detail in Section 5.3

The perchlorate ion is tetrahedrally shaped, but shows extreme thermal motion. This is not uncommon in complexes containing the perchlorate ion. (See section 5.6).

The ferric acetylacetonate moieties are arranged in a staggered array along the "z" direction of the unit cell to form a bulky sheet-like structure parallel to the bc plane. Because the three chelate rings of each acetylacetonate

molecule are mutually perpendicular these sheets create "cylindrical holes" which propagate in a direction parallel to the y axis. These "holes" are filled with ionic matter consisting of the silver (1) and perchlorate ions. (See 010 projection Fig. 23).

In other silver perchlorate complexes<sup>2,3,40</sup> the silver and perchlorate ions form layers of ionic matter which are made up of  $-AgO_2ClO_4 - Ag -$  chains. These chains are held together by weak  $\overset{\ddagger}{Ag}-O$  interactions and van der Waals forces. In the structure of  $Fe(acac)_3 \cdot AgClO_4 \cdot H_2O$  the silver ion is bound to only one perchlorate oxygen ( $O_8$ ) with the result that no bonded  $AgClO_4$  chains are formed. In this case the silver and perchlorate ions are found to zig-zag in a non bonded fashion down the 'cylindrical holes' created by the chelate rings in the direction of the 'Y' axis.

## 5.2 The Iron Acetylacetonate Molecule : Bond Lengths and Angles

The bond lengths and angles in the iron acetylacetonate molecule in  $Fe(acac)_3 \cdot AgClO_4 \cdot H_2O$  as obtained from visual and diffractometer data have been compared with the values obtained by Iball and Morgan<sup>2</sup> for the refined structure of ferric acetylacetonate (Figs. 15, 16, 17.)

As the iron acetylacetonate molecule contains groups of bonds and angles which are chemically equivalent it was possible to calculate a mean value for each group. Mean values of the bond lengths and angles for the three structures have been reported in Table XXV. Although some distortion of ring 3 in the structure of  $Fe(acac)_3 \cdot AgClO_4 \cdot H_2O$  was observed as a result of  $Ag - C_{13}$  bonding, it did not greatly affect the bonding distances in the ring. Therefore the values of the bond lengths and angles for this ring were also included in the calculation of the mean values.



TABLE XXV  
MEAN VALUES OF BOND LENGTHS AND ANGLES  
IN THE Fe(acac)<sub>3</sub> RING.

BOND LENGTH/ ANGLE	Fe(acac) <sub>3</sub> <sup>2</sup>	Fe(acac) <sub>3</sub> in Fe(acac) <sub>3</sub> ·AgClO <sub>4</sub> ·H <sub>2</sub> O	
		Diffractometer Data	Visual Data
Fe - O	1,992 Å <sup>o</sup>	1,998 Å <sup>o</sup>	1,99 Å <sup>o</sup>
C - C (ring)	1,377 Å <sup>o</sup>	1,385 Å <sup>o</sup>	1,42 Å <sup>o</sup>
C - O	1,258 Å <sup>o</sup>	1,285 Å <sup>o</sup>	1,26 Å <sup>o</sup>
C - CH <sub>3</sub>	1,530 Å <sup>o</sup>	1,522 Å <sup>o</sup>	1,52 Å <sup>o</sup>
O - Fe - O	87,1°	88,0°	87,1°
Fe - O - C	129,3°	127,6°	125,6°
C - C - C	124,8°	124,8°	112,7°
C - C - O (interior ring angle)	125,0°	124,5°	132,7°

The mean values of the bond lengths and angles of Fe(acac)<sub>3</sub> in the fully refined argentated complex compare very favourably with those reported for Fe(acac)<sub>3</sub> alone.

Fe - O bond lengths in the monoargentated complex varied between 1,97 Å<sup>o</sup> and 2,02 Å<sup>o</sup> in good agreement with the Fe - O bond distances found in the parent compound<sup>2</sup>. The regular octahedral arrangement of the oxygen atoms about the iron atom was confirmed by the O - Fe - O bond angles which varied only from 87,3° to 93,0° (Table XXII).

In addition three least squares planes were calculated through the atoms FeO<sub>1</sub>O<sub>2</sub>O<sub>4</sub>O<sub>5</sub>, FeO<sub>3</sub>O<sub>4</sub>O<sub>1</sub>O<sub>6</sub>, and FeO<sub>5</sub>O<sub>6</sub>O<sub>2</sub>O<sub>3</sub> (Table XXIIIa). The maximum deviation of any atom included in the least squares plane from that plane was 0,06 Å<sup>o</sup>.

This was not considered to be significant of any gross distortion from planarity. These planes also illustrated the symmetry of the chelate oxygens about the central iron atom.

The C - O bonds were observed to have a mean value of  $1,285 \overset{\circ}{\text{A}}$ . This value lies between the theoretical carbonyl bond length of  $1,23 \overset{\circ}{\text{A}}^{78}$  and the C - O paraffinic bond length of  $1,43 \overset{\circ}{\text{A}}^{78}$ . Intermediate between the theoretical values of the C = C bond length of  $1,34 \overset{\circ}{\text{A}}^{78}$  and the paraffinic C - C bond length of  $1,54 \overset{\circ}{\text{A}}^{78}$  were the values of the ring C - C bonds. Their mean value was  $1,377 \overset{\circ}{\text{A}}$ .

Although some of the electron density associated with the chelate oxygens must be used for Fe - O bonding, these intermediate C - O and C - C bond lengths can be interpreted as a result of the delocalization of the  $\pi$  electrons through a five membered section of the ring (Fig. 18). The delocalization of these  $\pi$  electrons through this part of the ring gives rise to the 'quasi aromatic' character of the chelate rings.

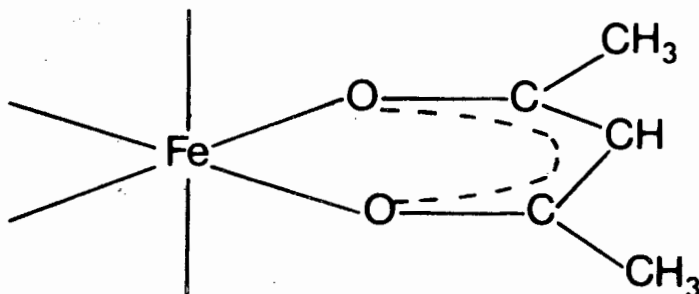


fig. 18

The mean value of  $1,522 \overset{\circ}{\text{A}}$  for the C - CH<sub>3</sub> bond lengths is in good agreement with the theoretical value of  $1,54 \overset{\circ}{\text{A}}^{78}$  for a paraffinic C - C bond length.

TABLE XXVI  
Ag - O BONDING INTERACTIONS

C O M P L E X	Ag - O SEPARATION
Bis-o-xylene·AgClO <sub>4</sub> <sup>39</sup>	2,56 Å; 2,60 Å
Biscyclohexylbenzene·AgClO <sub>4</sub> <sup>22</sup>	2,66 Å
Bis-m-xylene·AgClO <sub>4</sub> <sup>23</sup>	2,49 Å
Napthalene·4AgClO <sub>4</sub> ·4H <sub>2</sub> O <sup>40</sup>	2,34 Å; 2,38 Å
Anthracene·4AgClO <sub>4</sub> ·H <sub>2</sub> O <sup>40</sup>	2,41 Å; 2,47 Å; 2,48 Å
Indene·AgClO <sub>4</sub> <sup>21</sup>	2,46 Å
Trisilver Dinitrate Tris(acetyl- acetonato)nickelate II Monohydrate <sup>7</sup>	2,46 Å
Ag <sub>3</sub> PO <sub>4</sub> <sup>80</sup>	2,34 Å
Ag <sub>3</sub> AsO <sub>4</sub> <sup>81</sup>	2,42 Å
Ag <sub>2</sub> MoO <sub>4</sub> <sup>82</sup>	2,42 Å

### 5.3b Silver to Carbon Bonding

Table XXVII lists the shortest Ag - C distances reported in numerous structures in which a silver to aromatic and silver to olefin interaction occurs. These distances were considered to be bonding separations.

It can be seen that Ag - C distances between 2,45 Å and 2,61 Å are a feature of all silver to aromatic interactions whereas the Ag - C distance in silver to olefin interactions is shorter and is seen to vary between 2,31 Å and 2,46 Å.

Again it must be stated that there is no criterion by which a Ag - C interaction can be clearly defined.

TABLE XXVII  
Ag - C BONDING INTERACTIONS

COMPOUND (AROMATIC)	Ag - C SEPARATION
Benzene·AgClO <sub>4</sub> <sup>38</sup>	2,496 Å <sup>○</sup>
Benzene . AgAlCl <sub>4</sub> <sup>27</sup>	2,47 Å <sup>○</sup>
Biscyclohexylbenzene·AgClO <sub>4</sub> <sup>22</sup>	2,48 Å <sup>○</sup>
Indene . AgClO <sub>4</sub> <sup>21</sup>	2,47 Å <sup>○</sup>
Bis-m-xylene·AgClO <sub>4</sub> <sup>23</sup>	2,45 Å <sup>○</sup>
Bis-o-xylene·AgClO <sub>4</sub> <sup>39</sup>	2,53 Å <sup>○</sup>
Anthracene·4AgClO <sub>4</sub> ·H <sub>2</sub> O <sup>40</sup>	2,48 Å, 2,45 Å <sup>○</sup>
Napthalene·4AgClO <sub>4</sub> ·4H <sub>2</sub> O <sup>40</sup>	2,61 Å <sup>○</sup>
Trisilver Dinitrate tris(acetylacetonato)nickelate II Monohydrate <sup>7*</sup>	2,34 Å <sup>○</sup>
COMPOUND (OLEFINIC)	Ag - C SEPARATION
Norbornadiene . 2AgNO <sub>3</sub> <sup>83</sup>	2,31 Å <sup>○</sup>
Cyclooctatetraene·AgNO <sub>3</sub> <sup>84</sup>	2,46 Å <sup>○</sup>
Bullvalene . AgBF <sub>4</sub> ·H <sub>2</sub> O <sup>85</sup>	2,36 Å, 2,42 Å <sup>○</sup>
1,4,7 Cyclonatriene·3AgNO <sub>3</sub> <sup>86</sup>	2,38 Å <sup>○</sup>

\* This compound is considered to have "quasi aromatic character"

By comparing the values of significant Ag - O and Ag - C bonding separations of previously reported structures with those obtained for the structure of Fe(acac)<sub>3</sub>·AgClO<sub>4</sub>·H<sub>2</sub>O it was possible to formulate a theory as to the nature of the coordination of the silver ion.

### 5.3c The Coordination Number of the Silver Ion as Inferred from Visual Data

When the structure of the compound was initially solved using visual data it was not certain whether a hydrate molecule existed in the structure or not. The hydrate oxygen was not included in Fig. 12.

Considering Ag - O distances of 2,66 Å or greater to be non bonding, then the silver ion was seen to be bonded to O<sub>4</sub> (2,66 Å) of a chelate ring and to an oxygen of a perchlorate group O<sub>8</sub> (2,51 Å). The distance between the silver ion and the central carbon atom C<sub>13</sub> of an adjacent chelate ring, but of the same molecule, was 2,32 Å. This was considered to be a bonding interaction. Hence, without including the hydrate molecule in the structure, the coordination number of the silver ion was three, with the atoms O<sub>4</sub>, O<sub>8</sub> and C<sub>13</sub> arranged in a distorted trigonal pyramidal fashion around the silver ion (Fig. 12). The O<sub>4</sub> - Ag - O<sub>8</sub>, O<sub>8</sub> - Ag - C<sub>13</sub>, and O<sub>4</sub> - Ag - C<sub>13</sub> bond angles were 83,5° 108,0° and 89,5° respectively.

If the hydrate molecule was taken into consideration, then using the unrefined position of the oxygen atom (O<sub>11</sub>) the Ag - O<sub>11</sub> bond length was calculated as 2,07 Å.

Hence the existence of a hydrate molecule in the structure was seen to alter the coordination number of the silver ion from three to four. With the water molecule in its unrefined position the coordination tetrahedron was observed to be very distorted. The tetrahedron was very much flattened at its base with the O<sub>8</sub>, O<sub>11</sub>, C<sub>13</sub> and Ag atoms lying almost in the same plane. The sum of the angles O<sub>8</sub> - Ag - O<sub>11</sub>, O<sub>8</sub> - Ag - C<sub>13</sub> and O<sub>11</sub> - Ag - C<sub>13</sub> around the silver ion was 355,8° indicating a near trigonal planar

5.3e Confirmation of the Trigonal Planar Arrangement  
of O<sub>8</sub>, O<sub>11</sub>, C<sub>13</sub> Around the Silver Ion

The silver ion is closely surrounded by the four atoms O<sub>4</sub>, O<sub>8</sub>, O<sub>11</sub> and C<sub>13</sub>, all of which were initially considered to be possibly coordinated to the ion. There was originally some doubt as to whether the Ag - O<sub>4</sub> bond length of 2,73 Å constituted a significant bond or not, due to the fact that this value just exceeded the value of the sum of the silver and oxygen ionic radii (2,66 Å). In order to confirm that the arrangement of atoms about the silver ions was trigonal planar, four least squares planes were computed [See planes 10 - 13, Table XXIII b]. The calculation of least squares planes has been discussed on page 72. Each least squares plane was calculated using three of the four atoms O<sub>4</sub>, O<sub>8</sub>, O<sub>11</sub>, and C<sub>13</sub>. In each case the perpendicular distance of the silver ion to the plane was calculated.

If the silver ion was to be coordinated to all four atoms in a bonded fashion then a marked deviation of the silver ion from all four planes would be expected. In fact if the silver ion was to be tetrahedrally coordinated to the four atoms then theoretically the distance from the silver ion to each plane would be the same.

From Table XXIIIb it can be seen that the deviation of the silver ion from the first three planes varies markedly from 0,73 Å to 1,35 Å. Each of these planes contained the chelate oxygen O<sub>4</sub>. From the fourth least squares plane containing the atoms O<sub>8</sub>, O<sub>11</sub>, and C<sub>13</sub> the deviation was seen to be only 0,17 Å. Thus the silver ion was almost in the plane created by the atoms O<sub>8</sub>, O<sub>11</sub>, and C<sub>13</sub>. Least

squares plane No. 14 includes the silver ion in the calculation of the least squares plane.

The angles of these three atoms about the silver ion viz.  $C_{13} - Ag - O_8$ ,  $O_{11} - Ag - O_8$  and  $C_{13} - Ag - O_{11}$  were calculated to be  $106,2^\circ$ ,  $119,4^\circ$  and  $132,7^\circ$ . These angles have a total value of  $358,3^\circ$  which is very close to the theoretical value of  $360^\circ$  for a trigonal planar system.

It seemed favourable therefore to consider the coordination about the silver ion in terms of a trigonal planar arrangement rather than an irregular four fold arrangement.

Hence the evidence gained from the least squares planes supports the theory that the  $Ag - O_4$  bond distance of  $2,73 \text{ \AA}$  is not a bonding interaction. However it was considered as a very weak interaction and sterically to have a stabilizing influence on the silver ion [See Section 5.4].

The trigonal coordination of the silver ion may be explained by postulating  $sp^2$  hybridization of the empty  $5s$  and two  $5p$  orbitals of the silver ion. These orbitals would then act as acceptor orbitals to accommodate 'lone pair' electrons from the two oxygen atoms and the electron density associated with the methylene carbon atom of the chelate ring.

#### 5.4 The Planarity of the Chelate Rings

The three chelate rings in ferric acetylacetonate as reported by Iball and Morgan<sup>2</sup> were found to be planar within experimental error.

As the silver ion in the monoargentated complex was observed to be located in the vicinity of two of the chelate rings it was considered to be of interest to observe if any

deviations from planarity of the chelate rings had occurred.

Least squares planes for the three chelate rings were computed (Table XXIIIa). Planes 1 and 7 together contain the first chelate ring including the iron atom. Similarly planes 2 and 8 together contain the second chelate ring and planes 3 and 9 the third. Perpendicular distances of the atoms in each ring were calculated to the least squares planes (Equation 20).

Rings 1 and 2 (see least squares planes 7 and 8) were found to be planar. The greatest deviation of any one atom from the planes was  $0,03 \overset{\circ}{\text{A}}$ . This was not considered to represent a significant distortion of the rings.

Much larger distortions of ring 3 (least squares plane 9) were observed.  $C_{13}$  was displaced in the direction of the silver ion and was  $0,22 \overset{\circ}{\text{A}}$  from the least squares plane. The result of this displacement was that the two methyl carbon atoms  $C_{10}$  and  $C_{15}$  were located on the opposite sides of the plane (indicated by a negative sign in Table XXIIIa) at distances of  $0,13 \overset{\circ}{\text{A}}$  and  $0,14 \overset{\circ}{\text{A}}$  from the plane. The deviations of all the atoms in ring 3 from the least squares plane has been illustrated diagrammatically in Fig. 19.

It is possible that for each of the chelate rings a certain degree of bending can occur about an axis drawn through the dionato oxygens of each ring (Fig. 20). The extent by which each ring is bent about this axis can be obtained by measuring the angle between the pair of least squares planes constituting any one acetylacetonate ring (Table XXIV). For example the angle between least squares planes 1 and 7 gives the degree of bending in Ring 1.

The calculation of interplanar angles has been discussed on page 76.

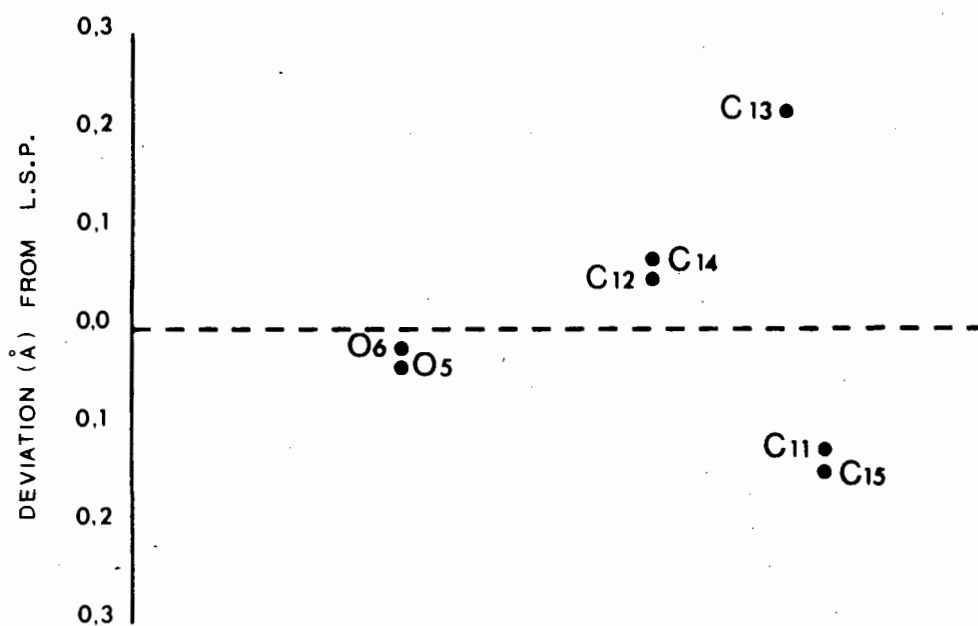


fig. 19

The dotted line represents the Least Squares Plane through atoms O5, O6, C11, C12, C13, C14, C15. The vertical scale is five times the horizontal scale.

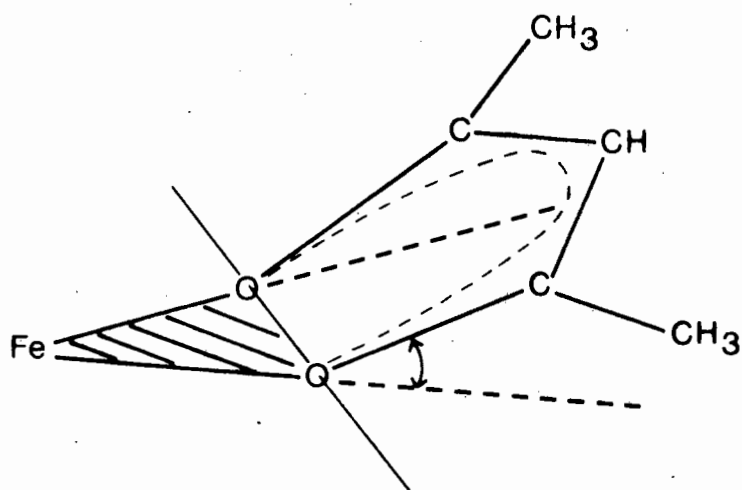


fig. 20

It is interesting to note that the bonding of the silver ion to  $C_{13}$  in ring 3 results in the ring being bent by  $15^{\circ} 47'$  in the direction of the silver ion. This clearly illustrates the significance of the  $Ag - C_{13}$  interaction.

As chelate ring 1 is not involved in any interaction with the silver ion or any other atom, the angle of deviation between planes 1 and 7 is expected to be minimal. The angle between the two planes was in fact found to be only  $2^{\circ} 54'$  which was not considered to be significant.

As the  $Ag - O_4$  interaction was considered to be non bonding, minimal bending of Ring 2 about the  $O_3 - O_4$  axis was expected. The angle between the planes in this case was found to be  $7^{\circ} 9'$ . The chelate ring was bent away from the silver ion as would be expected if the  $Ag - O_4$  bond was significant. Although the interplanar angle of  $7^{\circ} 9'$  was much smaller than was found for ring 3, it must be considered real, and for this reason the  $Ag - O_4$  interaction cannot be entirely discounted. It was concluded that although the  $Ag - O_4$  distance of  $2,73 \overset{\circ}{\text{Å}}$  reflected a very weak interaction, the dionato oxygen ( $O_4$ ) was considered to play an important part in stabilizing the structure.

The only other silver complex of a metal tris acetyl-acetate compound which has been solved by X-ray diffraction methods to date is the complex of trisilver dinitrate tris(acetylacetonato)nickelate II monohydrate<sup>7</sup>. In this complex however the silver ion was reported to be significantly bonded to the methylene carbon atom of one ring and also to a chelate oxygen of an adjacent ring. The  $Ag - O$  distance was given as  $2,46 \overset{\circ}{\text{Å}}$ . This is less than  $2,66 \overset{\circ}{\text{Å}}$  and therefore constitutes a significant bond (see page 87). The bonding of the silver ion to this

oxygen resulted in the chelate ring being bent by  $19^\circ$  about a line drawn through the two chelate oxygens. This deviation clearly reflects the strength of the Ag - O interaction in this complex in contrast to the much weaker interaction observed in the iron complex.

In the nickel complex the silver ion was also bonded to two oxygens of two separate nitrate ions to procure a coordination number of four.

### 5.5 Thermal Motion of the Methyl Groups

It is interesting to note that the thermal parameters of the methyl carbon atoms are relatively larger than the thermal parameters of the remaining atoms in the ferric acetylacetonate molecule. The methyl carbons were calculated to have a mean isotropic temperature factor of  $3,87 \text{ \AA}^2$  in contrast to the mean value of  $2,31 \text{ \AA}^2$  for the other atoms in the chelate ring.

This is not surprising as methyl groups are commonly known to exhibit large thermal motions and in some cases are in fact rotating.

### 5.6 The Perchlorate Ion

The perchlorate oxygens are arranged in a tetrahedral fashion around the chlorine ion. The tetrahedron is not extensively distorted from its theoretical shape. Three Cl - O distances are close to the expected Cl - O distance of  $1,43 \text{ \AA}$ . (Table XX). However the Cl - O<sub>7</sub> distance is very much contracted and is only  $1,27 \text{ \AA}$ . There seems to be no apparent reason for the shortening of the Cl - O<sub>7</sub> bond distance. However due to the extremely high thermal motion of this perchlorate oxygen the distortion in this

bond distance is probably not significant. The six tetrahedral angles are in relatively good agreement with the theoretical value of  $109^{\circ} 28'$ , and fall within the wide range generally found for perchlorate anions, viz.  $96^{\circ} - 117^{\circ 91}$ .

Large thermal parameters were observed for all four perchlorate oxygens (Table XIX). This thermal motion is illustrated in Fig. 13. Disorder and high thermal motion are not uncommon in perchlorate structures, and in the dioxane - silver perchlorate complex<sup>26</sup> the perchlorate oxygens were found to be rotating at room temperature.

The silver ion is bonded to only one perchlorate oxygen ( $O_8$ ). As a result of this interaction with the silver ion,  $O_8$  is stabilized and is hence observed to have the smallest isotropic thermal parameter ( $B = 10,03 \overset{\circ}{\text{A}}^2$ ) of all the perchlorate oxygens. The temperature factor of  $O_{10}$  was not much higher ( $B = 10,34 \overset{\circ}{\text{A}}^2$ ) but for  $O_7$  and  $O_9$  high isotropic temperature factor values of  $21,44 \overset{\circ}{\text{A}}^2$  and  $14,20 \overset{\circ}{\text{A}}^2$  were recorded. The lower value of  $B$  for  $O_{10}$  could possibly be attributed to stabilization of this atom through hydrogen bonding to the hydrate molecule. This will be discussed in the next section.  $O_7$  and  $O_9$  are not stabilized by any interaction with other atoms. This fact accounts for their very high  $B$  values in contrast to those of  $O_8$  and  $O_{10}$ .

The silver to oxygen ( $O_8$ ) distance of  $2,50 \overset{\circ}{\text{A}}$  is in agreement with the fact that perchlorate groups are important in the stabilization of these structures (Section 1.4). Shorter Ag - O distances have been reported in the silver perchlorate complexes of naphthalene<sup>40</sup> and anthracene<sup>40</sup>.

Values of the Ag - O distances in these structures varied from 2,34 Å to 2,46 Å. Similar Ag - O bonding distances have also been reported in the structures of  $\text{Ag}_3\text{PO}_4$ <sup>80</sup>,  $\text{Ag}_3\text{AsO}_4$ <sup>81</sup> and  $\text{Ag}_2\text{MoO}_4$ <sup>82</sup> (Table XXVI).

### 5.7 Hydrogen Bonding

In a recent account of the determination of the positions of hydrogen atoms in crystalline solids using X-ray diffraction data W.H.Bauer<sup>92</sup> states: "By X-ray diffraction the determination of the hydrogen atom positions is possible with a high degree of confidence in the presence of light atoms only. Therefore the hydrogen atom positions found in crystal structures of organic compounds where the heavy atoms are C, N, and O, are fairly reliable. In the presence of heavier atoms, the precision of the hydrogen atom coordinates is not only much lower but the probability of making a completely wrong assignment increases sharply. The reason for this is the low scattering power of hydrogen for X-rays so that the electron densities found in difference maps at the expected hydrogen atom sites are usually around  $5e \text{ \AA}^{-3}$ . This means that they are of approximately the same height as the background peaks even in the most precise structure determinations".

For this reason, as the structure of  $\text{Fe}(\text{acac})_3 \cdot \text{AgClO}_4 \cdot \text{H}_2\text{O}$  contains two heavy atoms viz. silver and iron, no attempt was made to locate any of the hydrogen atoms on a difference Fourier map.

However as it was possible that the hydrogen atoms of the hydrate molecule were H-bonded to one or two oxygen atoms in the structure, the model was studied in an attempt to locate possible positions for the hydrate hydrogens, from which H-bonding was likely to occur.

In the structure of ice<sup>93</sup> each oxygen atom is surrounded tetrahedrally by four other oxygen atoms. The O - O distance is 2,76 Å. There is one proton along each O - O axis resulting in the formation of hydrogen bonds (Fig. 21). The O - H bond distance was determined by neutron diffraction of deuterium oxide ice to be 1,01 Å.

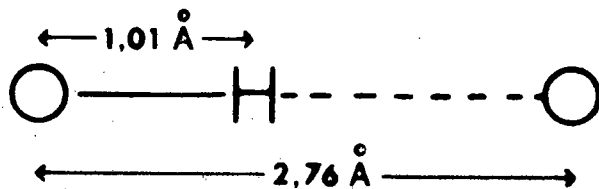


fig. 21

By means of the program "ORTEP" the vicinity of the hydrate oxygen ( $O_{11}$ ) was scanned. The two shortest oxygen to oxygen distances were computed to be 2,79 Å and 2,98 Å. These values corresponded to the separations  $O_{11} - O_2$  and  $O_{11} - O_{10}$ . The chelate oxygen atom  $O_2$  in this case belonged to an adjacent iron acetylacetonate molecule and the oxygen atom  $O_{10}$  to a neighbouring perchlorate ion. The next shortest O - O distance was 3,57 Å which corresponded to the separation  $O_{11} - O_9$ .

The oxygen to oxygen distances compared favourably with the value of 2,76 Å found in ice. The angle  $O_2 - O_{11} - O_{10}$  was computed to be  $107,7^\circ$  which is in close agreement with the theoretical tetrahedral angle of  $109^\circ 28'$  found in ice.

From this information it seemed highly probable that the hydrogen atoms of the hydrate molecule would be located along the lines drawn from  $O_{11}$  to the atoms  $O_2$  and  $O_{10}$ .

## 5.8 The Structure as Interpreted from Infrared Spectral Data

The infrared spectra of ferric acetylacetonate and its monoargentated adduct have been discussed in Section 1.10.

Numerous authors<sup>43,45</sup> have considered that in metal  $\beta$ -ketoenolate structures the ligand  $\pi$  electron density is extensively delocalized to equalize the bond orders of the C = O and C = C bonds in the chelate ring. Both of these groups have stretching frequencies in the  $1400\text{ cm}^{-1}$  to  $1600\text{ cm}^{-1}$  region. Various theories have been put forward as to which of the two bands in this region is the carbonyl stretching mode and which is the C = C stretching vibration. Kline *et al*<sup>46</sup> believed that the first strong band in the  $1600\text{ cm}^{-1}$  region was due to the C = C stretching mode, and that the lower frequency was attributed to a C = O stretch. More recent work has led to a reversal of these assignments<sup>48,49</sup>.

For this work the interpretation of the band frequencies was that given by Kline *et al*<sup>46</sup>. These authors postulated two types of structures for argentated complexes of metal acetylacetonates [Section 1.10e].

According to their theory, the silver ion in the monoargentated complexes was thought to be located directly above the C = C region of the chelate ring where  $\pi$  bonding as described by Dewar<sup>32</sup> could best be accomplished. In these complexes it was also believed that there was no bonding of the silver ion to any oxygen of the chelate rings. In the di and tri argentated complexes the silver ion was thought to be bonded to the oxygens of an adjacent chelate ring as well as being  $\pi$  bonded to the C = C regions of the chelate ring.

In the infrared spectra obtained for iron acetylacetonate and its monoargentated adduct no change in the C = O frequency was in fact observed (see Table I). This implied the absence of bonding from the silver ion to an

oxygen atom of a chelate ring. Structure analysis of the crystal confirmed this to be true. Although the  $\text{Ag} - \text{O}_4$  bond distance was found to be  $2.73 \overset{\text{O}}{\text{Å}}$ , this was considered to be a very weak interaction and was therefore not likely to affect the ring  $\text{C} = \text{O}$  stretching frequency.

The silver ion however was not located directly above the  $\text{C} = \text{C}$  region of the chelate ring, but was asymmetrically located above the central methylene carbon atom ( $\text{C}_{13}$ ). However even with the silver ion in this position a reduction in the  $\text{C} = \text{C}$  stretching frequency would still be expected as the silver ion acts as an electron acceptor, capable of withdrawing electrons from the ring. A reduction in the  $\text{C} = \text{C}$  frequency was observed on complexing ferric acetylacetonate with silver (Table I).

Thus the structure of the monoargentated complex of iron acetylacetonate as solved by X-ray diffraction techniques supports the theory in regard to  $\text{Ag} - \text{O}$  bonding as outlined by Kline *et al*<sup>46</sup>.

It must be pointed out that only small changes in the band frequencies were observed. Although the silver ion is considered to be an electron acceptor in this complex, the small amount of charge that is believed to be transferred from the ring to the ion to create a  $\text{Ag} - \text{C}$  interaction is not expected to alter the bond distances in the ring greatly.

When the values of the  $\text{C} - \text{O}$  bond lengths in rings 1, 2, and 3 are compared (Table XX) it was observed that the  $\text{C} - \text{O}$  bonds were not significantly different from one another. This evidence also inferred the absence of  $\text{Ag} - \text{O}$  bonding. The  $\text{C} - \text{C}$  bond lengths in ring 3 were however slightly longer than those found in rings 1 and 2.

If the Ag - C interaction was considered to be a real covalent interaction then electrons from the methylene carbon atom would be withdrawn from the ring to a greater extent than if the bonding was of an ionic nature. In the former case the withdrawal of electrons from the methylene carbon atom would most likely cause a greater increase in the C - C bond lengths adjacent to the Ag - C bond than was actually observed. It is difficult to postulate the exact nature of the Ag - C bond but in terms of Infrared and C - C bond length data it seems likely that the bonding is predominantly ionic.

### 5.9 INTERMOLECULAR STRUCTURE: Special Projections of the Structure.

The intermolecular structure of the adduct has been illustrated by viewing the structure down the X, Y and Z axes of the unit cell. These viewing directions yield the special projections [100], [010] and [001] respectively (Figs. 22, 23 and 24). These projections were obtained with the aid of the plotter program "ORTEP".

The symmetry of each of these projections is as follows:-

In the [100] projection which has pgg symmetry, the glide planes run parallel to the Y and Z\* directions (Fig. 22).

The [010] projection has p2 symmetry which is revealed by a centre of inversion located at the centre of the cell (Fig. 23).

The [001] projection has the plane group symmetry p<sub>g</sub>m. The glide and mirror planes run parallel to the Y and X\* directions respectively (Fig. 24).

### 5.10 STEREOSCOPIC ILLUSTRATION.

A stereo pair of the molecule (Fig. 25) was produced using the plotter program "ORTEP". The two figures were drawn from two different view points which were 6° apart.

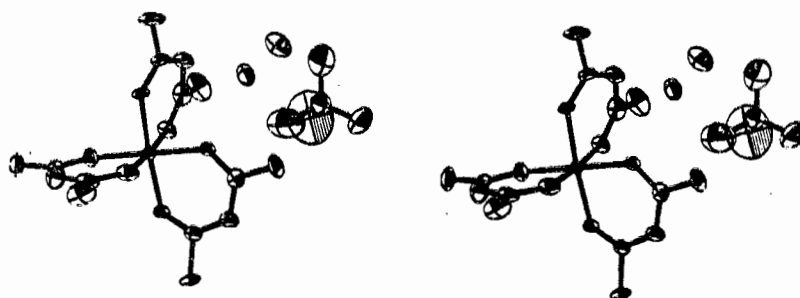


Fig. 25

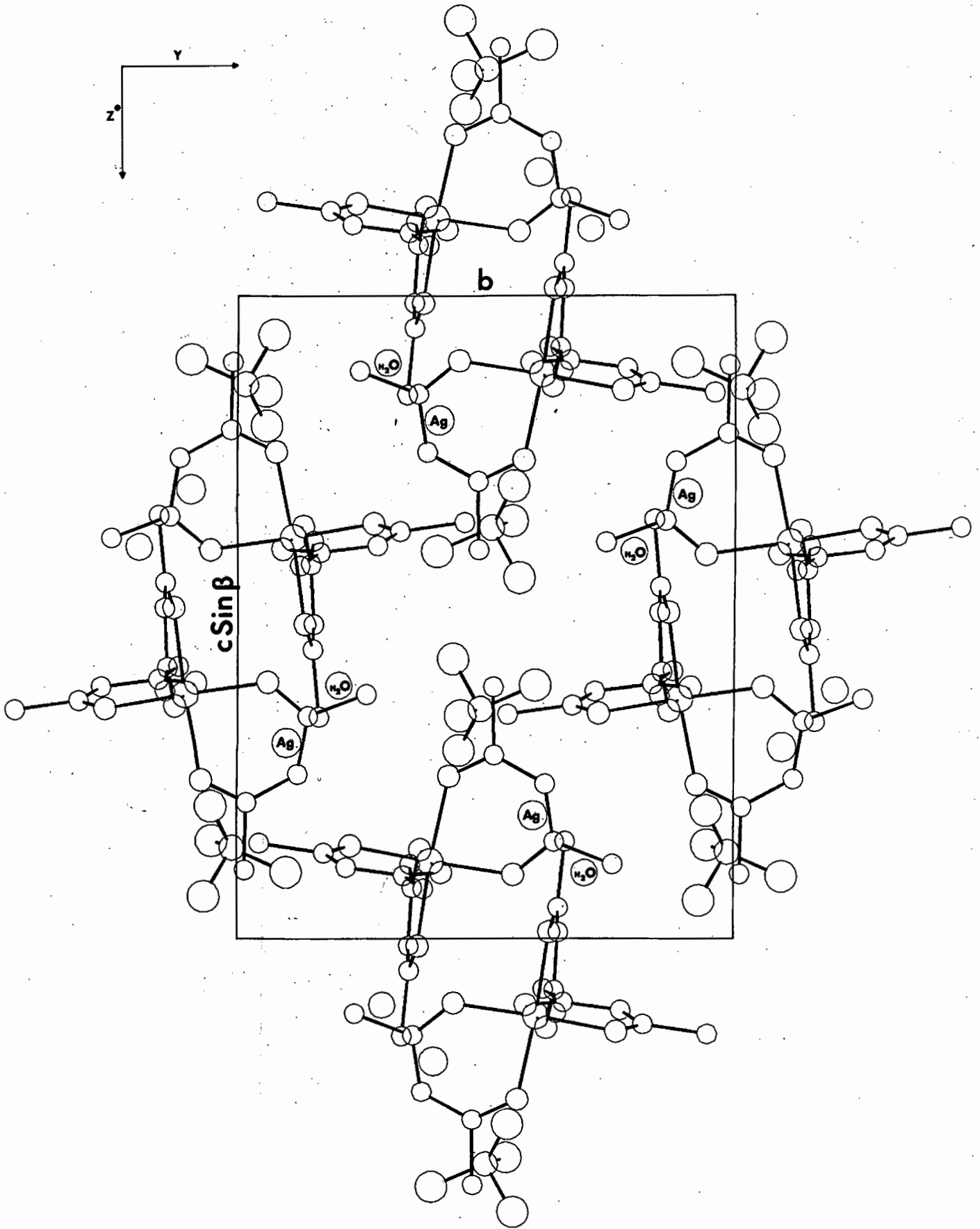
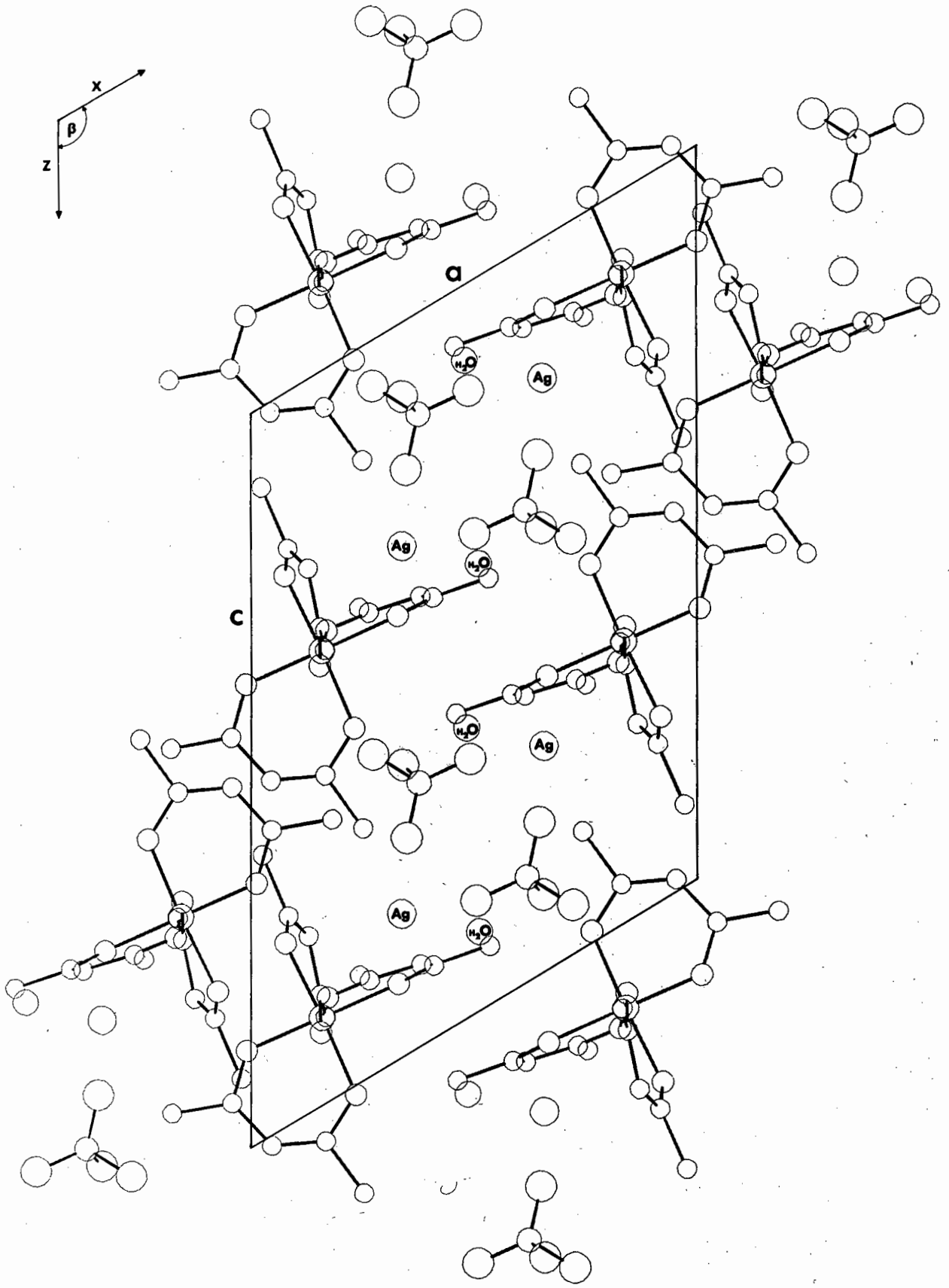


Fig. 22

(100) PROJECTION



**Fig.23**  
**( 010 ) PROJECTION**

5 Å

## LIST OF REFERENCES

1. R.B. Roof. *Acta Cryst.* 9, p781, (1956).
2. J. Iball and C.H. Morgan. *Acta Cryst.* 23, p239 (1967).
3. B. Morosin. *Acta Cryst.* 19, p131, (1965).
4. B. Morosin and J.R. Brathovde. *Acta Cryst.* 17, p705, (1964).
5. B. Morosin and H. Montgomery. *Acta Cryst.*(B). 25, p1354 (1969).
6. J.P. Collman. *Transition Metal Chem.* Vol.2, p35, (R.L. Carlin 1966)
7. W.H. Watson. Jr., and Chi-Tsun Ling. *Inorg. Chem.* 5, No. 6, p1074 (1966).
8. A.G. Swallow and M.R. Truter. *Proc. Roy. Soc. (London)* A254, p205, (1960).
9. A.C. Hazell and M.R. Truter. *Proc. Roy. Soc. (London)* A254, p218 (1960).
10. A.G. Swallow and M.R. Truter. *Proc. Roy. Soc. (London)* A266, p527 (1962).
11. J.P. Fackler Jr. T.S. Davis and I.D. Chawla, *Inorg. Chem.* 4, p130 (1965).
12. J. Endo. *J. Chem. Soc. Japan.* 65, p34 (1955).
13. P.D. Hopkins and B.E. Douglas, *Inorg. Chem.* 3, p357, (1964).
14. J.F. Steinbach, and J.H. Burns, *J. Am. Chem. Soc.* 80, p1839 (1958).
15. J.P. Fackler Jr., *Progress in Inorg. Chem.* 7, p361(1966).
16. P.C.L. Thorne, and E.R. Roberts. *Inorganic Chemistry* 5th ed. p390 (1948).
17. F.A. Cotton and G. Wilkinson. *Advanced Inorg. Chem.* 3rd ed. p478 (1972).
18. *Ibid.* p.644.
19. N.V. Sidgwick, *Chemical Elements and their Compounds* Vol. I, p129 (1950).
20. F.A. Cotton and G. Wilkinson. *Advanced Inorg. Chem.* 3rd ed. p1046 (1972).
21. P.F. Rodesiler, E.A. Hall Griffith and E.L. Amma. *J. Am. Chem. Soc.* 94, p761 (1972).
22. E.A. Hall Griffith and E.L. Amma. *J. Am. Chem. Soc.* 93, p3167 (1971).
23. I.F. Taylor Jr., E.A. Hall and E.L. Amma. *J. Am. Chem. Soc.* 91, p5745, (1969).
24. D.M. Barnhart, C.N. Caughlan, Mazhar-ol-Haque, *Inorg. Chem.* 8, p2768 (1969).
25. E.G. Cox, W. Wardlaw and K.C. Webster. *J. Chem. Soc.* p775, (1936).
26. R.J. Prosen and K.N. Trueblood. *Acta Cryst.* 9, p741 (1956).
27. R.W. Turner and E.L. Amma. *J. Am. Chem. Soc.* 88, p3243 (1966).

28. F.A. Cotton and G. Wilkinson. *Advanced Inorg. Chem.* 3rd ed. p730 (1972).
29. A.E. Hill. *J. Am. Chem. Soc.* 43, p254 (1921).
30. A.E. Hill. *J. Am. Chem. Soc.* 44, p1163 (1922).
31. A.E. Hill. *J. Am. Chem. Soc.* 47, p2702 (1925).
32. M.J.S. Dewar, *Bull. Soc. Chim. Fr.* C.71. (1951).
33. L.J. Andrews and R.M. Keefer. *J. Am. Chem. Soc.* 71, p3644 (1949).
34. L.J. Andrews and R.M. Keefer. *J. Am. Chem. Soc.* 72, p3113 (1950).
35. *Ibid.* p5034.
36. S. Winstein and H.J. Lucas. *J. Am. Chem. Soc.* 60, p836 (1938).
37. R.S. Mulliken, *J. Am. Chem. Soc.* 74, p811 (1952).
38. H.G. Smith and R.E. Rundle. *J. Am. Chem. Soc.* 80, p5075 (1958).
39. I.F. Taylor Jr., and E.L. Amma. *Chem. Comm.* p1442 (1970).
40. E.A. Hall and E.L. Amma. *J. Am. Chem. Soc.* 91, p6538(1969).
41. C.S. Ginsberg. *Diss. Abstr.*, 25, p2219 (1964).
42. C.H. Oestreich. *Diss Abstr.*, 22, p2184 (1962).
43. K. Nakamoto and A.R. Martell. *J. Chem. Phys.* 32, p588 (1960)
44. K. Nakamoto, P.J. McCarthy, A. Ruby, and A.R. Martell. *J. Am. Chem. Soc.* 83, p1066(1961).
45. K. Nakamoto, P.J. McCarthy and A.R. Martell. *J. Am. Chem. Soc.* 83, p1272 (1961).
46. R.J. Kline, C.S. Ginsberg and C.H. Oestreich. *Spectrochimica Acta.* 22, p1923 (1966).
47. M. Mikami, I. Nakagawa, and T. Shimanouchi, *Spectrochimica Acta.* 23A, p1037 (1967).
48. G.T. Behnke and K. Nakamoto. *Inorg. Chem.* 6, p433 (1967).
49. R.D. Hancock and D.A. Thornton. *Jour. Mol. Struct.* 4, p361(1969).
50. S. Pinchas, B.L. Silver and I. Laulicht. *J. Chem. Phys.* 46, p1506 (1967).
51. M.J. Buerger. *X-ray crystallography.* p372 (John Wiley 1942).
52. G.H. Stout and L.H. Jensen. *X-ray Structure Determination.* p66 (Macmillan 1968).
53. O. Weisz and W.F. Cole. *J. Sci. Instr.* 25, p213 (1948).
54. M.J. Buerger. *Crystal Structure Analysis.* p86 (John Wiley 1967).
55. M.J. Buerger. *X-ray crystallography.* Ch. 14 (John Wiley 1942).
56. M.J. Buerger. *Crystal Structure Analysis.* p86 (John Wiley 1967).
57. Stout and Jensen. *X-ray Structure Determination.* p167, p204(Macmillan 1968).

58. *International Tables for X-ray Crystallography*. II, p266 (1959).
59. M.J. Buerger. *Crystal Structure Analysis*. p554 (John Wiley 1967).
60. M.J. Buerger. *Vector Space*. p25 (John Wiley (1959)).
61. *International Tables for X-ray Crystallography*. I, p99 (1959).
62. G.H. Stout and L.H. Jensen. *X-ray Structure Determination*. p200 (Macmillan 1968).
63. D.T. Cromer and J.T. Waber. *Acta Cryst.* 18, p104 (1965).
64. G.H. Stout and L.H. Jensen. *X-ray Structure Determination*. p217 (Macmillan 1968).
65. *Ibid.* p222.
66. M.J. Buerger. *Crystal Structure Analysis*. p585 (John Wiley 1967).
67. G.H. Stout and L.H. Jensen. *X-ray Structure Determination*. p356 (Macmillan 1968).
68. L.R. Nassimbeni. *Ph.D. Thesis*. University of Cape Town (1969).
69. G.H. Stout and L.H. Jensen. *X-ray Structure Determination*. p385 (Macmillan 1968).
70. G.H. Stout and L.H. Jensen. *X-ray Structure Determination*. p.450 (Macmillan 1968).
71. G.H. Stout and L.H. Jensen. *X-ray Structure Determination*. p177 (Macmillan 1968).
72. *Ibid* p185
73. *Ibid* p183
74. *Ibid* p182
75. *International Tables for X-ray Crystallography*. II, p43 (1959).
76. G.H. Stout and L.H. Jensen. *X-ray Structure Determination*. p424 (Macmillan 1968).
77. K. Fukui, A. Imumara, T. Yonezawa, and C. Nagata. *Bull. Chem. Soc. Japan*. 34, p1046 (1961).
78. *Handbook of Chemistry and Physics*. F - 154 (R.C. Weast 1970 - 1971).
79. L. Pauling. *The Nature of the Chemical Bond*. p514, Cornell University Press. Ithaca, N.Y. (1960).
80. L. Helmholtz. *J. Chem. Phys.* 4, p316 (1936).
81. L. Helmholtz and R. Levine. *J. Am. Chem. Soc.* 64, p354 (1942).
82. J. Donohue and W. Shand Jr., *J. Am. Chem. Soc.* 69, p222 (1947).
83. N.C. Baenziger, H.L. Haight, R. Alexander and J.R. Doyle. *Inorg. Chem.* 5, p1399 (1966).
84. F.S. Mathews and W.N. Lipscomb. *J. Phys. Chem.* 63, p845 (1959).

85. J.S. McKechnie and I.C. Paul. *Jour. Chem. Soc. B.Part 2.* p1445 (1968).
86. R.B. Jackson and W.E. Streib. *J. Am. Chem. Soc.* 89, p2539 (1967).
87. A.G. Swallow and M.R. Truter. *Proc. Roy Soc. (London)* A254, p205 (1960).
88. A.C. Hazell and M.R. Truter. *Proc. Roy Soc.* A254, p218 (1960).
89. A.G. Swallow and M.R. Truter. *Proc. Roy Soc.* A266, p527 (1962).
90. A. Robson and M.R. Truter. *Jour. Chem. Soc.* p630 (1965).
91. P.E. Riley and K. Seff. *Inorg Chem.* Vol 11 No. 12. p2993 (1972).
92. W.H. Baur. *Acta Cryst.* B28, p1456 (1972).
93. L. Pauling. *The Nature of the Chemical Bond.* p464. Cornell University Press, Ithaca, N.Y. (1960).



	$h$	$k$	$F_O$	$F_C$		$h$	$k$	$F_O$	$F_C$		$h$	$k$	$F_O$	$F_C$
$\ell=-12$	6	-4	758	808		2	-5	295	329		4	-7	853	-878
	7	-4	973	994		3	-5	450	475		3	-7	284	-284
	8	-4	449	-442		5	-5	669	698		2	-7	387	409
	9	-4	72	71		6	-5	65	79		1	-6	703	695
	10	-3	631	-644		7	-5	1194	-1211		2	-6	775	829
	9	-3	711	732		8	-5	86	-84		3	-6	411	-417
	8	-3	942	964		9	-5	265	247		4	-6	189	171
	7	-3	248	-246		10	-5	219	-210		5	-6	329	-325
	6	-3	113	-104		10	-4	90	104		6	-6	792	-795
	5	-3	292	-324		9	-4	366	-388		7	-6	441	444
	4	-3	901	-983		8	-4	87	92		8	-6	214	204
	3	-3	615	661		7	-4	75	62		9	-6	240	-278
	2	-3	565	542		5	-4	410	421		8	-5	184	157
	1	-3	171	-195		4	-4	307	290		7	-5	180	187
	1	-2	313	-322		3	-4	372	-346		6	-5	408	394
	2	-2	198	166		2	-4	106	121		5	-5	83	102
	3	-2	359	-377		1	-4	285	-299		4	-5	322	-308
	4	-2	216	210		1	-3	311	-317		2	-5	107	144
	5	-2	487	487		2	-3	191	204		1	-5	354	372
	6	-2	270	-258		3	-3	178	183		1	-4	884	841
	8	-2	74	79		4	-3	431	450		2	-4	885	902
	9	-2	217	-231		5	-3	70	28		3	-4	346	-338
	10	-2	400	407		6	-3	175	-133		4	-4	211	208
	11	-2	159	140		7	-3	362	-356		5	-4	332	-345
	10	-1	518	-550		8	-3	359	-351		6	-4	770	-785
	9	-1	483	990		9	-3	260	225		7	-4	713	707
	8	-1	583	603		11	-3	72	46		8	-4	706	684
	7	-1	251	-246		11	-2	502	506		9	-4	92	-126
	5	-1	342	-357		10	-2	191	216		10	-4	90	97
	4	-1	305	-321		9	-2	939	-965		11	-3	426	-428
	3	-1	370	361		8	-2	186	148		10	-3	422	448
	2	-1	439	425		7	-2	396	395		9	-3	349	363
	1	0	664	-672		6	-2	131	138		8	-3	685	-707
	2	0	1254	1245		5	-2	1271	1322		7	-3	79	-61
	3	0	443	-487		4	-2	167	-203		6	-3	638	-607
	4	0	369	375		3	-2	1307	-1291		5	-3	486	-467
	5	0	801	850		2	-2	240	-236		4	-3	1121	1105
	6	0	1451	-1543		1	-2	85	73		3	-3	572	564
	7	0	373	-366		1	-1	1309	1230		2	-3	417	-372
	8	0	382	423		3	-1	569	-594		1	-3	303	265
	10	0	382	356		4	-1	563	605		1	-2	457	459
$\ell=-11$	6	-8	146	159		5	-1	839	-868		2	-2	581	-559
	5	-8	412	-408		7	-1	1550	1607		3	-2	376	366
	3	-8	543	546		8	-1	314	-328		5	-2	172	-233
	2	-8	280	-296		9	-1	167	161		6	-2	996	985
	5	-7	305	358		10	-1	404	403		8	-2	463	-462
	6	-7	387	415		11	-1	703	-726		9	-2	411	384
	9	-6	747	746	$\ell=-10$						10	-2	522	-517
	7	-6	167	-166		2	-8	471	-470		11	-2	132	145
	6	-6	160	-147		4	-8	545	534		11	-1	580	-579
	5	-6	484	-452		7	-8	494	-489		9	-1	177	199
	4	-6	272	254		8	-7	478	454		8	-1	423	-434
	3	-6	748	760		7	-7	238	-230		7	-1	84	99
	2	-6	114	-134		6	-7	571	537		6	-1	515	-458
	1	-5	863	-887		5	-7	525	554		5	-1	648	-656

$h$	$k$	$F_O$	$F_C$	$h$	$k$	$F_O$	$F_C$	$h$	$k$	$F_O$	$F_C$
$\ell=-7$											
4	-10	151	-129	4	-3	243	-285	9	-6	220	-169
3	-10	222	190	5	-3	589	586	9	-5	277	244
2	-10	239	277	8	-3	824	787	8	-5	225	-227
1	-10	133	-148	9	-3	372	-347	7	-5	403	-343
1	-9	369	-350	11	-2	549	-556	6	-5	96	-123
2	-9	494	-533	10	-2	828	825	5	-5	337	325
3	-9	650	639	9	-2	204	182	4	-5	521	493
4	-9	100	936	7	-2	982	891	3	-5	582	555
6	-9	281	279	6	-2	873	-835	2	-5	97	-74
7	-8	258	-266	5	-2	952	-868	1	-5	364	-334
6	-8	648	619	4	-2	1449	1418	2	-4	720	-590
5	-8	428	426	1	-2	1054	1019	3	-4	672	-689
4	-8	566	-550	1	-1	1548	-1432	4	-4	758	689
3	-8	154	163	2	-1	1609	-1479	5	-4	202	-119
1	-8	559	-560	3	-1	714	648	7	-4	454	384
1	-7	368	-389	4	-1	117	134	8	-4	1048	-993
2	-7	582	568	5	-1	200	-174	9	-4	535	-488
3	-7	80	659	6	-1	610	577	10	-4	583	528
4	-7	144	-123	7	-1	735	-738	11	-3	429	-418
5	-7	127	123	8	-1	649	-604	10	-3	636	-594
6	-7	526	-494	9	-1	313	322	9	-3	300	291
7	-7	103	103	10	-1	67	43	8	-3	432	-444
8	-7	132	99	$\ell=-6$				6	-3	1819	1710
9	-7	413	-358	1	-10	368	-363	5	-3	994	-858
9	-6	378	-362	2	-10	666	640	4	-3	204	-218
8	-6	72	48	3	-10	179	188	3	-3	1019	920
6	-6	846	784	4	-10	697	-698	2	-3	1206	-1159
5	-6	395	348	5	-10	213	227	1	-3	374	338
4	-6	330	-296	7	-9	207	202	1	-2	1309	-1223
3	-6	244	-207	6	-9	433	-429	2	-2	971	961
2	-6	244	-263	5	-9	190	165	4	-2	240	-183
1	-6	783	-765	4	-9	259	266	5	-2	666	619
1	-5	628	568	3	-9	535	-540	6	-2	583	-546
2	-5	1097	1073	2	-9	372	360	7	-2	351	-369
3	-5	808	-789	1	-9	89	-105	8	-2	376	382
4	-5	709	-737	2	-8	594	602	9	-2	233	-213
5	-5	743	700	3	-8	105	95	10	-2	152	109
6	-5	598	-555	4	-8	731	-703	11	-2	105	-84
7	-5	569	554	6	-8	141	-136	11	-1	77	-78
8	-5	974	936	8	-8	218	177	10	-1	382	-348
9	-5	887	-829	9	-7	214	-207	8	-1	397	-393
10	-5	239	-227	8	-7	245	241	7	-1	62	70
11	-4	429	-399	6	-7	1331	-1319	6	-1	1110	1017
10	-4	300	259	5	-7	424	402	5	-1	187	-224
9	-4	159	-154	4	-7	512	488	4	-1	548	-535
8	-4	70	-40	3	-7	102	-116	3	-1	1261	1042
7	-4	948	888	2	-7	728	682	2	-1	1709	-1602
6	-4	410	-374	1	-7	359	-377	1	-1	101	151
5	-4	493	-442	1	-6	235	155	2	0	1516	1562
4	-4	497	428	2	-6	869	-762	3	0	625	532
3	-4	473	-458	3	-6	254	-265	4	0	1485	-1429
1	-4	980	954	4	-6	932	867	5	0	598	644
2	-3	357	326	6	-6	242	-209	6	0	489	-497
3	-3	330	-255	7	-6	160	136	7	0	606	-574
				8	-6	652	-608	8	0	1787	1834

	$h$	$k$	$F_o$	$F_c$		$h$	$k$	$F_o$	$F_c$		$h$	$k$	$F_o$	$F_c$
$\ell=-6$	10	0	719	-731		8	-2	501	449		6	-5	269	263
	11	0	212	-195		7	-2	1320	-1284		5	-5	214	202
$\ell=-5$	5	-10	109	121		6	-2	782	-701		4	-5	128	97
	4	-10	288	293		5	-2	1841	1748		3	-5	615	-500
	2	-10	371	383		4	-2	697	-559		2	-5	423	-373
	1	-10	122	141		3	-2	307	268		1	-5	331	312
	2	-9	243	241		2	-2	1219	1138		1	-4	629	-461
	3	-9	774	-744		1	-2	1966	-1859		2	-4	823	773
	4	-9	377	337		1	-1	476	435		3	-4	1016	-979
	5	-9	167	144		2	-1	1029	923		4	-4	751	-680
	6	-9	170	-172		3	-1	2657	-2593		5	-4	825	790
	7	-9	462	455		4	-1	675	653		6	-4	210	200
	8	-8	367	-341		5	-1	1247	1181		7	-4	309	297
	7	-8	965	941		6	-1	487	-502		8	-4	313	273
	6	-8	127	104		7	-1	578	572		9	-4	424	-404
	5	-8	894	-863		8	-1	467	-453		10	-4	288	-268
	4	-8	593	589		9	-1	1048	-1065		10	-3	540	520
	3	-8	181	-159		10	-1	436	440		9	-3	360	-304
	2	-8	385	-403		11	-1	108	121		8	-3	311	260
	1	-8	1191	1172	$\ell=-4$	1	-10	252	234		7	-3	1150	1109
	1	-7	561	-517		2	-10	490	-496		6	-3	1760	-1652
	5	-7	217	256		3	-10	158	140		5	-3	414	-408
	7	-7	117	-114		4	-10	596	596		4	-3	801	718
	8	-7	203	-214		5	-10	484	-489		3	-3	1527	-1390
	7	-6	686	663		7	-9	602	-568		2	-3	353	329
	6	-6	128	97		6	-9	297	294		1	-3	1637	1534
	5	-6	912	-860		4	-9	263	-231		1	-2	205	198
	2	-6	348	-331		3	-9	546	524		2	-2	658	-614
	1	-6	1421	1333		2	-9	301	-298		3	-2	1025	-811
	1	-5	362	-373		1	-9	392	-372		4	-2	562	514
	3	-5	988	832		2	-8	96	-129		5	-2	296	-286
	4	-5	667	-581		3	-8	113	80		8	-2	493	-534
	5	-5	1059	-944		4	-8	569	555		9	-2	176	188
	7	-5	435	-446		5	-8	574	-552		10	-2	308	314
	8	-5	134	108		6	-8	480	-449		11	-1	150	-178
	9	-5	921	903		9	-7	311	313		10	-1	152	178
	10	-5	164	-206		8	-7	469	-444		9	-1	254	-244
	10	-4	163	-144		7	-7	977	-959		8	-1	319	289
	8	-4	322	257		6	-7	841	781		7	-1	533	513
	7	-4	760	-689		5	-7	586	555		6	-1	1011	-914
	6	-4	749	-702		4	-7	230	-208		5	-1	447	-400
	5	-4	969	855		3	-7	496	445		4	-1	461	378
	4	-4	980	-895		2	-7	1011	-985		3	-1	1232	-1160
	3	-4	397	353		1	-7	759	-792		2	-1	306	-249
	2	-4	875	828		1	-6	235	-169		1	-1	1622	1496
	1	-4	781	-778		2	-6	682	671		1	0	1709	1638
	3	-3	617	546		3	-6	981	-924		3	0	1039	834
	4	-3	275	-264		4	-6	711	-661		4	0	1260	1317
	5	-3	510	-417		5	-6	600	589		5	0	1894	-1883
	6	-3	392	-402		6	-6	339	291		6	0	1342	-1296
	9	-3	331	302		7	-6	295	272		8	0	999	-1073
	10	-3	64	-21		8	-6	350	327		9	0	1348	1369
	11	-3	334	-345		9	-6	294	-282		10	0	501	488
	11	-2	787	771		8	-5	335	-350		11	0	596	-606
	10	-2	299	-309		7	-5	305	287					



	$h$	$k$	$F_o$	$F_c$		$h$	$k$	$F_o$	$F_c$		$h$	$k$	$F_o$	$F_c$
$\ell=-1$	7	-8	564	-542		1	-2	1372	1201		9	-4	337	-296
	6	-8	519	502		2	-1	709	-742		9	-3	247	212
	5	-8	167	129		3	-1	1955	2053		8	-3	676	-686
	4	-8	160	-133		4	-1	1154	1267		7	-3	355	345
	3	-8	846	893		5	-1	1764	-1838		6	-3	289	287
	2	-8	328	-307		6	-1	649	-628		5	-3	613	-673
	1	-8	943	-919		7	-1	304	294		4	-3	658	740
	1	-7	661	-583		9	-1	147	168		3	-3	540	476
	2	-7	255	237		10	-1	349	353		2	-3	1392	-1453
	3	-7	312	346		$\ell=0$	2	-11	359		-440	1	-3	311
4	-7	725	-757	1	-11		117	-149	0	-2	1432	1659		
5	-7	184	-218	0	-10		575	611	1	-2	391	-478		
6	-7	95	83	1	-10		364	-456	3	-2	1145	1189		
7	-7	400	-391	2	-10		189	-209	4	-2	708	-747		
8	-7	364	361	3	-10		382	445	5	-2	286	-216		
8	-6	340	-360	4	-10		582	-626	6	-2	190	188		
7	-6	304	-276	6	-9		256	-266	7	-2	367	-371		
4	-6	132	142	5	-9		283	285	9	-2	155	139		
3	-6	972	990	3	-9		77	137	10	-1	350	296		
2	-6	596	-558	2	-9	553	626	9	-1	114	79			
1	-6	1480	-1415	1	-9	219	-256	8	-1	566	-579			
1	-5	1708	-1563	0	-8	805	884	7	-1	312	330			
2	-5	233	-257	1	-8	311	311	6	-1	90	90			
3	-5	78	164	3	-8	121	-94	5	-1	500	-536			
4	-5	1008	-1053	4	-8	400	-424	4	-1	733	819			
5	-5	1512	1548	5	-8	348	328	3	-1	375	373			
6	-5	813	823	6	-8	480	479	2	-1	533	-661			
7	-5	714	-712	7	-8	134	162	2	0	1018	1195			
8	-5	294	313	6	-7	223	-214	3	0	383	481			
9	-5	347	-337	4	-7	719	-800	4	0	1308	1463			
9	-4	488	-501	3	-7	94	-82	5	0	236	234			
8	-4	226	231	2	-7	1340	1514	6	0	1766	1825			
7	-4	306	297	1	-7	397	-469	7	0	392	-363			
6	-4	294	-337	0	-6	1045	-1035	9	0	140	-132			
4	-4	368	359	1	-6	235	266	10	0	752	-704			
3	-4	831	-877	2	-6	626	656	$\ell=1$	1	-11	375	-390		
2	-4	615	619	3	-6	197	-199		4	-10	87	-110		
1	-3	507	378	4	-6	776	829		3	-10	165	-140		
3	-3	253	235	5	-6	412	417		2	-10	317	359		
4	-3	120	134	6	-6	1010	-1029		1	-10	160	133		
5	-3	974	938	7	-6	190	211		0	-10	99	-90		
6	-3	652	655	8	-6	238	215		0	-9	239	-205		
7	-3	302	-329	8	-5	143	137		1	-9	749	-723		
8	-3	92	104	4	-5	302	-265		2	-9	344	382		
9	-3	134	-121	3	-5	255	-277		3	-9	139	126		
10	-3	366	-360	2	-5	308	341	4	-9	236	-251			
10	-2	261	238	0	-4	2086	-2308	5	-9	655	681			
9	-2	691	-640	1	-4	390	-436	6	-8	151	-168			
8	-2	242	258	2	-4	726	811	5	-8	92	102			
7	-2	529	556	3	-4	279	-259	4	-8	501	515			
6	-2	401	-474	4	-4	378	374	3	-8	741	-767			
5	-2	345	444	5	-4	112	203	2	-8	323	-372			
4	-2	105	4	6	-4	1084	-1111	1	-8	667	661			
3	-2	1301	-1294	7	-4	153	-173	0	-8	442	-503			
2	-2	1762	1796	8	-4	241	262	0	-7	379	-326			

$\ell=1$				$\ell=2$				$\ell=3$			
$h$	$k$	$F_O$	$F_C$	$h$	$k$	$F_O$	$F_C$	$h$	$k$	$F_O$	$F_C$
1	-7	209	-234	1	-11	207	223	2	-2	143	154
2	-7	115	-116	0	-11	243	279	3	-2	862	-864
3	-7	194	237	0	-10	442	-474	4	-2	405	477
4	-7	80	128	1	-10	460	488	6	-2	303	-296
5	-7	209	-209	2	-10	183	161	7	-2	570	600
6	-7	65	107	3	-10	277	-322	8	-2	171	-166
8	-6	247	-271	5	-9	257	-267	9	-1	429	-423
7	-6	408	416	4	-9	314	297	8	-1	158	126
5	-6	563	616	3	-9	225	246	7	-1	263	269
4	-6	790	775	2	-9	281	-309	5	-1	979	1011
3	-6	620	-632	1	-9	116	126	4	-1	374	-376
2	-6	223	-294	0	-9	168	125	3	-1	354	-390
0	-6	60	-35	1	-8	232	218	2	-1	572	590
0	-5	1781	1681	2	-8	454	475	1	-1	236	-215
1	-5	1968	1835	3	-8	191	-160	0	-1	568	476
2	-5	777	-750	5	-8	282	-306	1	0	2029	2305
4	-5	285	-331	6	-8	392	-397	2	0	896	702
5	-5	859	-858	7	-7	145	-189	3	0	1215	-1283
6	-5	455	468	6	-7	200	-212	4	0	747	759
7	-5	622	641	5	-7	679	-693	5	0	1146	-1241
8	-5	271	-235	4	-7	492	524	6	0	726	-717
9	-4	303	289	3	-7	835	892	7	0	967	1017
8	-4	134	152	2	-7	680	-673	8	0	194	182
7	-4	137	-172	1	-7	317	331	9	0	207	-178
6	-4	171	212	0	-7	409	-446				
4	-4	342	-390	0	-6	877	886	0	-11	355	430
3	-4	694	707	1	-6	1430	-1483	3	-10	205	208
1	-4	450	-405	3	-6	126	167	2	-10	117	-146
0	-3	2423	2350	4	-6	260	-306	1	-10	230	-263
2	-3	299	333	5	-6	779	810	0	-10	282	-291
3	-3	243	-277	7	-6	673	-691	0	-9	481	510
6	-3	65	-40	6	-5	145	-143	2	-9	507	-558
7	-3	134	170	5	-5	166	-141	3	-9	128	145
9	-3	96	-73	3	-5	182	210	4	-9	65	73
9	-2	457	462	1	-5	606	517	5	-8	105	99
8	-2	402	445	0	-5	759	-738	4	-8	632	-725
7	-2	568	-579	0	-4	267	255	0	-8	521	526
6	-2	349	322	1	-4	1300	-1377	0	-7	347	-325
5	-2	486	-486	2	-4	283	332	1	-7	317	276
4	-2	966	-1039	3	-4	163	172	2	-7	398	390
3	-2	933	1000	4	-4	668	-691	3	-7	609	-609
2	-2	286	-241	5	-4	670	747	4	-7	152	140
1	-2	870	-850	6	-4	429	434	5	-7	129	130
0	-2	962	788	7	-4	314	-322	6	-7	167	-165
1	-1	2000	-3161	8	-3	279	275	6	-6	376	398
2	-1	1183	1261	7	-3	155	176	4	-6	704	-768
3	-1	617	-672	6	-3	128	-93	3	-6	143	-161
4	-1	415	-367	5	-3	834	911	2	-6	237	327
5	-1	1254	1430	4	-3	64	-20	1	-6	178	133
6	-1	942	-998	3	-3	768	-826	0	-6	1341	1363
7	-1	551	-547	2	-3	1130	1141	0	-5	2072	-2063
8	-1	498	485	0	-3	139	-150	1	-5	308	282
9	-1	267	-217	0	-2	1172	-1076	2	-5	1245	1322

$\ell=3$								$\ell=5$			
$h$	$k$	$F_o$	$F_c$	$h$	$k$	$F_o$	$F_c$	$h$	$k$	$F_o$	$F_c$
3	-5	886	-890	2	-7	224	-184	1	-10	120	146
4	-5	392	351	1	-7	117	-143	0	-10	265	325
5	-5	180	-191	0	-7	751	-764	0	-9	257	-292
6	-5	991	-1018	1	-6	927	905	1	-9	699	717
7	-5	211	219	2	-6	1043	-1033	3	-9	506	-542
8	-4	394	-407	3	-6	445	-487	4	-8	201	207
6	-4	275	-278	4	-6	317	293	3	-8	242	253
5	-4	88	-63	5	-6	334	-346	1	-8	640	709
4	-4	475	517	6	-6	465	476	0	-7	105	60
3	-4	89	-96	7	-5	85	-92	1	-7	274	257
2	-4	593	-561	6	-5	223	266	2	-7	107	124
1	-4	1083	954	5	-5	166	171	3	-7	386	370
0	-4	694	-658	3	-5	212	159	4	-7	261	-314
0	-3	1431	-1337	2	-5	228	-164	6	-6	194	-196
1	-3	267	-190	1	-5	158	-155	5	-6	793	-820
2	-3	112	115	0	-5	176	-127	3	-6	457	484
3	-3	316	-296	1	-4	1479	1489	2	-6	154	183
4	-3	322	349	2	-4	702	-719	1	-6	174	168
6	-3	487	-482	3	-4	189	-206	0	-6	547	-594
8	-2	404	-374	4	-4	467	459	0	-5	296	242
7	-2	92	85	5	-4	452	-450	1	-5	1202	1184
6	-2	363	-359	6	-4	434	429	2	-5	464	-440
5	-2	342	-322	7	-4	617	601	3	-5	1052	1089
4	-2	1292	1367	7	-3	176	-162	4	-5	186	211
3	-2	357	-347	6	-3	496	491	5	-5	116	-139
2	-2	664	-672	5	-3	870	-910	6	-5	210	189
1	-2	1456	1455	4	-3	730	-742	7	-4	107	-112
0	-2	1723	-1641	3	-3	762	774	5	-4	530	529
0	-1	493	529	2	-3	352	-281	4	-4	461	-479
1	-1	224	155	1	-3	378	-349	3	-4	293	-261
2	-1	930	-900	0	-3	1698	1565	2	-4	464	433
3	-1	493	505	0	-2	114	60	1	-4	1066	-976
5	-1	139	91	2	-2	544	501	0	-4	184	143
6	-1	1006	1057	3	-2	76	-28	2	-3	931	-957
7	-1	68	40	4	-2	132	-114	3	-3	445	438
8	-1	703	-696	5	-2	99	-143	5	-3	156	-209
				6	-2	122	-155	7	-3	363	-379
				7	-2	109	-126	7	-2	181	-189
				8	-1	97	85	6	-2	322	334
				7	-1	175	-155	5	-2	1403	1414
				6	-1	126	116	4	-2	565	-549
				5	-1	621	-621	3	-2	778	-783
				4	-1	720	-727	2	-2	1017	931
				3	-1	856	810	1	-2	665	-657
				2	-1	559	-454	0	-2	208	142
				0	-1	1101	952	0	-1	336	-213
				0	0	2573	-2799	1	-1	1073	1061
				1	0	1047	-1031	3	-1	1105	-1035
				2	0	1064	986	4	-1	326	-336
				3	0	984	1036	5	-1	443	-448
				6	0	834	-834	6	-1	74	14
				7	0	965	-990	7	-1	627	607
				8	0	283	307				

$\ell=6$				$\ell=7$				$\ell=9$			
$h$	$k$	$F_o$	$F_c$	$h$	$k$	$F_o$	$F_c$	$h$	$k$	$F_o$	$F_c$
0	-10	111	91	1	-9	311	-356	1	-5	199	189
1	-9	482	-536	3	-8	249	-284	0	-5	465	459
0	-9	308	342	2	-8	406	430	0	-4	134	136
0	-8	283	294	1	-8	445	-473	1	-4	463	-436
2	-8	536	-539	0	-8	484	-533	2	-4	87	86
3	-8	119	110	0	-7	227	-294	3	-4	709	710
4	-7	727	-779	1	-7	87	-63	5	-4	170	-152
3	-7	82	77	2	-7	107	-111	5	-3	524	509
1	-7	362	-399	4	-7	77	-86	4	-3	319	-309
0	-7	1198	1185	4	-6	190	182	3	-3	167	124
0	-6	105	107	2	-6	209	254	2	-3	119	121
1	-6	275	262	1	-6	577	-551	1	-3	1154	-1070
2	-6	512	538	0	-6	1014	-1028	0	-2	182	-196
3	-6	89	-114	0	-5	174	164	2	-2	249	313
4	-6	428	-445	1	-5	219	221	3	-2	103	-91
5	-6	115	-90	2	-5	838	-876	5	-2	374	327
6	-5	128	127	3	-5	491	-544	5	-1	186	159
5	-5	307	318	4	-5	446	469	4	-1	112	-89
4	-5	202	210	5	-5	317	315	2	-1	260	241
3	-5	296	-285	5	-4	548	-523	1	-1	970	-874
1	-5	260	314	4	-4	187	-198	0	-1	102	-29
0	-5	521	446	3	-4	339	328	0	0	975	900
1	-4	53	-11	2	-4	218	-214	1	0	399	321
2	-4	843	782	1	-4	176	190	2	0	676	663
3	-4	292	-323	0	-4	636	601	3	0	1145	-1072
4	-4	773	-779	0	-3	248	275	4	0	87	-65
6	-4	169	-184	2	-3	361	-348	5	0	786	724
6	-3	666	-630	3	-3	82	-43	6	0	199	-159
5	-3	264	-247	4	-3	234	234	1	-8	290	-291
4	-3	797	792	5	-3	310	299	0	-8	585	625
3	-3	285	-275	6	-3	124	134	0	-7	126	119
2	-3	278	284	6	-2	529	465	1	-7	259	-253
1	-3	583	582	5	-2	331	-305	2	-7	203	214
0	-3	1955	-1882	4	-2	341	-296	3	-6	124	97
1	-2	371	-343	3	-2	342	320	2	-6	402	-443
2	-2	454	-503	2	-2	734	-707	1	-6	326	-307
3	-2	390	383	1	-2	929	881	0	-6	321	322
4	-2	84	-69	0	-2	1803	1715	0	-5	631	619
5	-2	147	-151	0	-1	268	355	2	-5	695	698
6	-2	291	266	1	-1	670	-721	3	-5	161	-140
7	-2	109	-92	2	-1	928	903	4	-5	607	-620
6	-1	439	-415	3	-1	843	788	4	-4	294	291
5	-1	456	-439	4	-1	733	-704	3	-4	237	-259
4	-1	679	645	0	-9	214	-257	2	-4	213	198
3	-1	77	-78	0	-8	261	269	1	-4	192	191
1	-1	115	-38	1	-8	102	114	0	-4	938	-926
0	-1	1817	-1710	3	-7	111	-155	0	-3	399	377
0	0	121	184	1	-7	639	698	1	-3	173	-150
1	0	928	-838	0	-7	177	-195	2	-3	645	629
2	0	2336	-2307	0	-6	242	228	4	-3	190	-184
3	0	708	737	1	-6	426	-413	2	-2	379	337
4	0	992	921	3	-6	672	689	3	-2	353	-316
5	0	93	68	4	-6	168	186	4	-2	288	263
6	0	525	469	4	-5	121	-112	0	-1	577	-578
7	0	143	-144	3	-5	373	-412	3	-3	76	-57
								1	-2	497	475

	$h$	$k$	$F_o$	$F_c$		$h$	$k$	$F_o$	$F_c$		$h$	$k$	$F_o$	$F_c$
$\ell=9$	0	-2	842	-759	$\ell=11$	0	-7	122	143	$\ell=13$	0	-3	80	-86
	1	-1	411	413		1	-6	478	486		1	-2	249	250
	2	-1	300	-247		0	-6	209	240		0	-2	89	101
	4	-1	615	581		1	-5	321	325		0	-1	664	643
	5	-1	168	-160		2	-5	273	-276					
$\ell=10$	0	-7	420	-433		1	-4	265	-286					
	1	-7	142	-160		0	-4	245	268					
	0	-6	514	-534		0	-3	130	-104					
	1	-6	129	165		2	-3	115	-121					
	2	-6	99	97		3	-3	97	108					
	3	-5	255	278		3	-2	577	572					
	2	-5	292	287		2	-2	152	141					
	1	-5	175	197		1	-2	658	-617					
	0	-5	89	-90		0	-2	172	185					
	0	-4	593	-561		0	-1	557	-528					
	1	-4	220	232		1	-1	158	-149					
	3	-4	484	-453		2	-1	234	200					
	4	-3	136	119		3	-1	517	-447					
	2	-3	683	-689	$\ell=12$	0	-6	243	279					
	1	-3	539	533		1	-5	127	-139					
	0	-3	606	580		0	-5	110	-83					
	0	-2	240	193		0	-4	197	220					
	3	-2	86	-69		1	-4	191	-196					
	4	-2	160	-147		2	-3	540	521					
	3	-1	142	-152		1	-3	255	236					
	2	-1	435	-400		0	-3	242	-227					
	1	-1	439	396		0	-2	237	-198					
	0	-1	482	427		1	-2	344	307					
	0	0	860	781		2	-1	325	322					
	1	0	195	-193		1	-1	137	115					
	2	0	453	382		0	-1	240	-247					
	3	0	337	343		0	0	801	-711					
	4	0	680	-631		1	0	634	566					
						2	0	249	-194					

$R = 6,6\%$

Note:- the values of  $F_o$  and  $F_c$  have been multiplied by a factor 10.

## APPENDIX B

PLANE NUMBER	PARAMETERS OF PLANE			
	L	M	N	P
1	-0,1413	0,9821	0,1249	11,1862
2	-0,1052	-0,1927	0,9756	3,5976
3	0,9914	0,0856	0,0991	0,0991
4	-0,1464	0,9760	0,1613	11,3647
5	-0,1092	-0,1722	0,9790	3,8191
6	0,9847	0,1196	0,1265	0,6328
7	-0,0945	0,9902	0,1028	11,0101
8	-0,1980	-0,1094	0,9741	4,4136
9	0,9572	-0,1383	0,2541	- 1,6987
10	0,5506	0,6832	0,4796	10,4738
11	-0,5415	0,3664	0,7567	8,0573
12	0,7519	-0,4908	0,4402	- 2,2414
13	-0,2416	-0,6464	0,7237	- 5,6183
14	-0,2409	-0,6495	0,7212	- 5,6246

ORTHOGONALIZED COORDINATES OF ATOMS USED IN THE LEAST SQUARES PLANES							
Atom	x	y	z	Atom	x	y	z
Ag	1,5108	12,9167	4,5149	C <sub>12</sub>	-0,8234	11,9678	3,1298
Fe	-1,3659	10,4803	5,6107	C <sub>13</sub>	-0,6497	13,1867	3,7985
C <sub>1</sub>	-5,6291	9,9890	5,6872	C <sub>14</sub>	-1,1301	13,4186	5,1197
C <sub>2</sub>	-4,2477	10,0600	6,2339	C <sub>15</sub>	-1,2771	14,8109	5,6302
C <sub>3</sub>	-3,9758	9,9828	7,5889	O <sub>1</sub>	-3,3116	10,2341	5,3467
C <sub>4</sub>	-2,7906	9,9961	8,1798	O <sub>2</sub>	-1,6246	10,1905	7,5962
C <sub>5</sub>	-2,6346	9,8403	9,7163	O <sub>3</sub>	-1,0159	8,5734	5,2717
C <sub>6</sub>	-0,1080	6,4069	5,2259	O <sub>4</sub>	0,5879	10,7343	5,8715
C <sub>7</sub>	0,0293	7,9396	5,4298	O <sub>5</sub>	-1,2055	10,9075	3,6375
C <sub>8</sub>	1,2840	8,4747	5,7701	O <sub>6</sub>	-1,5651	12,4588	5,8945
C <sub>9</sub>	1,5221	9,8208	5,9419	O <sub>8</sub>	2,5199	11,1602	3,0464
C <sub>10</sub>	2,8883	10,3105	6,2578	O <sub>11</sub>	2,8451	14,1554	5,8303
C <sub>11</sub>	-0,6014	11,9442	1,5841				